Accepted Manuscript

The eastern Sundaland margin in the latest Cretaceous to Late Eocene: Sediment provenance and depositional setting of the Kuching and Sibu Zones of Borneo

H. Tim Breitfeld, Robert Hall

PII: S1342-937X(18)30158-8
DOI: doi:10.1016/j.gr.2018.06.001
Reference: GR 1987

To appear in: *Gondwana Research*

Received date: 9 April 2018
Revised date: 17 May 2018
Accepted date: 10 June 2018

Please cite this article as: H. Tim Breitfeld, Robert Hall , The eastern Sundaland margin in the latest Cretaceous to Late Eocene: Sediment provenance and depositional setting of the Kuching and Sibu Zones of Borneo. Gr (2018), doi:10.1016/j.gr.2018.06.001

The eastern Sundaland margin in the latest Cretaceous to Late Eocene: Sediment provenance and depositional setting of the Kuching and Sibu Zones of Borneo

H. Tim Breitfeld [a*], Robert Hall [a]

[a] *SE Asia Research Group, Department of Earth Sciences, Royal Holloway University of London, Egham, TW20 0EX, UK*

*Corresponding author: t.breitfeld@es.rhul.ac.uk

Keywords: Kuching Supergroup; Rajang Group; Provenance; U-Pb detrital zircon dating; Borneo; SE Asia

Abstract

The Kuching Zone in Borneo comprises several large sedimentary basins of Late Cretaceous to Late Eocene age. In West Sarawak the Kayan Basin includes the Upper Cretaceous to Lower Eocene Kayan Group and further east in the Kuching Zone is the Ketungau Basin, consisting of the Middle to Upper Eocene Ketungau Group.

The Kayan Group is composed of the Kayan Sandstone and the Penrissen Sandstone. U-Pb detrital zircon ages and heavy minerals from the Kayan Sandstone suggest two major drainage systems: 1) Late Cretaceous to Paleocene rivers supplied sediment with abundant Cretaceous, Permian-Triassic and Precambrian zircons primarily from SW Borneo and East Malaya–Indochina and 2) Paleocene to Early Eocene rivers provided sediment containing almost entirely Cretaceous zircons from the Schwaner granites of SW Borneo. Differences in heavy minerals and zircon ages of the Lower Eocene Penrissen Sandstone support interpretations of an unconformity above Kayan Sandstone.

The Ketungau Group is interpreted to be unconformably above the Kayan Group, representing a new basin. The Ngili Sandstone, the oldest formation of the group, contains sediment derived from nearby sources, probably the Triassic Sadong and Kuching Formations. The Middle to Upper Eocene Bako-Mintu Sandstone, Silantek Formation and the probable Upper Eocene Tutoop Sandstone have similar sources to the Kayan Sandstone and have partly reworked the underlying sediments.

Field observations, heavy minerals and U-Pb zircon age data identify a large depositional system passing from the Kuching Zone terrestrial setting into Sibu Zone Rajang Group submarine fan deposits. This system was active for at least 25 to 30 Ma and at times the catchment area extended into the Malay Peninsula, possibly Sibumasu. The Kuching Supergroup sediments can be correlated with deep marine Rajang Group sediments based on detrital zircon ages and heavy mineral assemblages. There was some magmatism but the scarcity of contemporaneous zircons and compositional maturity of heavy mineral assemblages indicates that it was very minor. There is no support for subduction magmatism and the new observations are inconsistent with models suggesting the Sibu Zone was the source of sediments for a Kuching Zone forearc basin.

1. Introduction

In the western part of Borneo (Fig. 1) there are thick, mainly terrestrial, deposits of latest Cretaceous to Late Eocene age (Liechti et al., 1960; Wolfenden & Haile, 1963; Wilford & Kho, 1965; Muller, 1968; Tan, 1981; Pieters et al., 1987; Heryanto and Jones, 1996; Morley, 1998; Breitfeld et al., 2018) in the Kuching Zone of Haile (1974). These sedimentary rocks are separated by the Lupar Line from the Sibu Zone to the north where there are very thick deep water submarine fan deposits of similar depositional age forming the Rajang Group (Liechti et al., 1960; Tongkul, 1997; Galin et al., 2017). The Sibu Zone extends to the north up to the Bukit Mersing Line that separates it from the Miri Zone, where mostly Neogene sediments overly the deep marine Rajang Group (Haile, 1974). The West Baram Line in the northern part of the Miri Zone marked the southwestern limit of the Proto-South China Sea subduction in the Eocene to Early Miocene (Hall, 2013; Hall and Breitfeld, 2017). To the south of the three sedimentary zones lies the SW Borneo basement (Haile, 1974) or the SW Borneo block (Hall, 2012; Hennig et al., 2017).

The Kuching Zone sedimentary successions are the product of major fluvial systems and deltas that must have been active for at least 25 Ma. They are preserved in various basins of which the Melawi Basin of NW Kalimantan is the largest (Fig. 1). In West Sarawak are the Kayan Basin and its remnants, and the northern part of the Ketungau Basin which extends into Kalimantan (Fig. 2). Rocks of similar ages and depositional environments were previously assigned to different formations and groups (e.g. Liechti et al., 1960; Tan, 1981; Pieters et al., 1987; Doutch, 1992; Heryanto and Jones, 1996) and have recently been included in the Kuching Supergroup by Breitfeld et al. (2018). Williams et al. (1988) interpreted them as deposits of forearc basins north of a Schwaner Mountains arc, and the Rajang Group to the north has been interpreted as an accretionary complex related to southward-directed subduction (Hutchison, 1996). However, it is now known that the Schwaner arc had ceased activity by about 80 Ma (Davies et al., 2014), and there is little to indicate subduction in Sarawak in the latest Cretaceous, Paleocene or Eocene. Galin et al. (2017) argued against a subduction-related setting for the Rajang Group. This leads to questions about basin development on land. The distribution and

character of the basins along the Lupar Line and the Semitau Ridge suggests a strike-slip setting for some of the basins of the Kuching Zone (e.g. Doutch, 1992; Hall, 2012; Galin et al., 2017; Breitfeld et al., 2018).

Uppermost Cretaceous to Eocene sediments were not deposited or are not preserved in most parts of SE Asia. Therefore, Sarawak and NW Kalimantan provide a rare opportunity to gain insights into tectonic activity at this time, and the erosion and drainage of eastern Sundaland. We present new light and heavy mineral data accompanied by U-Pb detrital zircon age data from sediments in West Sarawak which provide insights into their provenance, link the terrestrial Kuching Zone and the deep marine Sibu Zone, and discuss the implications of these results for the latest Cretaceous and early Paleogene history of NW Borneo.

2. Geological background

The Kuching Zone in West Sarawak (Fig. 1 and Fig. 2) includes the Kayan Basin and the Ketungau Basin (Pieters et al., 1987; Tate, 1991; Doutch, 1992). The Mandai Basin to the east may be a lateral equivalent or former continuation of the Ketungau Basin (Pieters et al., 1987; Doutch, 1992). The sediments include the uppermost Cretaceous to Lower Eocene Kayan Group in the Kayan Basin (Muller, 1968; Morley, 1998; Breitfeld et al., 2018) and the Middle to Upper Eocene Ketungau Group in the Ketungau Basin (Tan, 1979; Breitfeld et al., 2018). Most age data comes from K-Ar dating of volcanic rocks that have been interpreted to occur at the base or are intercalated with the sedimentary sequences within the Mandai and West Kutei Basins in Kalimantan to the east of the research area. These include the Early Eocene (c. 48 Ma) Nyaan Volcanics and the Middle Eocene (c. 41 Ma) Muller Volcanics (Pieters et al., 1987; Bladon et al., 1989; Tate, 1991).

In the west the Kuching Zone is underlain by Paleozoic to Mesozoic rocks which formed part of the Triassic Sundaland margin (Breitfeld et al., 2017; Hennig et al., 2017a). In the east (Tan, 1979; Williams et al., 1988) rocks accreted at the Triassic to Cretaceous Paleo-Pacific subduction margin underlie the

Kuching Zone (Breitfeld et al., 2017; Hennig et al., 2017a). In the Cretaceous there was a magmatic arc in the Schwaner Mountains and a forearc basin to the (present) north in the Kuching Zone in which the Pedawan and Selangkai Formations (Fig. 3) were deposited (Pieters et al., 1993; Breitfeld et al., 2017). A Late Cretaceous (c. 80-90 Ma) Pedawan collision unconformity marks the end of Paleo-Pacific subduction beneath Borneo (Breitfeld et al., 2018).

The Sibu Zone is composed almost entirely of deep marine sediments of the Rajang Group (Haile, 1974). It is not known what underlies this zone. Moss (1998) proposed trapped oceanic crust whereas Breitfeld et al. (2017) and Hennig et al. (2017a) suggested a more complex mixture of Mesozoic accreted material. Galin et al. (2017) interpreted the Rajang Group as a submarine fan formed at a passive margin of the Proto-South China Sea (Hall and Breitfeld, 2017) and showed the Schwaner Mountains granites and the Malay-Thai Tin Belt-West Borneo province were probable source regions. The Kuching Supergroup sediments were deposited between those potential source regions and the Rajang Group in a number of terrestrial sedimentary basins.

Terrestrial sedimentation in the Kuching Zone initiated in the latest Cretaceous (Morley, 1998; Breitfeld et al., 2018). Some earlier studies, such as Doutch (1992) and Hutchison (1996, 2005) suggested the uplifted deep marine Rajang Group in the Sibu Zone to the north was the source area for Kuching Zone sediments, a conclusion supported by Erriyantoro et al. (2011) who reported similar light mineral compositions in both zones. However, dating by numerous workers (Haile, 1957; Kirk, 1957; Liechti et al., 1960; Wolfenden, 1960; Muller, 1968; Tan, 1979; Morley, 1998; Galin et al., 2017) shows that the sediments of both zones are of similar age and therefore the Rajang Group could not be the source for the Kuching Zone. Tan (1984) suggested parts of the Kuching Zone successions could have been derived by local reworking of older sediments in West Sarawak (e.g. Triassic Sadong and Jurassic-Cretaceous Pedawan Formations), although Tan (1984) and Hutchison (2005) raised questions concerning the quartz-rich character of the sediments and concluded that additional sources were required.

3. Stratigraphy of the Kuching Supergroup in West Sarawak

The stratigraphy of the Kayan and Ketungau Basins has undergone various revisions. Liechti et al. (1960) presented the first comprehensive stratigraphy for West Sarawak, and introduced the terms Silantek Formation and Plateau Sandstone for the sedimentary successions of the two basins. Haile (1968) and Tan (1981) made further subdivisions and distinguished the Kayan Sandstone, Penrissen Sandstone, Silantek Formation and Plateau Sandstone. Breitfeld et al. (2018) introduced a modified stratigraphy for West Sarawak based on new field observations. This divides the successions in West Sarawak into the Kayan Group, consisting of the Kayan Sandstone and the Penrissen Sandstone, and the Ketungau Group, consisting of the Ngili Sandstone, Bako-Mintu Sandstone, Silantek Formation and Tutoop Sandstone (Fig. 2). The Ketungau Group extends into Kalimantan where the Ketungau Formation marks the top of the group (Heryanto and Jones, 1996). Fig. 3 summarises the Cretaceous to Oligocene stratigraphy of West and Central Sarawak that is used in this paper for the Kuching and Sibu Zones.

3.1. Kayan Group

The Kayan Group comprises all sediments formerly named the Kayan Sandstone by Tan (1981) in West Sarawak (Breitfeld et al., 2018) and is subdivided into the Kayan Sandstone and Penrissen Sandstone (Fig. 3).

3.1.1. Kayan Sandstone

The Kayan Sandstone forms several isolated exposures in the Kayan Syncline (Fig. 2), including those at Gunung Serapi/Matang, Tanjung Santubong, the Pueh area and the Bungo Range (Breitfeld et al., 2018). The higher exposures at Gunung Penrissen previously included by Tan (1981) in the Kayan Sandstone were reassigned by Breitfeld et al. (2018) to the Penrissen Sandstone.

Muller (1968) introduced two palynological zones based on pollen analysis for the Kayan Sandstone, the *Rugubivesiculites* zone and the *Proxapertites* zone. The *Rugubivesiculites* zone is the oldest part of

the Kayan Sandstone and is exposed in the northern Pueh area, Lundu area (western part of the Kayan Syncline) and the Bungo Range (Muller, 1968). Morley (1998) suggested a Late Maastrichtian to Paleocene age. The *Proxapertites* zone of the Kayan Sandstone is exposed in the Pueh area, eastern Kayan Syncline, and in the Bungo Range. The age was reinterpreted by Morley (1998) to be probably Early to Late Paleocene.

Breitfeld et al. (2018) interpreted a terrestrial setting which started as an alluvial fan and developed with time into a fluvial system in a muddy floodplain environment with some tidal and deltaic influence; locally fine ash layers or pyroclastic material indicate contemporaneous volcanic activity.

3.1.2. Penrissen Sandstone

The Penrissen Sandstone is the sedimentary succession that caps the mountain range in the centre of the Bungo Syncline (Fig. 2) with a summit at Gunung Penrissen close to the border with Kalimantan (Breitfeld et al., 2018). The Penrissen Sandstone correlates with the *Retitriporites variabilis* palynology zone of Muller (1968) for which Morley (1998) interpreted an Early Eocene age making the Penrissen Sandstone the youngest part of the Kayan Group. Breitfeld et al. (2018) reported very thick alluvial conglomerates interbedded with fluvial channel sandstones and some lacustrine facies.

3.2. Ketungau Group

The term Ketungau Group was introduced by Breitfeld et al. (2018) for the Paleogene sequence that forms the synclinal Ketungau Basin in West Sarawak (Fig. 2). In West Sarawak (Fig. 3) it includes the Ngili Sandstone, Silantek Formation (named Kantu Formation in Kalimantan), Bako-Mintu Sandstone and Tutoop Sandstone (named Plateau Sandstone in Sarawak) and the Ketungau Formation exposed only in Kalimantan (Heryanto and Jones, 1996). In Kalimantan the term Merakai Group is used for the Ketungau Basin sequence (e.g. Williams and Heryanto, 1985). The Paleocene (to possible Early Eocene) Engkilili Formation is associated with the Ketungau Group in the Lupar Valley with uncertain stratigraphic relation (Haile, 1957; Muller, 1968; Tan, 1979; Haile, 1996).

3.2.1. Ngili Sandstone

The Ngili Sandstone was previously considered part of the Silantek Formation (Haile, 1954; Heng, 1992). In the lower part of Gunung Ngili the lower Ngili Sandstone includes alluvial conglomerates with a volcaniclastic component which pass upwards into sandstones deposited in small fluvial systems and extensive floodplain areas in a coal-producing coastal (estuarine) environment (Breitfeld et al., 2018).

3.2.2. Silantek Formation

The term Silantek Formation was introduced by Liechti et al. (1960) for rocks that form the lower part of the Klingkang Range close to the border between Sarawak and Kalimantan, south of the Lupar Valley. In Kalimantan the name Kantu Beds is used (e.g. Pieters et al., 1987; Heryanto and Jones, 1996). Breitfeld et al. (2018) subdivided the Silantek Formation into the Marup Sandstone Member, Temudok Sandstone Member and Shale Member.

Marup Sandstone Member

The Marup Sandstone Member is the lowermost part of the Silantek Formation and is exposed in the eponymous Marup Ridge, at the northern boundary of the Ketungau Basin (Fig. 2). Pieters et al. (1987) suggested the Haloq Sandstone of the Mandai Basin in Kalimantan is a lateral correlative, implying a former much larger extent of the member. Haile (1957) and Tan (1979) reported Middle to Upper Eocene foraminifera, and Tan (1979) and Breitfeld et al. (2018) interpreted a marginal marine, subtidal and near-shore facies environment.

Temudok Sandstone Member

The Temudok Sandstone Member forms the Temudok Ridge south of Sri Aman (Fig. 2) where it is composed of thick sandstone-mudstone alternations. Breitfeld et al. (2018) interpreted a floodplain environment with restricted peat formation and periodic clastic input by sheet flood events that formed the thick sandstone beds.

Shale Member

The Shale Member consists of thick mudstones interbedded with thin siltstone and sandstone beds (Breitfeld et al., 2018). It forms the thickest unit of the Silantek Formation, extending from the Marup Ridge to the Klingkang Range. Kanno (1978) reported brackish water molluscs, which indicate an estuarine or mangrove swamp environment.

3.2.3. Bako-Mintu Sandstone

The Bako-Mintu Sandstone was previously assigned to the Plateau Sandstone (Haile, 1957; Liechti et al., 1960; Wilford, 1955; Heng, 1992; Tan, 1993). It is exposed at Tanjung Bako, on top of Gunung Ngili and in the headwater area of the Sebuyau and Sebangan Rivers near Gunung Menuku (Fig. 2). Breitfeld et al. (2018) interpreted a predominantly fluvial environment with minor floodplain deposits which developed into larger mud-dominated successions with peat accumulation.

3.2.4. Tutoop Sandstone

The Tutoop Sandstone is widely distributed in Kalimantan and has its type locality in ridges around Gunung Tutoop (Williams and Heryanto, 1985; Heryanto and Jones, 1996). In Sarawak it was previously known as the Plateau Sandstone (Molengraaff and Hinde, 1902; ter Bruggen, 1935; Zeijlmanns van Emmichoven, 1935, 1939; Milroy, 1953; Haile, 1954, 1957; Liechti et al., 1960; Wolfenden and Haile, 1963; Wilford and Kho, 1965). Breitfeld et al. (2018) assigned exposures of the Klingkang Range near the border with Kalimantan to the Tutoop Sandstone, as well as the Upper Kantu Beds/Upper Silantek Redbeds (Haile, 1957; Tan, 1979) which were previously assigned to the Silantek Formation. The sequences at Bako and in the Mintu area formerly considered part of the Plateau Sandstone are now considered to be the Bako-Mintu Sandstone (Breitfeld et al., 2018). Liechti et al. (1960), Pieters et al. (1987), Doutch (1992) and Breitfeld et al. (2018) suggested a Late Eocene to possible Early Oligocene age. Haile (1957), Liechti et al. (1960), Tan (1979) and Breitfeld et al. (2018) interpreted a predominantly fluvial environment.

3.2.5. Ketungau Formation

The Ketungau Formation was not part of this study because it is the youngest unit of the Ketungau Group and is exposed only in Kalimantan in the core of the Ketungau syncline. It consists of sandstone with thicker beds in the lower part of the sequence and siltstone, carbonaceous mudstone and thin coal seams in the upper part (Heryanto and Jones, 1996). The formation is undated and assumed to be Late Eocene or Oligocene (Williams et al., 1988; Heryanto, 1991; Heryanto & Jones, 1996).

4. Sampling and methodology

Fieldwork in West Sarawak was undertaken at/within Tanjung Santubong, Tanjung Bako, Gunung Serapi/Kampung Matang, Kampung Pueh area, Kayan Syncline, Gunung Singai, Bungo Range, Gunung Penrissen, Gunung Ngili, Kampung Mintu area, Marup Ridge, Temudok Ridge and at Bukit Begunan and Bukit Mansul of the Klingkang Range (Fig. 2).

In total 74 samples were analysed for light minerals, 28 samples were analysed for heavy mineral assemblages and zircons of 26 samples were dated by U-Pb LA-ICP-MS or SHRIMP. Sample locations are shown on Fig. 2 and are listed in Supplementary Table 1. For light mineral modal analysis, the Gazzi-Dickinson point counting method was used to reduce the influence of grain size (Dickinson, 1970; Ingersoll et al., 1984). Alkali feldspars were stained using sodium cobaltinitrite and plagioclase stained using barium chloride and amaranth solution.

4.1. Sample preparation

Sample preparation was carried out at Royal Holloway University of London. A 63-250 µm fraction was used for zircon geochronology and heavy mineral analysis. Heavy minerals were separated by using standard heavy liquids sodium polytungstate (SPT) and lithium heteropolytungstate (LST) at a density of 2.89 g/cm^3. For zircon concentration the obtained fraction was further processed with a FRANTZ magnetic barrier separator and then immersed into di-iodomethane (DIM) at 3.3 g/cm^3 to maximise the purity of the zircon separates. Zircons were imaged in transmitted light to detect cracks or

inclusions and cathodoluminescence secondary electron microscopy (CL-SEM) was performed to identify growth zonation and rims of the zircons.

4.2. Geochronology

4.2.1. LA-ICP-MS U-Th-Pb dating

LA-ICP-MS (laser ablation inductively coupled plasma mass spectrometry) dating was performed at Birkbeck College, University of London with a New Wave NWR 193 and NWR 213 nm laser ablation system coupled to an Agilent 7700 quadrupole-based plasma mass spectrometer (ICP–MS) with a two-cell sample chamber. A spot size of 25 µm for the NWR 193 nm and of 30 µm for the NWR 213 nm system was used. The Plešovice zircon standard (337.13 ± 0.37 Ma; Sláma et al., 2008) and a NIST 612 silicate glass bead (Pearce et al., 1997) were used to correct for instrumental mass bias and depth-dependent inter-element fractionation of Pb, Th and U.

GLITTER software (Griffin et al., 2008) was used for data reduction. The data were corrected using the common lead correction method by Andersen (2002), which is used as a ^{204}Pb common lead-independent procedure.

4.2.2. SHRIMP U-Th-Pb dating

Sensitive high resolution ion microprobe (SHRIMP) dating was performed at IBERSIMS lab, University of Granada on a SHRIMP IIe/mc instrument. The GAL zircon (c. 480 Ma; Montero et al., 2009) was used for mass calibration, the SL13 zircon (Claoué-Long et al., 1995) was used as concentration standard (238 ppm U) and the TEMORA zircon (417 Ma, Black et al., 2003) was used as isotope ratio standard. Data reduction was done with SHRIMPTOOLS software for IBERSIMS developed by Fernando Bea.

4.2.3. Age presentation

The age obtained from the ^{207}Pb/^{206}Pb ratio is given for grains older than 1000 Ma. For ages younger than 1000 Ma, the age obtained from the ^{238}U/^{206}Pb ratio is given, because ^{207}Pb cannot be measured with sufficient precision in these samples resulting in large analytical errors (Nemchin and Cawood, 2005). Concordance was tested by using a 10 % threshold between the ^{207}Pb/^{206}Pb ^{206}Pb/^{238}U ages for

ages greater than 1 Ga and for ages below 1 Ga between the $^{207}Pb/^{235}U$ and $^{206}Pb/^{238}U$ ages. Age histograms and probability density plots were created using an R script written by Inga Sevastjanova based on the approach of Sircombe (2004) for calculating probability density. Results are presented for the Kayan Group in Supplementary Table 2 and for the Ketungau Group in Supplementary Table 3.

5. Light mineral detrital modes

The most common light minerals in the samples consist of varieties of quartz and both feldspar types with subordinate lithic fragments. Fig. 4 displays a selection of photomicrographs of the light minerals. Ternary sandstone diagrams are displayed in Fig. 5 that show the light mineral modes. The Kayan Group is shown in Figs. 5a to d and the Ketungau Group in Figs. 5e to h. Table 1 reports the light mineral modes for all samples. Feldspar and lithic fragments are susceptible to chemical and physical breakdown, especially in a tropical environment (Smyth et al., 2008; van Hattum et al., 2013; Galin et al., 2017), and therefore their abundance may not be indicative of source composition, but could indicate rapid deposition and/or shallow burial instead.

5.1. Kayan Group

Samples from the Kayan Sandstone are predominantly quartz-rich sublitharenites (Fig. 5a). Some samples are classified as lithic arenites and some as lithic greywackes (Fig. 5a and b). They are mainly composed of monocrystalline quartz, polycrystalline quartz and lithic fragments. Subordinate components are feldspar, chert and volcanic quartz. Feldspar is dominated by alkali feldspar indicating an acid igneous contribution. Metamorphic, sedimentary and abundant volcanic lithic fragments indicate multiple other sources. Samples from the Kayan Syncline, especially the basal conglomerate, are generally more lithic-rich. However, the QFL plots of the whole Kayan Group are rather similar and subdivision on the basis of light minerals is not possible. The enrichment in quartz may reflect erosion of quartz-rich protoliths and significant tropical weathering. All Kayan Sandstone samples have a recycled orogenic character on the QFL diagram (Fig. 5c). In the QmFLt diagram the samples are mainly

classed as transitional recycled with minor quartzose recycled and two samples fall into the craton interior field (Fig. 5d).

Penrissen Sandstone samples are sublitharenites to subarkoses with the most feldspathic falling into the lithic arkose field (Fig. 5a). They are mainly composed of monocrystalline quartz, polycrystalline quartz, feldspar and lithic fragments. Subordinate volcanic quartz and chert are present. Feldspar is dominated by alkali feldspar, but plagioclase is more abundant than in the underlying Kayan Sandstone. Microcline is present and indicates an igneous or pegmatite source. Lithic fragments are dominated by sedimentary and volcanic fragments, indicating reworking of older strata with input from a volcanic source. The overall abundance of feldspar indicates an additional fresh igneous source which was not available during deposition of the Kayan Sandstone, or relatively fast burial, diminishing breakdown of feldspar and unstable lithic fragments compared to the Kayan Sandstone. Penrissen Sandstone samples have a recycled orogenic character in the QFL diagram (Fig. 5c). In the QmFLt diagram they plot in the mixed field between recycled orogen and magmatic arc, and in the transitional orogen field (Fig. 5d).

5.2. Ketungau Group

The Ngili Sandstone samples are sublitharenites and lithic arenites (Fig. 5e). They are composed mainly of polycrystalline and monocrystalline quartz, with a wide compositional range. For example, STB75b has abundant polycrystalline quartz, indicating a predominantly metamorphic source. In contrast, the lowermost part of the Ngili Sandstone is a volcaniclastic conglomerate composed mainly of volcanic and sedimentary lithic fragments and polycrystalline quartz. Chert grains indicate a deep marine or marine sedimentary source. Three of the samples have only very minor or no feldspar but STB77 has a high feldspar content dominated by plagioclase (c. 14 % of the framework grains). Sandstones have a recycled orogen character in the QFL diagram (Fig. 5g), and plot in the QmFLt diagram in the transitional recycled and lithic recycled fields (Fig. 5h).

Silantek Formation samples are sublitharenites or lithic greywackes (Fig. 5 e and f), and all samples from the Shale Member are lithic greywackes (Fig. 5f). They are composed mainly of monocrystalline and polycrystalline quartz and lithic fragments. Subordinate components are chert, volcanic quartz and feldspar. Alkali feldspar and plagioclase are present within all samples, with alkali feldspar usually more abundant. Samples from the lowermost part of the Silantek Formation, the Marup Sandstone, have relatively high proportions of feldspar with c. 6 to 13 % of the framework grains (Table 1). Lithic fragments are mainly sedimentary and volcanic, with few metamorphic fragments. The Silantek Formation has a recycled orogen character on the QFL diagram (Fig. 5g) and on the QmFLt diagram samples plot in the quartzose to transitional recycled orogen fields (Fig. 5h).

The Bako-Mintu Sandstone samples are sublitharenites, lithic arenites and lithic greywackes (Fig. 5e and f). There is no compositional difference between samples from Tanjung Bako and the Mintu area. They are composed mainly of monocrystalline and polycrystalline quartz and lithic fragments. Chert, scarce feldspar and volcanic quartz are present. Lithic fragments include metamorphic, sedimentary and volcanic rocks. In contrast to the Silantek Formation, the Bako-Mintu Sandstone is characterised by the low abundance of feldspar. This could reflect a volcanic-dominated source, reworking or weathering. Sandstones plot into the recycled orogen field on the QFL diagram (Fig. 5g) and in the fields for quartzose to transitional recycled orogen on the QmFLt diagram (Fig. 5h).

The Tutoop Sandstone samples are sublitharenites (Fig. 5e) characterised by the abundance of monocrystalline quartz and low proportions of matrix (see Table 1). Polycrystalline quartz, chert, rare volcanic quartz, rare feldspar and lithic fragments indicate a variety of sources. Lithic grains are mainly sedimentary with some volcanic fragments. Feldspar is either absent or there are only small amounts of mainly alkali feldspar. Sandstones have a recycled orogen character on the QFL diagram (Fig. 5g) and quartzose recycled character on the QmFLt diagram (Fig. 5h). The Tutoop Sandstone is compositionally the most mature sediment of the Kayan and Ketungau Groups. This maturity may indicate a second- or multiple cycle sediment with minor input of volcanic material.

5.3. Textures

Sandstones of the Kayan Group and the Ketungau Group commonly have sub-rounded to sub-angular grains and sorting ranges from very poor to very good. This wide range, and common textural immaturity, is in contrast to the compositional maturity previously described.

The Kayan Sandstone is dominated by sub-rounded to sub-angular grains with subordinate angular grains and a wide range of sorting. This indicates various depositional processes and reworking. Rounding is generally better in the Kayan Syncline in contrast to the other areas of the Kayan Sandstone. The Penrissen Sandstone is texturally more immature than the Kayan Sandstone. It is composed predominantly of sub-angular grains characterised by moderate to poor sorting, suggesting less reworking of material than in the Kayan Sandstone and possibly shorter transport distances. The Ngili Sandstone is composed of sub-rounded to sub-angular grains. Sorting is generally poor, ranging from moderate to very poor, and suggests rapid deposition with a possible short transport distance. The volcaniclastic basal conglomerate and volcaniclastic sandstones have abundant angular grains and are especially poorly sorted. Silantek Formation samples usually have sub-rounded to sub-angular grains which are very well to moderately sorted. Samples from the lowermost part, the Marup Sandstone Member, have abundant sub-angular grains which are generally poorly to moderately sorted. The Bako-Mintu Sandstone samples are slightly better sorted than the Silantek Formation samples. Grains are usually sub-rounded to sub-angular, but rounded to sub-rounded grains are more common. Both indicate multiple reworking and a wide range of depositional processes. The Tutoop Sandstone samples are in general very well to moderately sorted. Grains are usually sub-rounded to sub-angular with scarce rounded grains, suggesting reworking. However, sorting and rounding are a function of a wide range of processes and therefore, there is considerable uncertainty in provenance interpretation from light mineral modes alone.

6. Heavy mineral assemblages

All samples are dominated by the ultra-stable minerals zircon, tourmaline and rutile. However, a wide range of heavy minerals are present as trace and minor constituents, indicating various sources. Zircon shapes range from euhedral to rounded and grains are colourless to pinkish (Fig. 6). Fig. 7 displays a selection of photomicrographs and backscattered SEM images of the most common heavy minerals in the samples.

Fig. 8 illustrates the heavy mineral composition of the samples in stratigraphic order. Table 2a and b record absolute and percentage amounts of the heavy minerals observed. Textures of zircons and tourmalines are listed in Table 3. Carbonate minerals (ankerite and siderite) and Ti-minerals (brookite and anatase) are present in most samples but may be the product of authigenic growth during burial and are not considered for source interpretation.

6.1. Kayan Group

6.1.1. Kayan Sandstone

14 samples from the Kayan Sandstone were analysed for heavy minerals. Assemblages are dominated by zircon (21 to 64 %), tourmaline (0 to 36 %) and rutile (5 to 42 %). Accessory heavy minerals include titanite, garnet, cassiterite, sillimanite, kyanite, apatite, hornblende, monazite, chrome spinel, augite, epidote, clinozoisite, chlorite, chloritoid, orthopyroxene and serpentine. The heavy mineral assemblages indicate acid igneous rocks and reworked sediments were the main sources with contributions from ultrabasic and basic igneous sources. Epidote and clinozoisite may indicate a metamorphic source or alteration of e.g. hornblende or plagioclase. The heavy mineral assemblage of sample TB21 is an exception. It is dominated by abundant andalusite (79 %) (Table 2b), which would indicate a metamorphic source, and contains very few zircons. However, the Gunung Serapi and the Gunung Bawang dykes are close to the sample location. Thus the abundance of andalusite may be a contact metamorphic overprint of the sediments and the sample was not considered for source specific interpretations and is also omitted from the heavy mineral figures.

There is a clear difference in zircon types between the Kayan Syncline/Tanjung Santubong and the Pueh area/Gunung Serapi/Bungo Range. While the samples from the former have angular (48.3 to 62.7%) and rounded to subrounded (37.3 to 51.7%) grains, samples from the latter are dominated by abundant angular grains (61.2 to 88.4%) and highly rounded zircons are scarce (Table 3). The zircon grains suggest first- to multiple-cycle and reworking for the Kayan Syncline/Tanjung Santubong, while the sediment for the Pueh area/Gunung Serapi/Bungo Range was primarily first-cycle. Variations in tourmaline types are not significant and show no differences in the two regions; angular grains dominate throughout the successions.

6.1.2. Penrissen Sandstone

Two samples (TB121, TB119) of the Penrissen Sandstone were analysed for heavy minerals. In contrast to the majority of sediments observed in West Sarawak, the heavy mineral assemblage of the Penrissen Sandstone is very diverse and interpreted to be immature. It is dominated by epidote (40 to 59 %), clinozoisite (7.4 to 10 %), apatite (4.9 %), garnet (9.2 to 10 %), zircon (8.2 to 16 %) and tourmaline (4 to 7 %). Accessory heavy minerals are rutile, chlorite, chloritoid, hypersthene and augite. The heavy mineral assemblage indicates acid igneous, metamorphic and basic igneous sources. Garnet, epidote, clinozoisite and chloritoid indicate a metamorphic contribution.

Zircons are dominated by colourless varieties. Angular zircon grain shapes are dominant (60.4 to 74.5 %) and indicate a relative high first-cycle input with only minor reworking. Tourmaline is predominantly brownish with angular shapes (59.1 to 69.6 %). The presence of rounded zircon and tourmaline grains suggests some reworking of older sediments.

6.2. Ketungau Group

6.2.1. Ngili Sandstone

Two samples of the Ngili Sandstone (STB75, STB75b) were analysed for heavy minerals. They are dominated by the ultra-stable heavy minerals zircon (46 to 81 %) and rutile (4 to 23 %). All other heavy minerals occur only in accessory quantities and include chlorite, epidote, tourmaline, hypersthene,

allanite, chrome spinel and titanite. The very low abundance of tourmaline is distinctive, which may be related to the source or be a function of hydraulic sorting. The heavy mineral assemblages suggest a primary acid igneous source with reworking of older sediments. Input from ultrabasic and metamorphic sources is very minor.

Zircon grains are angular (46.9 to 59.1 %) and rounded to subrounded (40.9 to 53.1 %) suggesting both reworking and fresh acid igneous input. Coloured zircon grains are predominantly rounded. Most tourmaline grains are rounded indicating reworking of older sediments.

6.2.2. Silantek Formation

Three samples of the Silantek Formation were analysed for heavy minerals, from the Marup Sandstone Member (TB210, TB217) and Temudok Sandstone Member (TB218). They are dominated by ultra-stable minerals including zircons (31 to 40 %), tourmaline (16 to 37 %) and rutile (5 to 20 %). The Marup Sandstone Member sample TB217 has abundant garnet (33 %) which is not present in the other samples. This indicates either hydraulic separation or a garnet-rich source which was not available for the rest of the Silantek Formation. Accessory heavy minerals comprise apatite, titanite, chrome spinel, hornblende, monazite, epidote, clinozoisite, chlorite and serpentinite. The heavy mineral assemblages indicate acid igneous and reworked older sediments as the main sources. Metamorphic and ultrabasic input is minor but present throughout the formation. Traces of wolframite ($(Fe,Mn)WO_4$) and huebnerite ($MnWO_4$) were identified in TB217. There have been some important metallic discoveries in West Sarawak (especially from the Bau district), including gold, antimony, silver, mercury, copper and nickel (Wilford, 1955; Wolfenden and Haile, 1963; Wolfenden, 1965; Hutchison, 2005, Breitfeld et al., 2018), but no tungsten mineralisation is recorded.

Zircon grains are commonly angular (44.2 to 63 %) and rounded to subrounded (37 to 55.8 %). Tourmaline shapes are predominantly angular (57.1 to 64.9 %). This indicates significant first-cycle input with some reworking of older sediments.

6.2.3. Bako-Mintu Sandstone

Two samples of the Bako-Mintu Sandstone were analysed for heavy minerals. The assemblages are dominated by zircons (c. 45 %), tourmaline (30 to 34 %) and rutile (8 to 12 %). Accessory minerals comprise chrome spinel, sillimanite, hornblende, monazite, epidote, cassiterite and serpentine. The heavy mineral assemblage indicates acid igneous and reworked older sediments as the main sources. Metamorphic and ultrabasic input is minor.

Zircons are dominated by angular grains (c. 63 %). Rounded to subrounded zircons form c. 38 % of the zircon assemblage. Tourmaline shapes are predominantly angular (59.4 to 72 %). This indicates first-cycle input with some reworking of older sediments.

6.2.4. Tutoop Sandstone

Five samples of the Tutoop Sandstone were analysed. The heavy mineral assemblages are dominated by zircon (38 to 69 %), tourmaline (11 to 31 %) and rutile (10 to 22 %). Accessory minerals comprise garnet, sillimanite, monazite, hornblende, monazite, chrome spinel, epidote, clinozoisite, chlorite and chloritoid. The heavy mineral assemblage indicates a major acid igneous source with reworking of older sediments. Input from ultrabasic and metamorphic sources is small. However, chrome spinel is found in 3 of the 5 samples at different stratigraphic levels and indicates ultrabasic input throughout Tutoop Sandstone deposition.

Zircon grains are angular (42.3 to 64.6 %) and rounded to subrounded (35.3 to 57.7 %) with angular being the more abundant, indicating primarily first-cycle input with reworked sediments. The tourmaline shapes are similar.

6.3. Heavy mineral ratios

Heavy mineral analyses used the ZTR index of Hubert (1962) and the zircon-tourmaline ratio (after Mange and Wright, 2007). The commonly used heavy mineral ratios of Morton & Hallsworth (1994) are not reported due to the low abundance of several important minerals. Fig. 8 illustrates the ZTR

index and ZTi ratio for the samples in stratigraphic order and heavy mineral ratios are listed in Table 4.

ZTR is generally very high for all samples, indicating very mature assemblages, with the exception of the Penrissen Sandstone, which has a very low ZTR indicative of immaturity. ZTi shows considerable variation throughout the successions. The Kayan Sandstone from the Kayan Syncline/Tanjung Santubong shows the most variation in the ZTi values, while samples from the Pueh area/Gunung Serapi/Bungo Range have generally similar ZTi values of 70 to 80. The Ngili Sandstone is characterised by the highest ZTi values. Samples from the Silantek Formation and the Bako-Mintu Sandstone show overall the lowest ZTi values.

7. U-Pb geochronology

The U-Pb detrital zircon histograms for the Kayan Group and for the Ketungau Group are illustrated in Figs. 9 and 10 in stratigraphic order. Histograms of individual samples can be found in the supplementary figures.

7.1. Kayan Group

7.1.1. Kayan Sandstone

Zircons were analysed in 12 Kayan Sandstone samples from different areas, which include Tanjung Santubong, the Kayan Syncline, the Bungo Range, Gunung Serapi/Matang and the Pueh area.

Kayan Syncline

The Kayan Sandstone in the Kayan Syncline was sampled at the “Buffer Wall” outcrop (STB01) at 82 m above sea level and STB10 was sampled from Gunung Sepada/Bukit Chupin at 67 m above sea level.

A total of 201 concordant U-Pb ages were obtained from 202 zircons (Fig. 9). The zircon age populations consist of 149 Phanerozoic, 48 Proterozoic and 4 Archean ages. The two samples have two dominant age peaks in the Cretaceous and in the Permian-Triassic. The youngest population comprises almost the whole Cretaceous period. STB10 has a significant peak between 70 and 80 Ma

and STB01 is characterised by a peak at 100 to 110 Ma. The Triassic population covers the whole Triassic and extends into the Late Permian with a major peak between 230 to 250 Ma. Besides these two main populations, there is a small Late Jurassic peak in sample STB01 whereas this population is absent in STB10. There are a small number of older Paleozoic zircons. The Proterozoic zircon age populations in each sample differ. There is a dominant Proterozoic peak at 600 Ma in sample STB01, a wide peak with varying amplitude is present at 1 to 1.2 Ga in both samples, and a single peak at c. 1.5 Ga in STB01. The oldest Proterozoic zircons are c. 2.4 Ga. Archean zircons are 3 Neoarchean grains and 1 Mesoarchean grain.

The oldest age is 2964 ± 32 Ma (Mesoarchean) in sample STB10. The youngest age is 71 ± 1 Ma (Maastrichtian, Late Cretaceous) in sample STB10 and 73 ± 2 (Campanian, Late Cretaceous) in sample STB01.

Tanjung Santubong

STB48c was sampled from a beach exposure. STB50 was sampled from a large block at the beach (assumed to be very locally derived) and TB167 was sampled from an outcrop near the summit of Gunung Santubong at 607 m above sea level.

A total of 348 concordant U-Pb ages were obtained from 360 zircons (Fig. 9). The zircon age populations are very similar in the three samples, consisting of 297 Phanerozoic, 45 Proterozoic and 6 Archean ages. The Cretaceous population comprises almost the whole Cretaceous with a major peak between 80 and 90 Ma in sample STB50 and around 110 to 130 Ma in STB48c and TB167. There is a significant Permian-Triassic component in the samples with peaks at 210 to 230 Ma and 240 to 260 Ma. Minor zircon populations are Jurassic, with peaks in the Late and Early Jurassic, and there are scattered Paleozoic ages. Prominent Proterozoic peaks are at 1.2 Ga, 1.8 Ga and around 2.4 Ga with the 1.8 Ga peak being the largest.

The oldest age is 2655 ± 20 Ma (Neoarchean) in sample TB167. The youngest age is 44 ± 0.7 Ma (Lutetian, Eocene) in sample TB167. There are no other Eocene or Paleocene zircons in the three samples.

Bungo Range

In the Bungo Range STB20a was sampled at 86 m above sea level, STB21 at 106 m above sea level and TB124b at 240 m above sea level. Sample STB21 was analysed by SHRIMP. The other two samples were analysed using LA-ICP-MS. A total of 213 concordant U-Pb ages were obtained from 221 zircons.

The three samples have very similar zircon age distributions, consisting in total of 199 Phanerozoic, 12 Proterozoic and 2 Archean ages (Fig. 9). The samples are composed almost entirely of Cretaceous zircons, in contrast to other samples of the Kayan Sandstone, with very few non-Cretaceous zircons. The zircons range across almost the whole Cretaceous period with a major peak between 90 and 130 Ma. There are a few Jurassic, Triassic and Permian grains. Only sample STB21 contains Precambrian zircons with 14 grains scattering from around 600 Ma to a single Archean zircon of 3006 ± 10 Ma. The youngest zircon of 62.1 ± 2.2 Ma (Danian, Paleocene) is in STB21. The youngest zircons in samples STB20a and TB124b have significantly older Late Cretaceous ages.

Gunung Serapi

At Gunung Serapi STB18a and STB18b were sampled at 19 m above sea level in the Matang area and TB21 from near the summit of Gunung Serapi at 790 m. A total of 394 concordant U-Pb ages were obtained from 428 zircons.

The zircons include 345 Phanerozoic, 47 Proterozoic and 2 Archean grains (Fig. 9). Again all samples are dominated by Cretaceous zircons covering almost the whole period with a main peak between 80 and 110 Ma. There are minor Jurassic and Permian-Triassic populations with a few scattered Paleozoic ages. All samples contain a few Precambrian zircons ranging from Neoproterozoic to Paleoproterozoic with a peak at 1.2 Ga in STB18b. The oldest age of 2652 ± 70 Ma (Neoarchean) is from TB21. The

youngest age of 50 ± 1 Ma (Ypresian, Eocene) is also from sample TB21. There are no other Eocene or Paleocene zircons and the next youngest grains are Maastrichtian (68 ± 2 Ma) in sample STB18b.

Pueh area

The Kayan Sandstone sample TB89b in the Pueh area was collected at 33 m above sea level. 135 concordant U-Pb ages were obtained from 137 zircons with 133 Phanerozoic and 2 Proterozoic ages (Fig. 9). Like the Bungo Range samples there are mainly Cretaceous zircons with a population in two parts: a younger group from 90 to 100 Ma and an older group from 110 to 130 Ma. A few Jurassic, Triassic, Permian and Proterozoic grains are present. The oldest zircon is 1070 ± 33 Ma and the youngest is 63 ± 1 Ma (Danian, Paleocene) with an age similar to the youngest grain from the Bungo Range.

7.1.2. Penrissen Sandstone

The Penrissen samples were collected from Gunung Penrissen at different stratigraphic levels. TB121 was sampled in an outcrop at 440 m above sea level and TB119 from a large boulder, close to an in situ exposure, at 705 m above sea level near the summit.

A total of 282 concordant U-Pb ages were obtained from 296 zircon grains (Fig. 9). The zircon populations of the two samples are similar. Both have major Cretaceous populations between 90 and 120 Ma, and smaller Jurassic and Triassic populations. TB119 differs from TB121 in larger Eocene and Triassic peaks. There are small numbers of Palaeozoic grains in each sample. Older grains range from early Cambrian into the Precambrian, which scatter from Neoproterozoic to Neoarchean (541 Ma to 2.9 Ga) with a small peak at about 1.2 Ga. The oldest grain is 2870 ± 88 Ma (Mesoarchean) in TB119 and the youngest grains are of similar age at 46.9 ± 0.8 Ma (Lutetian, Eocene) in TB119 and 50.9 ± 0.8 Ma (Ypresian, Eocene) in TB121.

7.2. Ketungau Group

7.2.1. Ngili Sandstone

The Ngili Sandstone were collected at Gunung Ngili at various altitudes from 5 to 40 metres; samples STB75b, STB77 and TB60a were analysed by LA-ICP-MS and STB75 with SHRIMP. The four samples have very similar zircon age distributions which are quite different from other sandstone samples from West Sarawak.

The four samples yielded a total of 407 concordant U-Pb ages, obtained from 392 zircon grains (Fig. 10). There are 356 Phanerozoic, 50 Proterozoic and 1 Archean ages. The majority of U-Pb ages are Permian-Triassic and form a major narrow peak. Three of the samples have a very small number of Cretaceous zircons. There is a small number of Carboniferous to Ordovician zircons and a second minor Phanerozoic peak of Carboniferous-Devonian age. Precambrian zircons have a narrow Paleoproterozoic peak at 1.8 Ga accompanied by widely scattered ages from 1.4 Ga to 2.5 Ga. The youngest age is 85.5 ± 0.9 Ma (Santonian, Late Cretaceous) and the oldest age is 2530 ± 4.6 Ma (Neoarchean).

7.2.2. Silantek Formation

The Silantek Formation was sampled from the Marup Ridge at 75 m above sea level (Marup Sandstone Member, TB210), and from the upper section of the Temudok Ridge at 59 m above sea level (Temudok Sandstone Member, TB218).

Marup Sandstone Member

152 concordant U-Pb ages were obtained from 161 zircons of sample TB210 (Fig. 10) which include 111 Phanerozoic, 38 Proterozoic and 3 Archean ages. The large Cretaceous population comprises the whole Cretaceous with a major peak between 100 and 120 Ma. The whole Jurassic is recorded in the sample, peaking at 150 to 160 Ma. The Permian-Triassic population comprises several sub-peaks, with the strongest between 240 and 260 Ma. There are scattered Paleozoic ages. Proterozoic peaks at 1.2 and 1.8 Ga are accompanied by other Precambrian ages from 541 Ma to around 2.5 Ga and a few early

Cambrian ages. The oldest age is 3243 ± 63 Ma (Paleoarchean) and the youngest is 41.6 ± 0.7 Ma (late Lutetian, Eocene).

Temudok Sandstone Member

166 concordant U-Pb ages were obtained from 178 zircon grains of sample TB218 (Fig. 10). The zircon populations are similar to the Marup Sandstone Member, including 110 Phanerozoic, 55 Proterozoic and 1 Archean ages.

In contrast to the Marup Sandstone Member sample, the Eocene population is missing. The Cretaceous population comprises the whole Cretaceous with a major peak between 90 and 100 Ma. Jurassic ages are recorded throughout the Jurassic with a peak at 180 to 190 Ma. There are populations in the Triassic between 220 and 240 Ma and in the Permian with a small peak between 260 to 280 Ma. There are scattered Paleozoic ages from Carboniferous to Ordovician. The Proterozoic peaks at 1.2 Ga, 1.8 Ga and 2.4 Ga are accompanied by ages between 600 Ma and 2.6 Ga. The oldest age is 2634 ± 35 Ma (Neoarchean) and the youngest is 62 ± 1 Ma (Danian, Paleocene).

7.2.3. Bako-Mintu Sandstone

The Bako-Mintu Sandstone was sampled at different locations. TB144 is from a sea cliff at the northern tip of Tanjung Santubong at c. 114 m above sea level. STB74b was sampled from a boulder derived from the upper part of Gunung Ngili (> 100 m above sea level) and TB171 was sampled from 144 m above sea level in the Mintu area. 379 concordant U-Pb ages were obtained from 399 zircon grains (Fig. 10).

The three samples have similar zircon age distributions including 279 Phanerozoic, 93 Proterozoic and 7 Archean ages. All samples have a small Cenozoic (Eocene to Paleocene) zircon population. The dominant Cretaceous population comprises the whole Cretaceous with major peaks between 80 and 110 Ma in all samples and 120 to 130 Ma in sample TB144. There are two Jurassic peaks, one at 160 to 170 Ma in sample TB144 and the other at 180 to 190 in sample STB74b. There is a Permian-Triassic population between 240 and 260 Ma. There are a few zircons from Carboniferous to Cambrian with a

Silurian-Ordovician peak at 440 Ma. There are a moderate number of Proterozoic ages with Paleoproterozoic peaks at c. 1.8 Ga and c. 2.5 Ga. The oldest age is 3486 ± 10 Ma (Paleoarchean) in sample TB171 and the youngest age is 39.8 ± 0.5 Ma (Bartonian, Eocene) in sample TB171. The other samples yield similar Middle Eocene (c. 41 to 44 Ma) zircon ages.

7.2.4. Tutoop Sandstone

The Tutoop Sandstone samples were collected in the Klingkang Range. STB88 was at 174 m above sea level at Bukit Begunan. STB95 was from a large block at 37 m above sea level below c. 200 m high Gunung Segundang. TB227 was from 470 m above sea level near Bukit Mansul. Samples STB88 and TB227 were dated using LA-ICP-MS and sample STB95 with SHRIMP.

398 concordant U-Pb ages were obtained from 423 zircon grains (Fig. 10) and include 339 Phanerozoic, 58 Proterozoic and 1 Archean ages. There are a small number of Eocene zircons in samples STB88 and TB227. The Cretaceous population comprises the whole Cretaceous with a major peak between 100 and 120 Ma. The Jurassic shows several smaller populations from the Early to Late Jurassic, peaking at 150 to 170 Ma in the two LA-ICP-MS samples. The three samples differ slightly in their Triassic peaks. The Triassic population peaks between 200 and 230 Ma and in the Permo-Triassic between 240 to 250 Ma. There are scattered ages from Carboniferous to Ordovician. Proterozoic ages are scattered from around 541 Ma to 2.5 Ga with weak peaks at 600 Ma and 1.8 Ga and are accompanied by some early Cambrian ages. The oldest age is 2563 ± 40 Ma (Neoarchean) and the youngest age is 51 ± 3 Ma (Ypresian, Paleocene).

8. Discussion

8.1. Stratigraphic subdivision

As summarised above, the Kayan Group includes two formations separated by the Bungo Unconformity (Fig. 3): the Kayan Sandstone and the Penrissen Sandstone which differ significantly in their light and heavy minerals and detrital zircon U-Pb ages.

Within the Kayan Sandstone there are two different groups of zircon ages. Samples from the Kayan Syncline and Tanjung Santubong are dominated by Cretaceous and Triassic, with a moderate proportion of Precambrian, zircons whereas samples from the Bungo Range, Gunung Serapi/Matang and Pueh area contain predominantly Cretaceous zircons, with very few older grains. This can be correlated with the palynology zones of Muller (1968). The Kayan Syncline is part of the *Rugubivesiculites* zone, while the Pueh area and the Bungo Range are part of *Proxapertites* zone.

The Ketungau Group includes 5 formations: the Ngili Sandstone, the Bako-Mintu Sandstone, the Silantek Formation and the Tutoop Sandstone which differ in heavy minerals and detrital zircon ages, plus the Ketungau Formation of Kalimantan. The Ngili Sandstone has zircon ages and heavy mineral assemblages which are completely different from all other formations. Different members of the Silantek Formation show lithological differences observable in the field, but only minor differences in their mineral assemblages and zircon ages. The zircon ages and heavy mineral assemblages from the Bako-Mintu Sandstone resemble the Silantek Formation and it is regarded as a lateral equivalent of the Silantek Formation (Breitfeld et al., 2018). The Tutoop Sandstone is reported to be conformable above the Silantek Formation (e.g. Haile, 1957; Tan, 1979), however there is a small difference in zircon ages between this and both the Silantek Formation and the Bako-Mintu Sandstone (Fig. 10) which may suggest a change in provenance. The environment of deposition also changes from the estuarine-deltaic Silantek Formation to fluvial deposits of the Tutoop Sandstone (Breitfeld et al., 2018). The Tutoop Sandstone could therefore overlie the Silantek Formation, with a parallel unconformity or disconformity representing the Rajang Unconformity on land. Alternatively, the Tutoop Sandstone could be below the Rajang Unconformity and have a conformable contact with the Silantek Formation which is the preferred stratigraphic interpretation shown in Fig. 3.

8.2. Age of deposition

Fig. 11 summarises the maximum depositional ages (MDA) of the Kuching Supergroup formations and correlates them with interpreted equivalents in the deep marine Rajang Group (Galin et al., 2017),

based on heavy mineral assemblages and detrital zircon ages, with stratigraphic ages partly based on palaeontological data reviewed by Liechti et al. (1960).

8.2.1. Kayan Group

The maximum depositional age (MDA) for the Kayan Sandstone in the Kayan Syncline is c. 71 to 73 Ma (Maastrichtian to Campanian) based on zircons in samples STB01 and STB10. This age is similar to that indicated by palynology for the *Rugubivesiculites* zone of the Kayan Sandstone (Muller, 1968; Morley, 1998). There are no palynology data for the Kayan Sandstone at Tanjung Santubong. The zircon age populations resemble those from the Kayan Syncline. Sample STB50 has Maastrichtian to Campanian zircons with an MDA of c. 71 Ma. TB167 is similar but contains a single grain of 44 ± 0.7 Ma (Lutetian) although the next youngest grain is 76 ± 1 Ma (Campanian). Extension of the Kayan Sandstone into the Middle Eocene is not likely, based on age data from the overlying Penrissen Sandstone and the Ketungau Group. We therefore interpret the single Eocene age as affected by lead-loss and disregard it for MDA interpretation and consider the succession at Tanjung Santubong as part of the *Rugubivesiculites* zone with an MDA of c. 71 Ma similar to the Kayan Syncline.

The MDA of the Kayan Sandstone in the Pueh area and at the Bungo Range is c. 62 to 63 Ma (Danian) based on zircons in samples STB21 and TB89b. This age corresponds to the Paleocene *Proxapertites* zone (Muller, 1968; Morley, 1998). The MDA of the Kayan Sandstone at the base of Gunung Serapi in the Matang area is interpreted to be c. 68 to 70 Ma (Maastrichtian) based on zircons in samples STB18a and STB18b. Sample TB21 from near the summit of Gunung Serapi has one younger grain of 50 ± 1 Ma (Ypresian). It is located close to the contact of a Miocene dyke (Schmidkte et al., 1990) and could have been reset to a younger age. However, the sample was collected much higher (790 m above sea level) than the other two samples and alternatively could indicate an extension of the Kayan Sandstone at Gunung Serapi into the Ypresian.

The Penrissen Sandstone samples contain a number of Eocene zircons with ages between 47 to 52 Ma and an MDA of c. 47 Ma (Ypresian). This corresponds to the Early Eocene age suggested by Muller

(1968) and Morley (1998) for the *Retitriporites variabilis* zone (which is included in the Penrissen Sandstone) based on palynology data.

8.2.2. Ketungau Group

The age of deposition of the Ngili Sandstone is uncertain. Most samples contain a few Cretaceous grains indicating an MDA of c. 85 Ma (Santonian) but an age as young as Middle Eocene age (? early Lutetian) is possible since the formation is overlain by the Middle to Upper Eocene Bako-Mintu Sandstone (see below).

The MDA of the Silantek Formation is c. 42 Ma (Lutetian) from TB210 (Marup Sandstone Member), an age which is consistent with foraminifera ages for the lowermost part of the Marup Sandstone Member (Tan, 1979; Breitfeld et al., 2018). The Temudok Sandstone Member overlies the Marup Sandstone Member and therefore the MDA is Middle Eocene or younger but no zircons close to the depositional age were obtained.

The MDA of the Bako-Mintu Sandstone is c. 40 to 43 Ma (Bartonian to Lutetian), based on several zircons in samples STB74b, TB144 and TB171. The Bako-Mintu Sandstone is therefore considered a lateral equivalent of the Silantek Formation with a Middle to Late Eocene age as suggested by Breitfeld et al. (2018).

The age of deposition of the Tutoop Sandstone is uncertain. The youngest grain of 51 ± 3 Ma is significantly older than the youngest zircons from the underlying Silantek Formation and Bako-Mintu Sandstone. The youngest grain from the underlying formations is 39.8 ± 0.5 Ma providing the MDA of the Tutoop Sandstone and a Bartonian to Priabonian (late Middle to Late Eocene) depositional age is interpreted.

8.3. Sedimentary basin development in the latest Cretaceous to early Cenozoic

Paleo-Pacific subduction terminated at c. 80 to 86 Ma (Breitfeld et al., 2017; Hennig et al., 2017a) and the regional Pedawan unconformity (Fig. 3) marks collision and initiation of uplift (Breitfeld et al. 2018). Large areas that previously formed Triassic to Cretaceous forearc basins (Sadong/Kuching

Formation, Pedawan/Selangkai Formation) or consisted of Mesozoic melanges (Lubok Antu/Boyan Melange) were the basement for new sedimentary basins. In West Sarawak, the Maastrichtian to Lower Eocene Kayan Basin and its remnants is the oldest fluvial/marginal marine basin above the Pedawan Unconformity. The Ketungau Basin formed in the late Middle Eocene. In NW Kalimantan, the Melawi and Mandai Basins are lateral equivalents of the West Sarawak basins.

The Kayan Sandstone in the Kayan Syncline and Tanjung Santubong is about 800 m thick, which results in a minimum depositional rate of c. 130 m/Ma, assuming deposition took place between c. 65 to 71 Ma. At Gunung Serapi and the Bungo Range, it is approximately 1000 m thick, which results in a minimum depositional rate of c. 80 m/Ma, assuming deposition between 51 to 63 Ma. If the 51 Ma zircon is disregarded, deposition took place between 63 to 66 Ma, which results in a minimum depositional rate of c. 330 m/Ma. However, an erosional surface marks the top of the Kayan Sandstone in many places and a significant thickness may have been removed. Therefore, the real depositional rates for the two members might be much higher. The Penrissen Sandstone is approximately 2000 m thick, which results in a minimum depositional rate of 400 m/Ma, assuming deposition between 52 to 47 Ma. This increase in deposited material within the Kayan Group may reflect a pulse linked to a tectonic event. The whole Ketungau Group is approximately 4000 to 8000 m thick, which results in minimum depositional rates from 400 m/Ma up to more than 800 m/Ma, assuming deposition between 44 to 34 Ma. The lower part of the Silantek Formation may also indicate a major sedimentation pulse. The Marup Sandstone is predominantly medium to coarse grained with conglomerate beds (Tan, 1979; Breitfeld et al., 2018). Soft-sediment deformation within the succession indicates high deposition rates (Breitfeld et al., 2018). No depositional rates for the Ngili Sandstone can be estimated.

The uplift of SW Borneo and West Borneo on land was potentially compensated by subsidence of present-day Central Sarawak (Sibu Zone) and development of a deep marine basin in which the Rajang Group was deposited. The Lupar Line is approximately at the position of the shelf edge, separating the largely terrestrial sedimentary rocks south of the Lupar Line from the contemporaneous deep-water

equivalents north of it. Galin et al. (2017) reported abundant deformation features such as slump-folds within the Rajang Group and interpreted them as mainly syn-depositional, and low grade metamorphism and development of schistosity to be related to burial depth. In contrast, the Kuching Supergroup is not metamorphosed and bedding is predominantly horizontal or dips at low angles associated with large broad synclines (Breitfeld et al., 2018).

8.4. Kuching Zone – Sibu Zone provenance similarities

The deep water sediments of the Rajang Group (Sibu Zone) and the largely terrestrial/marginal marine sediments of the Kuching Supergroup (Kuching Zone) are of similar age and share many features and suggest the two zones were part of the same depositional system.

Light and heavy mineral data, as well as zircon U-Pb ages for the Rajang Group were presented by Galin et al. (2017) and can be compared with the results of this study. The zircon U-Pb age populations have distinctive patterns over time which are similar in both Kuching and Sibu Zones. Fig. 12 shows the Kayan Sandstone and Rajang Group Unit 1 of Galin et al. (2017). The Kayan Sandstone of Tanjung Santubong closely resembles the lowest part of Unit 1 (Lupar Formation). Both are dominated by Cretaceous and Permian-Triassic zircon ages, and Precambrian zircons are subordinate with populations at c. 1.8 Ga and c. 2.5 Ga. Higher in the succession, zircon ages of the Kayan Sandstone in the Kayan Syncline are very similar to those from the upper part of Rajang Unit 1, still dominated by Cretaceous and Permian-Triassic zircons, but with an increase in the number of Precambrian zircons with age peaks at c. 500 Ma, 1.2 Ga, 1.6 Ga and 2.5 Ga. The populations at 1.8 Ga are either much smaller (Rajang Group Unit 1) or absent (Kayan Sandstone/Kayan Syncline).

Continuing up-section the Paleocene to ?Lower Eocene Rajang Group Unit 2 and the Kayan Sandstone of the Bungo Range, Pueh area and Gunung Serapi/Matang are dominated by Cretaceous zircons (Fig. 13). The number of early Mesozoic, Paleozoic and Precambrian zircons is small; in both groups there is a small age peak at 1.8 Ga.

The best match of the Kuching Supergroup and the Rajang Group can be found in the upper Middle Eocene successions. The zircon ages of the Silantek Formation and Bako-Mintu Sandstone are almost identical to those of Rajang Unit 3 (Fig. 13) with abundant Phanerozoic and Precambrian grains. The Phanerozoic zircons include a few Eocene ages, a broad Cretaceous age peak, a Late Jurassic peak, a very broad Permian-Triassic age peak and an Ordovician to Early Devonian peak. Precambrian age populations comprise of two narrow age peaks at c. 1.8 Ga and 2.5 Ga and a very broad age peak from c. 700 Ma to 1.2 Ga. The Tutoop Sandstone shows similar zircon age populations with some small variations (Fig. 13) which could reflect reworking or additional sources.

Fig. 14 displays a multi-dimensional (MDS) plot of the zircon ages (Vermeesch et al., 2016) of the Kuching Supergroup, the Rajang Group sediments and three potential source areas (Schwaner Mountains of SW Borneo, Malay-Thai Tin Belt, West Borneo), supporting the similarities, differences and correlations described above. This approach is based on the Kolmogorov–Smirnov effect size, which groups samples with similar age spectra together, while samples with different spectra plot farther apart. The Upper Eocene Tutoop Sandstone and the Lower Eocene Penrissen Sandstone have similar zircon populations, which are also similar to the Lupar Formation and the Kayan Sandstone at Santubong. This could indicate reworking of the older deposits.

The compositionally immature Penrissen Sandstone is different from the time-equivalent Unit 2 of the Rajang Group (Fig. 13). It has a significant Permian-Triassic population of zircons as well as Eocene and Jurassic zircons; Precambrian zircons also lack the strong 1.8 Ga peak of Unit 2. It is more similar to Unit 3 of the Rajang Group (Fig. 13), although lacking the small lower Paleozoic peak, and has fewer Precambrian zircons and lacks the strong 1.8 and 2.5 Ga peak. It is very similar to the Tutoop Sandstone (Fig. 13 and Fig. 14). This could indicate a lack of connection of the Kuching and Sibu Zones during deposition of the Penrissen Sandstone.

There is no Rajang Group equivalent of the Middle Eocene Ngili Sandstone (Fig. 11) which has zircon ages very different from all other formations. It contains almost entirely Permian-Triassic and some

Paleoproterozoic zircons, which require a source with a very limited age range. The zircon ages closely resemble those from the (meta-) sedimentary Triassic Sadong and Kuching Formations to the west with a bimodal Permo-Triassic and Paleoproterozoic signature (Breitfeld et al., 2017). Permian-Triassic zircons could also be derived from Triassic (meta-) granitoids or their eruptive equivalents (e.g. the Jagoi intrusion or meta-granitoids SE of Pontianak) reported to the southwest (Setiawan et al., 2013; Breitfeld et al., 2017; Hennig et al., 2017a). It therefore might be a very limited deposit by a local river system isolated from the main drainage system. This could explain the missing deep water equivalent in the Sibu Zone.

Overall the U-Pb zircon ages and heavy mineral assemblages show similar patterns for the Sibu and Kuching Zones and indicate that the Rajang Group is the deeper marine equivalent of the Kuching Supergroup. Although these signatures are very similar, it is noteworthy that the MDA ranges for the Paleocene to Middle Eocene successions show an offset, suggesting a diachronous character (Fig. 11). Rajang Group Unit 2, dominated by Cretaceous zircons, has a MDA range from c. 55 to 40 Ma, while its onshore equivalent part of the Kayan Sandstone shows a range from 64 to 61 Ma or possibly 51 Ma. The Layar Member and Lupar Formation of the Rajang Group Unit 1 have a MDA range from c. 76 to 69 Ma, similar to part of the Kayan Sandstone of the Kayan Syncline. The lower Kapit Member, also part of Unit 1, however extends the MDA up to c. 58 or 51 Ma.

Heavy minerals are mostly dominated by ultra-stable varieties, such as zircon, tourmaline and rutile. Fig. 15 displays the most common heavy minerals and their abundance in the Kuching Supergroup and the Rajang Group. There are some similarities that support the zircon age data. The Kayan Sandstone at Santubong and in the Kayan Syncline is comparable to Unit 1 of the Rajang Group in having a similar percentage in zircon. Up sequence the amount of zircon increases in Unit 2 and in the Kayan Sandstone at the Bungo Range, Gunung Serapi and in the Pueh area. The youngest part of the Rajang Group, Unit 3, shows a decrease in zircon abundance similar to the Silantek Formation and the Bako-Mintu Sandstone of the Kuching Zone. However, there are some differences, including greater heavy mineral diversity and the larger abundance of rutile in the Kuching Supergroup. In the Rajang Group heavy

mineral diversity is lower and the dominant heavy minerals are usually only zircon and tourmaline. This could reflect hydraulic sorting and breakdown of unstable heavy minerals during storage/transport into the deeper parts of the basin or indicate multiple recycling phases before deposition in the deeper parts of the basin. The lower abundance of rutile in the Rajang Group is difficult to interpret. Rutile has generally comparable density to zircon, but can exceed it with increased trace element contents (Deer et al., 1982; Mange and Maurer, 1992) which could therefore account for hydraulic sorting. Alternatively, our study may indicate that rutile is less stable in tropical environments than previously assumed.

Light mineral data shows compositional maturity and textural immaturity for sandstones from both zones. Feldspar is generally more abundant in the Rajang Group (Galin et al., 2017), which might be related to breakdown of feldspar in the Kuching Supergroup due to acid groundwater.

8.5. Sources for the sediments

Most of the samples from the Kuching Supergroup are quartz-dominated, with various lithic fragments and rare feldspar. The conventional QFL/QmFLt provenance diagrams suggest a quartzose to transitional recycled orogenic provenance (Fig. 5c, d, g and h). Feldspar dissolution and breakdown of unstable lithic fragments during transport, erosion or storage of sand in a humid tropical environment (Suttner et al., 1981; Johnsson et al., 1988; Smyth et al., 2008; van Hattum et al., 2013) may have altered the original composition significantly. Volcanic quartz and volcanic-derived lithic fragments indicate volcaniclastic input. Only the provenance of the Ngili Sandstone, which is composed mainly of polycrystalline quartz which was derived from a metamorphic source, can be established from the light mineral fraction. For all other formations a multi-method approach is needed to assess the provenance.

The heavy mineral assemblages in most of the clastic sediments from this study in West Sarawak are compositionally very similar. They are dominated by the ultra-stable heavy minerals zircon, tourmaline and rutile in different proportions, reflecting significant alteration of the original assemblage by deep

burial or acid dissolution (Morton, 1984; Mange and Maurer, 1992; Morton and Hallsworth, 1994). Generally, the heavy mineral assemblages and textures indicate acid igneous input with reworking of older sediments as the main sources. Ultrabasic to basic igneous and metamorphic input is present in low abundance, but present throughout the formations. Hypersthene in the Kayan Group sediments indicates volcanic input throughout the succession. Only the heavy mineral assemblage of the Penrissen Sandstone, which includes abundant less stable or unstable heavy minerals, including apatite, garnet, epidote and titanite, has not been changed by post-depositional processes.

Zircon grain shapes in the Kayan Sandstone indicate reworking in samples in the Kayan Syncline and Tanjung Santubong, but only very minor reworking of older sediments in the Bungo Range, Pueh area and Gunung Serapi. The Penrissen Sandstone has a very immature heavy mineral assemblage and a wide range of different heavy minerals. Abundant apatite, which is sensitive to chemical weathering, may indicate that the Penrissen Sandstone has not experienced similar acid weathering that affected most of the other formations in which apatite is rare. The Ngili Sandstone samples have a very low abundance of tourmaline, not a feature in other samples, which may reflect hydraulic sorting, potentially in a very high energy environment, or a different source.

The different zircon age populations vary. Most important are the Cretaceous and Triassic age peaks, indicating input from at least two source regions for many samples. Sandstones from the Bungo Range, Pueh area and Gunung Serapi of the Kayan Sandstone are dominated by Cretaceous zircons and have few Precambrian zircons indicating only one source. Paleogene zircons in some samples indicate contemporaneous magmatic activity. Precambrian populations are variable but are usually linked to abundant Permian-Triassic zircons. Source regions for zircons of the Rajang Group have been discussed in detail in Galin (2017). We interpret the Kuching Supergroup to be the onshore terrestrial equivalent of the Rajang Group submarine fan with the same provenance. Fig. 16 displays the principal blocks of the region in the Latest Cretaceous to Eocene that could be potential source regions.

8.5.1. Paleogene zircons

The youngest zircons observed in the samples cluster around 41 Ma (39-44 Ma) and around 50 Ma (47-52 Ma). They represent (almost) contemporaneous magmatic activity. These zircon ages are similar to the youngest zircons reported by Galin et al. (2017) from the Rajang Group. K-Ar ages reported by Pieters et al. (1987) and Bladon et al. (1989) for the Muller Volcanics (c. 41 Ma), Piyabung Volcanics (c. 50 Ma) and Nyaan Volcanics (c. 49 Ma) in Kalimantan are similar to the zircon ages. The Muller Volcanics are located in the Mandai Basin where they form part of the base of the Eocene sedimentary succession (Pieters et al., 1987). The Piyabung Volcanincs are adjacent to the Melawi and Mandai Basins, and the Nyaan Volcanics are located further to the east in the Kutai Basin (Pieters et al., 1987). They suggest that localised nearby (c. 50-200 km) magmatism is the most likely source of the Paleogene zircons. The low abundance of these zircons suggests only minor activity and the overall mature mineral assemblage of the sediments does not support prolonged active margin magmatism resulting from subduction. A similar interpretation was given by Galin et al. (2017) for the Rajang Group.

8.5.2. Cretaceous zircons

The Schwaner Mountains c. 200-400 km to the south of the research area are interpreted as an important source for Cretaceous material (Fig. 16). Cretaceous igneous rocks in the Schwaner Mountains were dated with the K-Ar method (e.g. Haile et al., 1977; Bladon et al., 1989). Cretaceous zircons have since been reported from the Schwaner granites and the Pinoh Metamorphics from SW Borneo by Davies et al. (2014) and for the Northwest Schwaner Zone (NWSZ) by Hennig et al. (2017a). Ages range from 70 to 140 Ma.

A distinctive characteristic of the Schwaner region in SW Borneo is the low abundance of non-Cretaceous zircons; Palaeozoic and Precambrian zircons are almost entirely absent. This suggests that sediments that contain predominantly Cretaceous zircons are likely derived from this area (Fig. 14). Additional possible sources for some Late Cretaceous zircons are post-collisional granites with K-Ar

ages of 70 to 80 Ma in NW Kalimantan (Williams et al., 1988) and similar zircon ages for post-collisional granites in West Borneo (Hennig et al., 2017a). Zircons with these ages are not abundant in the Kuching Supergroup which suggests that these granites or their volcanic equivalents (e.g. Pueh, Gading) were not widely exposed at the time of deposition.

Other Cretaceous granite provinces in the region (Fig. 16) that could have contributed to the sediments are in the Malay Peninsula (Searle et al., 2012) and SE Vietnam (Nguyen et al., 2004; Shellnutt et al., 2013; Hennig et al., 2017b). However, both would require significantly greater transport distances of up to 1000 to 2000 km. Furthermore, Cretaceous ages from the Malay-Thai Tin Belt are c. 80 to 95 Ma (e.g. Searle et al., 2012) and cannot account for the wide range of Cretaceous ages observed.

8.5.3. Jurassic zircons

There are two Jurassic igneous plutons in SW Borneo (Haile et al., 1977; Davies, 2013) interpreted to indicate igneous activity during separation of SW Borneo from Gondwana in the Jurassic. Jurassic zircons with similar ages were reported by Zimmermann and Hall (2016) from West Timor and by Hennig et al. (2016) from NW Sulawesi and were related to rifting of blocks from Australia (Hall, 2012). Hennig et al. (2017a) reported Jurassic magmatism from West Borneo in part of Indochina-East Malaya, a zone that has been interpreted (Breitfeld et al., 2017; Hennig et al., 2017a) as a long-lived Mesozoic subduction margin of the Paleo-Pacific. Breitfeld et al. (2017) reported Jurassic zircons from this active margin in the Cretaceous Pedawan Formation that underlies the Kuching Supergroup, and reworking of the Pedawan Formation is indicated by a basal conglomerate in the Kayan Sandstone (Breitfeld et al., 2018).

A significant Jurassic igneous province outside Borneo is the Khorat Plateau in eastern Thailand and Laos. Clastic terrestrial sediments of Mesozoic age yielded a significant number of Jurassic zircons (Carter & Moss, 1999). Clements et al. (2011) suggested a much greater extent of the Khorat continental basin to the south into the Malay Peninsula, which has now been largely eroded. There

are poorly dated probable Jurassic volcanic rocks in the Tembeling Group (Koopmans, 1968; Hutchison, 1989; Abdullah, 2009) of the Malay Peninsula. This basin could have supplied material to Sarawak, either reworked from Thailand or from the Malay Peninsula.

8.5.4. Permian-Triassic

Triassic zircons have been reported from Triassic granitoids and sediments in West Borneo (Setiawan et al., 2013; Breitfeld et al., 2017; Hennig et al., 2017a) and in the Cretaceous Pedawan Formation of West Sarawak (Breitfeld et al., 2017), which could indicate a nearby source in West Borneo. The Malay-Thai Tin Belt of East Malaya is potentially an important source. Permian-Triassic ages have been reported by e.g. the Rb-Sr and K-Ar methods by Bignell & Snelling (1977), Darbyshire (1988), Cobbing et al. (1992) and by zircon U-Pb geochronology by Liew & Page (1985), Sevastjanova et al. (2011), Searle et al. (2012) and Oliver et al., (2014). Zircon data from these areas is displayed in the MSD plot (Fig. 14).

Permian-Triassic zircons are also known from Indochina and the Cathaysia block in SE China, although these are much more distant possibilities. Possible sources include the Kontum Massif in Vietnam (Hieu et al., 2015), Hainan (Li et al., 2006; Jiang et al., 2015; Yan et al., 2017) and northern Vietnam-Laos-SE China (Shu et al., 2008; Halpin et al., 2016; Wang et al., 2016). Hennig et al. (2018) reported significant amounts of Permian-Triassic zircons in the Neogene Proto-Mekong deposits and concluded their origin was in northern Indochina or South China.

8.5.5. Lower Paleozoic zircons

The relatively small numbers of lower Paleozoic zircons (e.g. Silantek Formation and Bako-Mintu Sandstone; Fig. 13) have no obvious nearby sources. Chen et al. (2017) reported U-Pb zircon ages of c. 440 Ma with Triassic and c. 1.0 Ga zircons from the Yunkai Massif (SE China). Xianhua et al. (1989) dated the Tanghu Granite in southeast China at c. 435 Ma. Carter and Moss (1999) reported similar zircons of c. 440 Ma from the Khorat Group. Additionally, Permian-Triassic and Precambrian zircons of c. 750 Ma, 1.8 Ga and 2.5 Ga in the Khorat Group (Carter and Moss, 1999) have similarities to the

Kuching Supergroup and the Rajang Group. Ordovician-Silurian zircons in the Proto-Mekong sediments were also interpreted to be derived from northern Indochina and southern South China (Hennig et al., 2018). Detrital Ordovician zircons have been reported from Laos (Indochina) by Burrett et al. (2014), by Sevastjanova et al. (2011) and Basori et al. (2018) from the East Malaya terrane, and by Cai et al. (2017) from the Sibumasu terrane in Myanmar. These ages suggest that recycling of material from SE China and/or Indochina, East Malaya and Sibumasu is a possible source for lower Paleozoic zircons.

8.5.6. Precambrian zircons

Breitfeld et al. (2017) reported abundant c. 1.8 Ga and 2.5 Ga zircons in the Triassic Sadong and Kuching Formations from West Sarawak. In the sandstones analysed in this study these ages are common and could indicate either reworking of older sediments or similar sources. A limited number of Precambrian zircons with these age peaks have also been reported from the Malay Peninsula (Sevastjanova et al., 2011) and they are more abundant in the Khorat Group of Indochina (Carter & Moss, 1999), in SE Vietnam (Hennig et al., 2018) and in SE China (Liu et al., 2009a; Chen and Xing, 2013; Chen et al., 2016).

Neoproterozoic zircons with ages of c. 800-850 Ma are reported from the Cathaysia Block of SE China by Li et al. (2005) but are more common in the Yangtze Block (e.g. Li, 1999; Wang et al., 2012; Ma et al., 2016).

Zircons with ages of 500 Ma and 1.2 Ga, which are common in the Sarawak sandstones, are not known or rare in Indochina and SE China. Galin et al. (2017) suggested a potential Sibumasu source for zircons of these ages in the Rajang Group based on Hall and Sevastjanova (2012). Zircon ages of c. 500 Ma from Sibumasu have been reported by Song et al. (2007) and from Tengchong-Baoshan (northern Sibumasu) by Liu et al. (2009b) and Lin et al. (2013). They are also common in Cenozoic sediments of Sumatra (Liebermann et al., 2017), which is part of Sibumasu. Zircons of c. 1.2 Ga have been reported

so far only from West Java, which was part of the SW Borneo block (Clements and Hall, 2011; Clements et al., 2012), East Java (Smyth et al., 2007) and Thailand (Burrett et al., 2014; Arboit et al., 2016).

8.6. Reconstruction

The Kuching Zone Supergroup is interpreted here to be the onshore equivalent of the deep marine Rajang Group. Termination of Paleo-Pacific subduction at about 90-80 Ma (Breitfeld et al., 2017; Hennig et al., 2017) resulted in uplift of southern Borneo and the development of large terrestrial basins in present-day NW Kalimantan and West Sarawak and a deep marine basin in Central Sarawak between the latest Cretaceous (Maastrichtian) and Late Eocene (Priabonian).

Haile (1974) suggested large scale strike-slip faulting associated with upper Paleogene successions that could account for pull-apart basins. The Ketungau Basin in particular is bounded by the linear feature of the Lupar Line to the north and the Semitau ridge fault to the south and can be interpreted as a pull-apart basin. Palaeocurrents reported by Breitfeld et al. (2018) are similar to the present-day Batang Lupar, suggesting a proto-Lupar River and strike-slip movement along the Lupar Line at the time of deposition. Counter-clockwise rotation of Borneo (e.g. Schmidtke et al., 1990) might be associated with large-scale strike-slip fault systems, such as the Lupar Line, that are responsible for pull-apart basin development. Fuller et al. (1999) interpreted CCW rotation of c. 40 degrees of Mesozoic rocks which occurred after 80 Ma and before the Neogene.

Galin et al. (2017) identified the Rajang Group as deposits of a submarine fan similar in size to some modern river fans like the Amazonas or the Mississippi. The large volume of sediment in the Rajang Group and Kuching Supergroup requires a large catchment area and the relative positions of the terrestrial basins and deep water fan imply sediment sources to the west and south. The river systems that fed the Melawi, Kayan and Ketungau Basins must have been active from the Maastrichtian onwards until the Late Eocene. Palaeocurrent data presented by Tan (1984) and Breitfeld et al. (2018) suggest a predominantly southern source for all sediments. The heavy minerals and zircon ages suggest drainage of West Borneo, SW Borneo, the East Malaya block, and possibly Sumatra, with

reworking of sediment from Sibumasu and Indochina. The Rajang Group presents the submarine fan beyond the outer shelf or shelf break of this depositional system.

None of the present-day active fluvial systems in Borneo are of similar size, but the bathymetry of the Sunda Shelf suggests much larger rivers (e.g. Molengraaff and North Sunda river system) may have drained the region from Sumatra to the South China Sea, and Thailand-Indochina to offshore Sarawak, during glacial lowstands (e.g. Dickerson, 1941; Kuenen, 1950; Voris, 2000). Fig. 16 illustrates the catchment area of the fluvial system and the paleogeography of SE Asia with potential source regions. Inferred rivers are quite similar in size to Late Pleistocene rivers of SE Asia. As indicated by the detrital zircon results rivers must have drained back from SW Borneo into the Malay Peninsula, and possibly Sibumasu and Indochina in the latest Cretaceous to Late Paleocene/Early Eocene and in the Middle to Late Eocene. Drainage in the Late Paleocene to Early/Middle Eocene seems to have been restricted to SW Borneo. This fluvial system was in the position of the present-day Sungai Sarawak and predated the Molengraaff River as the major north-eastwards directed drainage system of eastern Sundaland. We suggest it to be named proto-Sungai Sarawak. The shape of the submarine fan and slight variations in provenance signature suggest an eastward-draining river system to the east of the Kuching Zone during deposition of the Rajang Group (Fig. 16). With the onset of subduction of the Proto-South China Sea beneath Sabah from the Late Eocene and during the Oligocene, the drainage patterns in Borneo changed drastically. The Kuching Supergroup and the Rajang Group depositional systems terminated. The Miri Zone and western Sabah (Crocker fan) formed the main depocenter for sediments in the Oligocene to Miocene in northern Borneo. No deposition occurred in the Kuching Zone, which suggests that the area may have been uplifted during this time. The shelf break and coastline that previously were close to the position of the present-day Lupar Line (Breitfeld et al., 2018), shifted northwards into the Miri Zone.

9. Conclusions

The terrestrial sediments of the Kuching Supergroup have a granitic, metamorphic and reworked sediment provenance with a minor contribution from ultrabasic and basic igneous rocks. Material was mainly derived from the south (SW Borneo, West Borneo province) and west (Malay Peninsula), and probably recycled from Indochina–East Malaya and a previously larger Khorat Basin. The inferred river systems drained a large region to the south and west during most of the history of the Kuching Supergroup, but were partly restricted to SW Borneo in the Paleocene to Middle Eocene. The younger Ketungau Group sediments are compositionally more mature than the older Kayan Group and their zircon age populations are the most diverse. This suggests that the Kayan Group sediments were potentially reworked into the Ketungau Group, especially the Tutoop Sandstone. Very limited volcanic input into the sediments indicates some contemporaneous magmatism but the scarcity of Late Cretaceous to Eocene zircons indicates that this was very minor. The new observations are inconsistent with models suggesting the Sibu Zone was the source of sediments for a Kuching Zone forearc basin and provide no support for subduction magmatism or a forearc setting. Field observations, heavy minerals and U-Pb zircon age data identify a large depositional system passing from Kuching Zone alluvial fans, fluvial channels, deltas and floodplain environment into Sibu Zone submarine fan deposits. The terrestrial Kuching Supergroup sediments can be correlated with deep marine Rajang Group sediments based on similar U-Pb detrital zircon ages and heavy mineral assemblages. The Kuching Supergroup formations tend to be slightly older than their inferred Rajang Group equivalents consistent with progradation of sediments into the offshore region beyond the Lupar Line which is suggested to be an important strike-slip zone at the shelf edge. The Kuching Supergroup and Rajang Group depositional systems terminated in the Late Eocene during plate reorganisation as new subduction zones developed around SE Asia (Hall, 2012; Hall and Sevastjanova, 2012). Subduction of the Proto-South China Sea beneath northern Borneo began, accompanied by uplift of the Kuching and Sibu Zones in Sarawak (Hall and Breitfeld, 2017).

Acknowledgements

This project was funded by the SE Asia Research Group of Royal Holloway University of London, which is supported by a consortium of oil companies. The Economic Planning Unit of Malaysia and the State Planning Unit of Malaysia made the fieldwork possible, and the Mineral and Geoscience Department Malaysia, Sarawak assisted in the field and with logistics. Richard Mani Banda is especially thanked. Thomson Galin is thanked for his contribution in and off the field. We thank Juliane Hennig for helpful discussions that improved the manuscript, Martin Rittner and Andy Carter (UCL/Birkbeck College) for help and support with the LA-ICP-MS dating. Cathodoluminescence imaging was aided by Andy Beard (UCL/Birkbeck College) and Dominique Tanner (now University of Wollongong). Fernando Bea and Pilar Montero (IBERSIMS, University of Granada) are thanked for the SHRIMP dating and data calculation for three SHRIMP samples. Inga Sevastjanova (Getech Group) is thanked for help with the SHRIMP samples. Reviewers Mike Cottam, Chris Morley and an anonymous reviewer are thanked for their valuable input that improved figures and the text.

References

Abdullah, N.T., 2009. Mesozoic stratigraphy. In: Hutchison, C.S. and Tan, D.N.K. (Eds.), Geology of Peninsular Malaysia. University of Malaya and Geol. Soc. Malaysia, 87-131.

Andersen, T., 2002. Correction of common lead in U–Pb analyses that do not report 204 Pb. Chemical Geology 192, 59-79.

Arboit, F., Collins, A.S., Morley, C.K., King, R., Amrouch, K., 2016. Detrital zircon analysis of the southwest Indochina terrane, central Thailand: Unravelling the Indosinian orogeny. Geological Society of America Bulletin 128, 1024-1043.

Basori, M.B.I., Leman, M.S., Zaw, K., Meffre, S., Large, R.R., Mohamed, K.R., Makoundi, C., Mohd Zin, M., 2018. Implications of U–Pb detrital zircon geochronology analysis for the depositional age, provenance, and tectonic setting of continental Mesozoic formations in the East Malaya Terrane, Peninsular Malaysia. Geological Journal. 2018; 1-10.

Bignell, J.D., Snelling, N.J., 1977. K-Ar ages on some basic igneous rocks from peninsular Malaysia and Thailand. Bulletin of the Geological Society of Malaysia 8, 89-93.

Black, L.P., Kamo, S.L., Allen, C.M., Aleinikoff, J.N., Davis, D.W., Korsch, R.J., Foudoulis, C., 2003. TEMORA 1: a new zircon standard for Phanerozoic U–Pb geochronology. Chemical Geology 200, 155-170.

Bladon, G.M., Pieters, P.E., Supriatna, S., 1989. Catalogue of isotopic ages commissioned by the Indonesia-Australia Geological Mapping Project for igneous and metamorphic rocks in Kalimantan, Preliminary Report. Geological Research and Development Centre, Bandung.

Breitfeld, H.T., Hall, R., Galin, T., BouDagher-Fadel, M.K., 2018. Unravelling the stratigraphy and sedimentation history of the uppermost Cretaceous to Eocene sediments of the Kuching Zone in West Sarawak (Malaysia), Borneo. Journal of Asian Earth Sciences 160, 200-223.

Breitfeld, H.T., Hall, R., Galin, T., Forster, M.A., BouDagher-Fadel, M.K., 2017. A Triassic to Cretaceous Sundaland–Pacific subduction margin in West Sarawak, Borneo. Tectonophysics 694, 35-56.

Burrett, C., Zaw, K., Meffre, S., Lai, C.K., Khositanont, S., Chaodumrong, P., Udchachon, M., Ekins, S.,

Halpin, J., 2014. The configuration of Greater Gondwana—evidence from LA ICPMS, U–Pb geochronology of detrital zircons from the Palaeozoic and Mesozoic of Southeast Asia and China. Gondwana Research 26, 31-51.

Cai, F., Ding, L., Yao, W., Laskowski, A.K., Xu, Q., Zhang, J.e., Sein, K., 2017. Provenance and tectonic evolution of Lower Paleozoic–Upper Mesozoic strata from Sibumasu terrane, Myanmar. Gondwana Research 41, 325-336.

Carter, A., Moss, S.J., 1999. Combined detrital-zircon fission-track and U-Pb dating: A new approach to understanding hinterland evolution. Geology 27, 235–238.

Chen, C.-H., Liu, Y.-H., Lee, C.-Y., Sano, Y., Zhou, H.-W., Xiang, H., Takahata, N., 2017. The Triassic reworking of the Yunkai massif (South China): EMP monazite and U-Pb zircon geochronologic evidence. Tectonophysics 694, 1-22.

Chen, Z.-H., Xing, G.-F., 2013. Petrogenesis of a Palaeoproterozoic S-type granite, central Wuyishan terrane, SE China: implications for early crustal evolution of the Cathaysia Block. International Geology Review 55, 1445-1461.

Chen, Z.-H., Xing, G.-F., Zhao, X.-L., 2016. Palaeoproterozoic A-type magmatism in northern Wuyishan terrane, Southeast China: petrogenesis and tectonic implications. International Geology Review 58, 773-786.

Claoué-Long, J.C., Compston, W., Roberts, J., Fanning, C.M., 1995. Two Carboniferous ages: a comparison of SHRIMP zircon dating with conventional zircon ages and 40Ar/39Ar analysis. In: Berggren, W.A., Kent, D.V., Aubry, M.P., Hardenbol, J. (Eds.), Geochronology Time Scales and Global Stratigraphic Correlation, SEPM (Society for Sedimentary Geology) Special Publications 4, 3-21.

Clements, B., Burgess, P.M., Hall, R., Cottam, M.A., 2011. Subsidence and uplift by slab-related mantle dynamics: a driving mechanism for the Late Cretaceous and Cenozoic evolution of continental SE Asia? Geological Society, London, Special Publications 355, 37-51.

Clements, B., Hall, R., 2011. A record of continental collision and regional sediment flux for the

Cretaceous and Palaeogene core of SE Asia: implications for early Cenozoic palaeogeography. Journal of the Geological Society 168, 1187-1200.

Clements, B., Sevastjanova, I., Hall, R., Belousova, E.A., Griffin, W.L., Pearson, N., 2012. Detrital zircon U-Pb age and Hf-isotope perspective on sediment provenance and tectonic models in SE Asia. Geological Society of America Special Papers 487, 37-61.

Cobbing, E.J., Mallick, D.I.J., Pitfield, P.E.J., Teoh, L.H., 1986. The granites of the Southeast Asian tin belt. Journal of the Geological Society 143, 537-550.

Darbyshire, D.P.F., 1988. Geochronology of Malaysian granites. Natural Environment Research Council, Isotope Geology Centre Open File Report 88/3.

Davies, L., Hall, R., Armstrong, R., 2014. Cretaceous crust in SW Borneo: petrological, geochemical and geochronological constraints from the Schwaner Mountains, Proceedings Indonesian Petroleum Association, 38th Annual Convention and Exhibition, IPA14-G-025.

Davies, L.B., 2013. SW Borneo Basement: Age, origin and character of igneous and metamorphic rocks from the Schwaner Mountains. Ph.D. Thesis, Royal Holloway University of London, 391 pp.

Deer, W.A., Howie, R.A., Zussman, J., 1982. Rock forming minerals. Volume 1A-Orthosilicates, Longman, London, 919 pp.

Dickerson, R.E., 1941. Molengraaff River: a drowned Pleistocene stream and other Asian evidences bearing upon the lowering of sea level during the Ice Age. In: Speiser, E.A. (Ed.), Proceedings University of Pennsylvania, Bicentennial Conference, pp. 13-20.

Dickinson, W.R., 1970. Interpreting detrital modes of graywacke and arkose. Journal of Sedimentary Research 40.

Dickinson, W.R., Suczek, C.A., 1979. Plate tectonics and sandstone composition. American Association of Petroleum Geologists Bulletin 63, 2164-2182.

Doutch, H.F., 1992. Aspects of the structural histories of the Tertiary sedimentary basins of East, Central and West Kalimantan and their margins. BMR Journal of Australian Geology and

Geophysics 13, 237-250.

Erriyantoro, E.S., Basuki, N.I., Heryanto, R., Santy, L.D., 2011. Provenance of the Kantu Formation sandstones, Nanga Kantu Area, Ketungau Basin, West Kalimantan, Proceedings Indonesian Petroleum Association, 35th Annual Convention and Exhibition. IPA11-SG-038.

Fuller, M., Ali, J.R., Moss, S.J., Frost, G.M., Richter, B., Mahfi, A., 1999. Paleomagnetism of Borneo. Journal of Asian Earth Sciences 17, 3-24.

Galin, T., Breitfeld, H.T., Hall, R., Sevastjanova, I., 2017. Provenance of the Cretaceous–Eocene Rajang Group submarine fan, Sarawak, Malaysia from light and heavy mineral assemblages and U-Pb zircon geochronology. Gondwana Research 51, 209-233.

Griffin, W.L., Powell, W.J., Pearson, N.J., O'Reilly, S.Y., 2008. GLITTER: data reduction software for laser ablation ICP-MS. In: Sylvester, P.J. (Ed.), Laser Ablation-ICP-MS in the earth sciences: current practices and outstanding issues. Mineralogical association of Canada, Short course series 40, 308-311.

Haile, N.S., 1954. The geology and mineral resources of the Strap and Sadong Valleys, West Sarawak, including the Klingkang Range Coal. British Territories Borneo Region Geological Survey, Memoir 16, 150pp.

Haile, N.S., 1957. The geology and mineral resources of the Lupar and Saribas Valleys, West Sarawak: Malaysia Geological Survey Borneo Region, Memoir,5, 123 pp.

Haile, N.S., 1968. The northwest Borneo geosyncline in its geotectonic setting. Bulletin of the Geological Society of Malaysia, Studies in Malaysian Geology 1, 59-60.

Haile, N.S., 1974. Borneo. In: Spencer, A.M. (Ed.), Mesozoic-Cenozoic Orogenic Belts, Geological Society of London Special Publication, 4, 333-347.

Haile, N.S., 1996. Note on the Engkilili Formation and the age of the Lubok Antu Melange, West Sarawak, Malaysia. Warta Geologi, Geological Society of Malaysia Newsletter 22, 67-70.

Haile, N.S., McElhinny, M.W., McDougall, I., 1977. Palaeomagnetic data and radiometric ages from the Cretaceous of West Kalimantan (Borneo), and their significance in interpreting regional

structure. Journal of the Geological Society of London 133, 133-144.

Hall, R., 2009. Southeast Asia's changing palaeogeography. Blumea-Biodiversity, Evolution and Biogeography of Plants 54, 148-161.

Hall, R., 2012. Late Jurassic–Cenozoic reconstructions of the Indonesian region and the Indian Ocean. Tectonophysics 570–571, 1-41.

Hall, R., 2013. Contraction and extension in northern Borneo driven by subduction rollback. Journal of Asian Earth Sciences 76, 399-411.

Hall, R., 2017. Southeast Asia: New Views of the Geology of the Malay Archipelago. Annual Review of Earth and Planetary Sciences 45, 331-358.

Hall, R., Breitfeld, H.T., 2017. The demise of the Proto-South China Sea. Geological Society of Malaysia Bulletin 63, 61-76.

Hall, R., Sevastjanova, I., 2012. Australian crust in Indonesia. Australian Journal of Earth Sciences 59, 827-844.

Halpin, J.A., Tran, H.T., Lai, C.-K., Meffre, S., Crawford, A.J., Zaw, K., 2016. U–Pb zircon geochronology and geochemistry from NE Vietnam: A 'tectonically disputed'territory between the Indochina and South China blocks. Gondwana Research 34, 254-273.

Heng, Y.E., 1992. Geological Map of Sarawak, 1:500,000. Geological Survey of Malaysia.

Hennig, J., Breitfeld, H.T., Gough, A., Hall, R., Long, T.V., Kim, V.M., Quang, S.D., 2017b. SE Vietnam U-Pb zircon ages and provenance: Correlating the Da Lat Zone on land with the Cuu Long Basin offshore, AGU Fall Meeting 2017, New Orleans, USA.

Hennig, J., Breitfeld, H.T., Gough, A., Hall, R., Long, T.V., Kim, V.M., Quang, S.D., 2018. U-Pb zircon ages and provenance of upper Cenozoic sediments from the Da Lat Zone, SE Vietnam: implications for an intra-Miocene unconformity and paleo-drainage of the proto-Mekong River. Journal of Sedimentary Research 88, 495-515.

Hennig, J., Breitfeld, H.T., Hall, R., Nugraha, A.M.S., 2017a. The Mesozoic tectono-magmatic evolution at the Paleo-Pacific subduction zone in West Borneo. Gondwana Research 48, 292-

310.

Hennig, J., Hall, R., Armstrong, R.A., 2016. U-Pb zircon geochronology of rocks from west Central Sulawesi, Indonesia: Extension-related metamorphism and magmatism during the early stages of mountain building. Gondwana Research 32, 41-63.

Heryanto, R., Jones, B.G., 1996. Tectonic development of Melawi and Ketungau Basins, Western Kalimantan, Indonesia. Bulletin Geological Research and Development Centre, Bandung 19, 151-179.

Heryanto, R.S., 1991. Sedimentology of the Melawi and Kentungau Basins, West Kalimantan, Indonesia. Doctor of Philosophy thesis Thesis, Wollongong, Australia, 255 pp.

Hieu, P.T., Yang, Y.-Z., Binh, D.Q., Nguyen, T.B.T., Dung, L.T., Chen, F., 2015. Late Permian to Early Triassic crustal evolution of the Kontum massif, central Vietnam: zircon U–Pb ages and geochemical and Nd–Hf isotopic composition of the Hai Van granitoid complex. International Geology Review 57, 1877-1888.

Hubert, J.F., 1962. A zircon-tourmaline-rutile maturity index and the interdependence of the composition of heavy mineral assemblages with the gross composition and texture of sandstones. Journal of Sedimentary Petrology 32, 440-450.

Hutchison, C.S., 1989. Geological Evolution of South-East Asia: Oxford Monographs on Geology and Geophysics,13, Clarendon Press, Oxford, 376 pp.

Hutchison, C.S., 1996. The 'Rajang Accretionary Prism' and 'Lupar Line' problem of Borneo. In: Hall, R., Blundell, D.J. (Eds.), Tectonic Evolution of SE Asia, Geological Society London Special Publication, 106, 247-261.

Hutchison, C.S., 2005. Geology of North-West Borneo, Elsevier, Amsterdam, 421 pp.

Ingersoll, R.V., Bullard, T.F., Ford, R.L., Grimm, J.P., Pickle, J.D., Sares, S.W., 1984. The effect of grain size on detrital modes: a test of the Gazzi-Dickinson point-counting method. Journal of Sedimentary Research 54, 103-116.

Jiang, X.-Y., Li, X.-H., Collins, W.J., Huang, H.-Q., 2015. U-Pb age and Hf-O isotopes of detrital zircons

from Hainan Island: Implications for Mesozoic subduction models. Lithos 239, 60-70.

Johnsson, M.J., Stallard, R.F., Meade, R.H., 1988. First-cycle quartz arenites in the Orinoco River basin, Venezuela and Colombia. The Journal of Geology 96, 263-277.

Kanno, S., 1978. Brackish molluscan fauna (Upper Eocene) from the Silantek Formation in West Sarawak, Malaysia. Geology and Palaeontology of S.E. Asia (University of Tokyo Press) 20, 103-112.

Kirk, H.J.C., 1957. The Geology and Mineral Resources of the Upper Rajang and adjacent areas: British Territories Borneo Region Geological Survey, Memoir,8, 181 pp.

Koopmans, B.N., 1968. The Tembeling Formation - A Litho-Stratigraphic Description (West Malaysia). Bull. Geol. Soc. Malaysia 1, 23-43.

Kuenen, P.H., 1950. Marine Geology, John Wiley & Sons, New York, 568 pp.

Li, W.-X., Li, X.-H., Li, Z.-X., 2005. Neoproterozoic bimodal magmatism in the Cathaysia Block of South China and its tectonic significance. Precambrian Research 136, 51-66.

Li, X.H., 1999. U–Pb zircon ages of granites from the southern margin of the Yangtze Block: timing of Neoproterozoic Jinning: Orogeny in SE China and implications for Rodinia Assembly. Precambrian Research 97, 43-57.

Li, X.-H., Li, Z.-X., Li, W.-X., Wang, Y., 2006. Initiation of the Indosinian Orogeny in South China: evidence for a Permian magmatic arc on Hainan Island. The Journal of Geology 114, 341-353.

Liebermann, C., Hall, R., Gough, A., 2017. Provenance of sediments from Sumatra, Indonesia-Insights from detrital U-Pb zircon geochronology, heavy mineral analyses and Raman spectroscopy, AGU Fall Meeting 2017, New Orleans, USA.

Liechti, P., Roe, F.W., Haile, N.S., 1960. The Geology of Sarawak, Brunei and the western part of North Borneo: Geological Survey Department, British Territories of Borneo, Bulletin,3, 360 pp.

Liew, T.C., Page, R.W., 1985. U-Pb zircon dating of granitoid plutons from the West Coast of Peninsular Malaysia. Journal of the Geological Society of London 142, 515-526.

Lin, Y.-L., Yeh, M.-W., Lee, T.-Y., Chung, S.-L., Iizuka, Y., Charusiri, P., 2013. First evidence of the Cambrian basement in Upper Peninsula of Thailand and its implication for crustal and tectonic evolution of the Sibumasu terrane. Gondwana Research 24, 1031-1037.

Liu, R., Zhou, H., Zhang, L., Zhong, Z., Zeng, W., Xiang, H., Jin, S., Lu, X., Li, C., 2009a. Paleoproterozoic reworking of ancient crust in the Cathaysia Block, South China: Evidence from zircon trace elements, U-Pb and Lu-Hf isotopes. Chinese Science Bulletin 54, 1543-1554.

Liu, S., Hu, R., Gao, S., Feng, C., Huang, Z., Lai, S., Yuan, H., Liu, X., Coulson, I.M., Feng, G., 2009b. U–Pb zircon, geochemical and Sr–Nd–Hf isotopic constraints on the age and origin of Early Palaeozoic I-type granite from the Tengchong–Baoshan Block, Western Yunnan Province, SW China. Journal of Asian Earth Sciences 36, 168-182.

Ma, X., Yang, K., Li, X., Dai, C., Zhang, H., Zhou, Q., 2016. Neoproterozoic Jiangnan Orogeny in southeast Guizhou, South China: evidence from U–Pb ages for detrital zircons from the Sibao Group and Xiajiang Group. Canadian Journal of Earth Sciences 53, 219-230.

Mange, M.A., Maurer, H.F.W., 1992. Heavy minerals in colour, Chapman & Hall, London, 147 pp.

Mange, M.A., Wright, D.T. (eds.), 2007. Heavy minerals in use, Developments in Sedimentology 58. Elsevier, Amsterdam, 1328 pp.

Milroy, W.V., Crews, W.E., 1953. Geology of West Sarawak with notes on the palaeontology of West Sarawak. Sarawak Shell Oilfields ds Ltd. Report GR 602 (unpubl.).

Molengraaff, G.A.F., Hinde, G.J., 1902. Borneo-expedition: Geological Explorations in Central Borneo (1893-94), E.J. Brill, Leyden, 489 pp.

Montero, P., Bea, F., Corretgé, L.G., Floor, P., Whitehouse, M.J., 2009. U-Pb ion microprobe dating and Sr and Nd isotope geology of the Galiñeiro igneous complex: A model for the peraluminous/peralkaline duality of the Cambro-Ordovician magmatism of Iberia. Lithos 107, 227-238.

Morley, R.J., 1998. Palynological evidence for Tertiary plant dispersals in the SE Asian region in relation to plate tectonics and climate. In Hall, R. & Holloway, J. D. (eds.) Biogeography and

Geological Evolution of SE Asia. Backhuys Publishers, Leiden, The Netherlands 211-234.

Morton, A.C., 1984. Stability of detrital heavy tertiary sandstones from sea basin. Clay Minerals 19, 287-308.

Morton, A.C., Hallsworth, C.R., 1994. Identifying provenance-specific features of detrital heavy mineral assemblages in sandstones. Sedimentary Geology 90, 241-256.

Moss, S.J., 1998. Embaluh Group turbidites in Kalimantan: evolution of a remnant oceanic basin in Borneo during the Late Cretaceous to Palaeogene. Journal- Geological Society London 155, 509-524.

Muller, J., 1968. Palynology of the Pedawan and Plateau Sandstone Formations (Cretaceous - Eocene) in Sarawak, Malaysia. Micropaleontology 14, 1-37.

Nemchin, A.A., Cawood, P.A., 2005. Discordance of the U–Pb system in detrital zircons: implication for provenance studies of sedimentary rocks. Sedimentary Geology 182, 143-162.

Nguyen, T.T.B., Satir, M., Siebel, W., Chen, F., 2004. Granitoids in the Dalat zone, southern Vietnam: age constraints on magmatism and regional geological implications. International Journal of Earth Sciences 93, 329-340.

Oliver, G., Zaw, K., Hotson, M., Meffre, S., Manka, T., 2014. U–Pb zircon geochronology of Early Permian to Late Triassic rocks from Singapore and Johor: A plate tectonic reinterpretation. Gondwana Research 26, 132-143.

Pearce, N.J.G., Perkins, W.T., Westgate, J.A., Gorton, M.P., Jackson, S.E., Neal, C.R., Chenery, S.P., 1997. A Compilation of New and Published Major and Trace Element Data for NIST SRM 610 and NIST SRM 612 Glass Reference Materials. Geostandards Newsletter 21, 115-144.

Pieters, P.E., Surono, Noya, Y., 1993. Geology of the Putussibau Sheet area, Kalimantan. Geological Survey of Indonesia, Directorate of Mineral Resources, Geological Research and Development Centre, Bandung, Quadrangle 1616, Scale 1:250000. 31-63.

Pieters, P.E., Trail, D.S., Supriatna, S., 1987. Correlation of Early Tertiary rocks across Kalimantan. Indonesian Petroleum Association, Proceedings 16th annual convention Jakarta, 1987, 291-

306.

Schmidtke, E.A., Fuller, M., Haston, R.B., 1990. Paleomagnetic data from Sarawak, Malaysian Borneo and the Late Mesozoic and Cenozoic tectonics of Sundaland. Tectonics 9, 123-140.

Searle, M.P., Whitehouse, M.J., Robb, L.J., Ghani, A.A., Hutchison, C.S., Sone, M., Ng, S.W., Roselee, M.H., Chung, S.-L., Oliver, G.J.H., 2012. Tectonic evolution of the Sibumasu-Indochina terrane collision zone in Thailand and Malaysia: constraints from new U-Pb zircon chronology of SE Asian tin granitoids. Journal of the Geological Society 169, 489.

Setiawan, N.I., Osanai, Y., Nakano, N., Adachi, T., Setiadji, L.D., Wahyudiono, J., 2013. Late Triassic metatonalite from the Schwaner Mountains in West Kalimantan and its contribution to sedimentary provenance in the Sundaland. Berita Sedimentologi 12, 4-12.

Sevastjanova, I., Clements, B., Hall, R., Belousova, E.A., Griffin, W.L., Pearson, N., 2011. Granitic magmatism, basement ages, and provenance indicators in the Malay Peninsula: Insights from detrital zircon U-Pb and Hf-isotope data. Gondwana Research 19, 1024-1039.

Shellnutt, J.G., Lan, C.-Y., Van Long, T., Usuki, T., Yang, H.-J., Mertzman, S.A., Iizuka, Y., Chung, S.-L., Wang, K.-L., Hsu, W.-Y., 2013. Formation of Cretaceous Cordilleran and post-orogenic granites and their microgranular enclaves from the Dalat zone, southern Vietnam: Tectonic implications for the evolution of Southeast Asia. Lithos 182, 229-241.

Shu, L., Faure, M., Wang, B., Zhou, X., Song, B., 2008. Late Palaeozoic–Early Mesozoic geological features of South China: response to the Indosinian collision events in Southeast Asia. Comptes Rendus Geoscience 340, 151-165.

Sircombe, K.N., 2004. AgeDisplay: an EXCEL workbook to evaluate and display univariate geochronological data using binned frequency histograms and probability density distributions. Computers & Geosciences 30, 21-31.

Sláma, J., Košler, J., Condon, D.J., Crowley, J.L., Gerdes, A., Hanchar, J.M., Horstwood, M.S.A., Morris, G.A., Nasdala, L., Norberg, N., Schaltegger, U., Schoene, B., Tubrett, M.N., Whitehouse, M.J., 2008. Plešovice zircon — A new natural reference material for U–Pb and Hf isotopic

microanalysis. Chemical Geology 249, 1-35.

Smyth, H.R., Hall, R., Nichols, G.J., 2008. Significant volcanic contribution to some quartz-rich sandstones, East Java, Indonesia. Journal of Sedimentary Research 78, 335-356.

Smyth, H.R., Hamilton, P.J., Hall, R., Kinny, P.D., 2007. The deep crust beneath island arcs: inherited zircons reveal a Gondwana continental fragment beneath East Java, Indonesia. Earth and Planetary Science Letters 258, 269-282.

Song, S., Ji, J., Wei, C., Su, L., Zheng, Y., Song, B., Zhang, L., 2007. Early Paleozoic granite in Nujiang River of northwest Yunnan in southwestern China and its tectonic implications. Chinese Science Bulletin 52, 2402-2406.

Suttner, L.J., Basu, A., Mack, G.H., 1981. Climate and the origin of quartz arenites. Journal of Sedimentary Research 51.

Tan, D.N.K., 1979. Lupar Valley, west Sarawak: Geological Survey of Malaysia, Report 13, 159 pp.

Tan, D.N.K., 1981. Nomenclature of the Upper Cretaceous - Tertiary molasse deposits in west Sarawak. Malaysia Geol. Survey Ann. Rept. 1981, 348-355.

Tan, D.N.K., 1984. Palaeocurrents in the Tertiary sedimentary deposits in western Sarawak. Bulletin of the Geological Society of Malaysia 17, 258-264.

Tan, D.N.K., 1993. Geology of the Kuching area. West Sarawak, Malaysia. Geological Survey of Malaysia, Report 16, 161 pp.

Tate, R.B., 1991. Cross-border correlation of geological formations in Sarawak and Kalimantan. Bulletin of the Geological Society of Malaysia 28, 63-96.

ter Bruggen, G., 1935. De Eocene Fyllietformatie in Centraal-Borneo. N.V. Drukkerij Waltman, Delft, the Netherlands 133pp.

Tongkul, F., 1997. Sedimentation and tectonics of Paleogene sediments in central Sarawak. Bulletin of the Geological Society of Malaysia 40, 135-140.

van Hattum, M.W.A., Hall, R., Pickard, A.L., Nichols, G.J., 2013. Provenance and geochronology of Cenozoic sandstones of northern Borneo. Journal of Asian Earth Sciences 76, 266-282.

Vermeesch, P., Resentini, A., Garzanti, E., 2016. An R package for statistical provenance analysis. Sedimentary Geology 336, 14-25.

Voris, H.K., 2000. Maps of Pleistocene sea levels in Southeast Asia: shorelines, river systems and time durations. Journal of Biogeography 27, 1153-1167.

Wang, S., Mo, Y., Wang, C., Ye, P., 2016. Paleotethyan evolution of the Indochina Block as deduced from granites in northern Laos. Gondwana Research 38, 183-196.

Wang, W., Zhou, M.-F., Yan, D.-P., Li, J.-W., 2012. Depositional age, provenance, and tectonic setting of the Neoproterozoic Sibao Group, southeastern Yangtze Block, South China. Precambrian Research 192, 107-124.

Wilford, G.E., 1955. The geology and mineral resources of the Kuching-Lundu area, West Sarawak including the Bau mining district: British Territories Borneo Region Geological Survey Department, Memoir 3, 254 pp.

Wilford, G.E., Kho, C.H., 1965. Penrissen area, west Sarawak, Malaysia: Malaysian Geol. Survey, Borneo Region, Rept. 2., 195 pp.

Williams, P.R., Heryanto, R., 1985. Geological Map of the Sintang 1:250 000 Quadrangle, Kalimantan (preliminary). Geological Research and Development Centre, Bandung.

Williams, P.R., Johnston, C.R., Almond, R.A., Simamora, W.H., 1988. Late Cretaceous to Early Tertiary structural elements of West Kalimantan. Tectonophysics 148, 279-298.

Wolfenden, E.B., 1960. The Geology and Mineral Resources of the Lower Rajang Valley and adjoining areas, Sarawak: British Territories Borneo Region Geological Survey Department, Memoir 11, 167 pp.

Wolfenden, E.B., 1965. Bau Mining District, West Sarawak, Malaysia, part I. Bau. Geological Survey of Malaysia, Borneo Region, Bulletin 7, 147pp.

Wolfenden, E.B., Haile, N.S., 1963. Semantan and Lundu area, West Sarawak: British Borneo Geological Survey Report,1, 159 pp.

Xianhua, L., Tatsumoto, M., Premo, W.R., Xuntang, G., 1989. Age and origin of the Tanghu Granite,

southeast China: Results from U-Pb single zircon and Nd isotopes. Geology 17, 395-399.

Yan, Q., Metcalfe, I., Shi, X., 2017. U-Pb isotope geochronology and geochemistry of granites from Hainan Island (northern South China Sea margin): Constraints on late Paleozoic-Mesozoic tectonic evolution. Gondwana Research 49, 333-349.

Zeijlmans van Emmichoven, C.P.A., 1939. De geologie van het centrale en oostelijke deel van de Westerafdeeling van Borneo. Jaarboek Mijnwezen Nederlandsch Oost Indië, Verhandelingen 1939 68, 7-186.

Zeijlmans van Emmichoven, C.P.A., ter Bruggen, G., 1935. Voorlopige mededeeling over het tertiair ten W van het Merengebied in de Wester-afdeeling van Borneo [Provisional report on the Tertiary west of the Lake District in the Western Division of Borneo]. De Ingenieur in Ned. Indië sect. IV, 99-102.

Zimmermann, S., Hall, R., 2016. Provenance of Triassic and Jurassic sandstones in the Banda Arc: Petrography, heavy minerals and zircon geochronology. Gondwana Research 37, 1-19.

Figure captions

Figure 1: Tectonic provinces of NW Borneo (modified from Haile, 1974; Breitfeld et al., 2017; Hennig et al., 2017a). The SW Borneo Basement represents the SW Borneo block. The West Borneo province includes the lower Mesozoic basement that was part of Sundaland in the Triassic, which underlies the Kuching Zone in the west. The Kuching Zone is composed of mainly Cenozoic terrestrial sedimentary basins. Extend of basins is shown adapted from Doutch (1992) and Breitfeld et al. (2018). The Sibu Zone consists mainly of Paleogene deep marine rocks of the Rajang Group. The Miri Zone is composed of mainly fluvio-marine Neogene sediments.

Figure 2: Distribution of sediments from the Kayan and Ketungau Groups with location of U-Pb detrital zircon dated samples (modified from Liechti et al., 1960; Heng, 1992; Breitfeld et al., 2018).

Figure 3: Stratigraphy of the Late Cretaceous to Early Oligocene in the Kuching Zone (West Sarawak), Sibu Zone (Central Sarawak) and Miri Zone (North Sarawak) (modified from Breitfeld et al., 2018).

Figure 4: Selection of thin section photomicrographs of light minerals. A) Monocrystalline undulose quartz (crossed polars; STB21). B) Euhedral bipryramidal volcanic quartz grains (crossed polars; TB92c). C) Polycrystalline quartz (crossed polars; TB81). D) Detrital chert fragment composed of mega- and microquartz (crossed polars; STB21). E) Detrital chert fragment (crossed polars; TB143). F) Plagioclase (crossed polars; TB127). G) Plagioclase, polycrystalline quartz and volcanic rock fragment composed entirely of sericite (crossed polars; STB50). H) Yellow stained alkali feldspar (plane polars; TB122). I) Euhedral alkali feldspar (crossed polars; STB50). J) Microcline grain (crossed polars; TB127). K) Metamorphic rock fragment composed of elongated polycrystalline quartz and muscovite (crossed polars; STB06). L) Rock fragment of either sedimentary or metamorphic origin probably derived from the Sejingkat Formation. (crossed polars; TB158). M) Sedimentary rock fragment composed of fibrous chalcedony (crossed polars; TB60a). N) Sedimentary rock fragment, well rounded (crossed polars; TB130). O) Volcanic rock fragment composed of fine glass matrix and idiomorph prismatic plagioclase needles (plane polars; TB60a).

Figure 5: Light mineral modes. Sandstone classification for sediments with A) < 15% matrix and B) 15-75% matrix for the Kayan Group (after Pettijohn et al., 1987). Light mineral provenance after Dickinson and Suczek (1979) displaying C) the QFL (total quartz-feldspar-lithic fragments) and D) the QmFLt (monocrystalline quartz-feldspar-total lithics including chert and polycrystalline quartz) diagrams for the Kayan Group. Sandstone classification for the Ketungau Group displaying E) samples with < 15% matrix and F) with 15-75% matrix. Light mineral provenance displaying G) the QFL diagram and H) the QmFLt diagram.

Figure 6: Detrital zircon photomicrographs and SEM backscattered images. Zircon varieties are dominated by colourless euhedral and subhedral and pinkish rounded grains. Colourless anhedral and rounded as well as pinkish euhedral grains are less abundant.

Figure 7: Heavy mineral slide photomicrographs and backscatter SEM images. A) Brown rutile (plane polars); B) Deep red rutile (plane polars); C) Anatase (plane polars); D) Brookite (plane polars); E) Fractured chrome spinel (SEM); F) Huebnerite (SEM); G & H) Titanite (plane polars, SEM); I) Yellowish rounded monazite (plane polars); J) Colourless garnet (plane polars); K) Garnet with rhombic dodecahedron crystals (SEM); L) Elongated andalusite (plane polars); M & N) Brown euhedral tourmaline (plane and crossed polars); O & P) Dark green rounded tourmaline (plane and crossed polars); Q & R) Colourless apatite and light green-yellow epidote (plane and crossed polars); S) Apatite (SEM); T) Elongated epidote (SEM); U & V) Kyanite (plane and crossed polars); W & X) Clinopyroxene, ?hedenbergite (plane and crossed polars); Y) Clinopyroxene, augite (plane polars); Z & i) Orthopyroxene, ?hypersthene (plane and crossed polars); ii) Brown hornblende (plane and crossed polars).

Figure 8: A) Most abundant heavy minerals in the Kayan and Ketungau Group in relative stratigraphic order, shown as 100 % vertical stacked area plots. Andalusite which occurs only in sample TB21 (78% of the heavy minerals are andalusite) is not displayed. B) Zircon-tourmaline-rutile (ZTR) index and

zircon-tourmaline (ZTi) ratio plots for samples in stratigraphic order. Sample TB21 (anomalous heavy mineral assemblage) is excluded.

Figure 9: Age histograms for detrital zircons of samples from the Kayan Group. The Kayan Sandstone in the Kayan Syncline and at Tanjung Santubong shows predominantly Cretaceous and Permian-Triassic zircon age populations. The Kayan Sandstone in the Pueh area, at the Bungo Range and at Gunung Serapi/Matang area consists predominantly of Cretaceous zircons. The Penrissen Sandstone shows heterogeneous zircon populations ranging from the Early Eocene to the Archean comparable to the lower Kayan Sandstone. Bin size of 10 Ma for Phanerozoic ages and 50 Ma for Precambrian ages.

Figure 10: Age histograms for detrital zircons of samples from the Ketungau Group including the Ngili Sandstone, the Silantek Formation, the Bako-Mintu Sandstone and the Tutoop Sandstone. The Ngili Sandstone is mainly composed only of two significant zircon age populations. The majority of zircons are Permian-Triassic with a small number Paleoproterozoic (c. 1.8 Ga) ages. The Silantek Formation samples and the Bako-Mintu Sandstone show very variable zircons age populations ranging from the Middle Eocene to the Archean. The Tutoop Sandstone show slight variations in the amount of Paleozoic, Neoproterozoic and Archean zircon peaks compared to the underlying Silantek Formation/Bako-Mintu Sandstone. Bin size of 10 Ma for Phanerozoic ages and 50 Ma for Precambrian ages.

Figure 11: Summary diagram of U-Pb detrital zircon ages for sediments of the Kuching and Sibu Zones, showing the interpreted maximum depositional ages based on the youngest zircon populations and the interpreted palaeontology/palynology age range. Rajang Group U-Pb detrital zircon data from Galin et al. (2017). Paleontology and palynology data based on Haile (1957), Liechti et al. (1960), Wolfenden (1960), Muller (1968), Tan (1979) and Morley (1998). Unimodal zircon populations means the zircon distribution is dominated by one maximum (Cretaceous), while multimodal means the

distribution has more than 2 maxima (Cretaceous, Permian-Triassic, and e.g. Jurassic, Neoproterozoic, Paleoproterozoic).

Figure 12: Comparison of detrital U-Pb zircon age histograms of Latest Cretaceous units from the Kuching and Sibu Zones. Similar age peaks are in the Cretaceous and Permian-Triassic present in all four histograms. The Kayan Sandstone at Santubong and the Lupar Formation (base of Unit 1) have a peak in the Paleoproterozoic at c. 1.8 Ga. The Kayan Sandstone in the Kayan Syncline and the Rajang Group Unit 1 have similar peaks at c. 500 Ma, c. 1.2 Ga and 1.6 Ga, and are missing the prominent 1.8 Ga peak.

Figure 13: Comparison of detrital U-Pb zircon age histograms of Paleocene to Late Eocene units from the Kuching and Sibu Zones. The Kayan Sandstone in the Pueh area, at Gunung Serapi/Matang and at the Bungo Range are very similar to the Rajang Group Unit 2, showing a very strong Cretaceous age population and only minor other populations. Characteristic is also the low abundance of Precambrian zircons, peaking at c. 1.8 Ga. The Silantek Formation and the Bako-Mintu Sandstone have an almost identical age signature compared to the Rajang Group Unit 3. Similar peaks are in the Middle Eocene, Cretaceous, Jurassic, Permian-Triassic, Ordovician to Early Devonian, ca. 0.8 to 1.2 Ga, c. 1.8 Ga and c. 2.5 Ga. The Tutopp Sandstone is overall similar to the underlying units, but shows slight variation. Prominent populations are missing or are only weak in the Middle Eocene, Ordovician to Early Devonian and at c. 2.5 Ga.

Figure 14: Multi-dimensional scaling (MDS) plot of detrital zircon data (Vermeesch et al., 2016), showing similarities of successions south and north of the Lupar Line. Source data compiled for SW Borneo from Davies (2013), Davies et al. (2014) and Hennig et al. (2017a), for West Borneo from Breitfeld et al. (2017) and Hennig et al. (2017a) and for the Malay-Thai Tin Belt from Sevastjanova et al. (2011), Searle et al. (2012) and Oliver et al. (2014).

Figure 15: Comparison of heavy mineral analysis of sediments from the Kuching Supergroup and the Rajang Group, displaying a more diverse assemblage with more abundant rutile for the Kuching

Supergroup. The abundance of zircon for both groups is comparable, supporting the U-Pb zircon provenance similarities. There are no Rajang Group equivalents for the Penrissen and Ngili Sandstones. Heavy mineral data for the Rajang Group from Galin et al. (2017).

Figure 16: A) Principal blocks of SE Asia, and their position in the Latest Cretaceous (Terranes: NWS – North Sulawesi + Sabah; EJWS – East Java + West Sulawesi; Cretaceous granites: SG – Schwaner granites; DLZG – Da Lat Zone granites). B–D) Paleogeography and reconstruction of the major fluvial system that deposited the Kuching Supergroup in the Latest Cretaceous to Late Eocene (proto-Sungai Sarawak/proto-Sarawak). The Rajang Group was the submarine fan that was fed by the paleo-river(s) of the Kuching Zone. Figures based on this study and earlier work (Watkinson et al., 2008; Hall, 2009; 2012, 2013, 2017; Hall and Sevastjanova, 2012; Morley, 2012; Hennig et al., 2016; Breitfeld et al., 2017; Hennig et al., 2017a; Galin et al., 2017).

Table captions

Table 1: Light mineral modes for the Kuching Supergroup in West Sarawak (Kuching Zone). (Qm = monocrystalline quartz, Qmu = monocrystalline undulary quartz, Qv = volcanic quartz, Qp = polycrystalline quartz, Ch = chert, Fp = plagioclase, Fk = K-feldspar, Lm = metamorphic lithic fragments, Ls = sedimentary lithic fragments, Lv = volcanic lithic fragments, H = heavy mineral, Mt = matrix, Lithics (L) = Lm+Ls+Lv, Total lithics (Lt) = Lm+Ls+Lv+Qp+Ch, Total Qm = Qm+Qmu+Qv).

Table 2a: Heavy mineral assemblage of the Kuching Supergroup in West Sarawak (Kuching Zone) as total counts.

Table 2b: Heavy mineral assemblage of the Kuching Supergroup in West Sarawak (Kuching Zone) as percentage.

Table 3: Zircon and tourmaline varieties and percentage of rounded-angular zircon and tourmaline in the analysed sample. Rounded zircon % comprises counts of subrounded and rounded. Angular zircon % includes counts of euhedral, subhedral and anhedral.

Table 4: Heavy mineral ratios and counts of heavy minerals for index calculation after Hubert (1962); Morton and Hallsworth (1994) and Mange and Wright (2007).

Table 1

Sample	Formation	Qm	Qmu	Qv	Qp	Ch	Fp	Fk	Lm	Ls	Lv	H	Mt	mica	organic or iron	calcite	Total	Framework grains	% matrix	Total lithics	Total feldspar	Total Qm	Total Q
TB227	Tutoop Sst	159	121	22	93	21	1	10	2	25	19	0	22	0	5	0	500	473	4.4	160	11	302	416
TB223	Tutoop Sst	143	107	25	69	18	1	12	4	41	34	0	45	0	1	0	500	454	9.0	166	13	275	362
TB215	Tutoop Sst	174	89	20	82	20	2	0	6	26	46	2	30	0	3	0	500	465	6.0	180	2	283	385
STB95	Tutoop Sst	219	97	0	42	19	0	2	10	40	20	0	41	2	8	0	500	449	8.2	131	2	316	377
STB90a	Tutoop Sst	168	125	6	64	22	4	6	0	36	15	0	45	4	5	0	500	446	9.0	137	10	299	385
STB89	Tutoop Sst	223	135	4	52	4	4	1	14	33	16	3	10	0	1	0	500	486	2.0	119	5	362	418
STB88	Tutoop Sst	139	90	20	82	35	5	1	3	42	21	2	48	2	0	0	500	448	9.6	183	16	249	366
STB96a	Tutoop Sst	163	93	63	53	13	5	16	13	28	20	0	30	1	2	0	500	467	6	127	21	319	385
TB177b	Bako-Mintu Sst	139	69	17	52	13	0	0	39	21	49	0	80	4	7	0	500	409	16.0	174	10	225	290
TB175-2	Bako-Mintu Sst	196	70	0	24	4	5	5	12	35	24	0	86	1	38	0	500	375	17.2	99	10	266	294
TB175	Bako-Mintu Sst	137	72	23	50	9	6	6	0	26	31	0	104	5	31	0	500	360	20.8	116	12	232	291
TB173	Bako-Mintu Sst	124	81	32	72	22	4	0	40	23	39	1	59	1	2	0	500	437	11.8	196	4	237	331
TB171	Bako-Mintu Sst	143	71	7	81	14	0	6	21	8	61	0	73	0	5	0	500	422	14.6	185	16	221	316

STB79b	Bako-Mintu Sst	141	104	6	78	11	0	0	36	54	44	2	19	1	4	0	500	474	3.8	223	0	251	340
STB79a	Bako-Mintu Sst	147	92	26	51	26	3	7	5	16	22	0	49	3	53	0	500	395	9.8	120	10	265	342
STB74a	Bako-Mintu Sst	141	112	38	83	30	2	13	0	38	14	0	28	1	0	0	500	471	5.6	165	15	291	404
TB164	Bako-Mintu Sst	158	103	37	66	3	3	0	23	19	24	1	59	0	4	0	500	436	11.8	135	3	298	367
TB158	Bako-Mintu Sst	129	105	21	8	21	2	0	33	18	27	0	34	2	0	0	500	464	6.8	207	2	255	384
TB145	Bako-Mintu Sst	100	80	66	80	18	9	0	27	47	43	2	27	0	1	0	500	470	5.4	215	9	246	344
TB144	Bako-Mintu Sst	117	80	40	81	28	5	5	7	61	36	0	39	1	0	0	500	460	7.8	213	10	237	346
TB143	Bako-Mintu Sst	124	92	19	84	17	0	2	6	30	62	0	57	1	6	0	500	436	11.4	199	2	235	336
STB60	Bako-Mintu Sst	130	101	6	88	14	4	2	4	51	29	1	75	1	10	0	500	413	15.0	170	6	237	339
TB216	Silantek Fm (Shale Mbr)	138	55	3	37	30	8	7	0	23	17	1	121	2	48	0	500	328	24.2	107	25	196	263
STB97b	Silantek Fm (Shale Mbr)	107	79	12	64	30	8	3	5	30	24	0	118	3	7	0	500	372	23.6	153	21	198	292
TB218	Silantek Fm (Temudok Sst)	139	93	17	62	30	2	7	5	20	58	1	62	1	3	0	500	433	12.4	175	9	249	341
STB109	Silantek Fm (Temudok Sst)	130	120	40	59	24	5	13	3	31	31	0	42	2	0	0	500	456	8.4	148	18	290	373
TB217	Silantek Fm (Marup Sst)	121	104	10	94	15	3	39	16	18	49	0	22	0	9	0	500	469	4.4	192	42	235	344
TB213b	Silantek Fm (Marup Sst)	105	72	70	54	20	34	26	22	36	28	1	20	1	4	7	500	467	4	160	60	247	321
TB208	Silantek Fm (Marup Sst)	104	48	6	34	16	2	8	3	39	66	1	146	3	14	0	500	336	29.2	158	20	158	208

TB210	Silantek Fm (Marup Sst)	114	73	19	102	22	17	26	6	55	42	0	19	1	4	0	500	476	3.8	227	43	206	330
STB113b	Silantek Fm (Marup Sst)	107	55	12	16	23	1	17	7	36	31	2	29 4	14	50	0	665	305	44.2	113	18	174	213
TB60a	Ngili Sst	31	52	4	142	30	0	0	18	67	119	0	31	1	5	0	500	463	6.2	376	0	87	259
STB77	Ngili Sst	76	83	13	104	25	19	1	1	26	34	2	39	1	36	0	500	422	7.8	190	60	172	301
STB75b	Ngili Sst	68	55	3	216	44	0	4	26	13	25	2	39	5	0	0	500	454	7.8	324	4	126	386
STB75	Ngili Sst	107	134	0	89	24	8	1	47	20	5	0	60	0	5	0	500	435	12.0	185	9	241	354
TB119	Penrissen Sandstone	100	73	11	60	23	33	79	3	23	37	5	42	2	5	4	500	442	8.4	146	112	184	267
TB127	Penrissen Sandstone	113	96	15	55	26	31	21	0	44	44	0	41	4	8	0	500	447	8.2	169	54	224	305
TB121b	Penrissen Sandstone	95	72	51	61	24	90	3	39	27	1	16	2	0	0	500	481	3.2	174	89	218	303		
TB121	Penrissen Sandstone	110	70	22	70	76	61	1	1	1	59	2	25	0	2	14	500	457	5.0	178	77	202	289
TB130	Penrissen Sandstone	102	111	25	63	83	39	24	22	46	0	36	1	10	0	500	453	7.2	163	52	238	309		
TB89b	Kayan Sst (Pueh area)	119	87	24	60	13	53	10	38	44	0	84	2	11	0	500	403	16.8	165	8	230	303		
TB84	Kayan Sst (Pueh area)	160	110	43	10	0	87	0	12	15	0	13 4	0	1	0	500	365	26.8	37	15	313	323		
TB83	Kayan Sst (Pueh area)	152	74	10	43	27	21	12	47	20	2	95	3	12	0	500	388	19.0	139	13	236	306		
TB81	Kayan Sst (Pueh area)	181	74	58	4	0	15	1	00	21	0	13 3	0	3	0	500	364	26.6	35	16	313	317		
TB118	Kayan Sst (Bungo Range)	163	98	17	11 9	14	44	77	17	21	11	1	26	1	1	0	500	471	5.2	182	11	278	411

STB38	Kayan Sst (Bungo Range)	102	79	18	80	17	3	2	8	16	66	1	94	0	14	0	500	391	18.8	187	5	199	296
STB36a	Kayan Sst (Bungo Range)	83	86	26	82	21	8	4	12	15	45	3	62	0	2	1	500	432	12.4	175	62	195	298
STB31b	Kayan Sst (Bungo Range)	142	186	18	89	3	0	0	17	14	17	0	13	1	0	0	500	486	2.6	140	0	346	438
STB31	Kayan Sst (Bungo Range)	99	110	8	77	9	0	0	43	25	30	0	96	1	2	0	500	401	19.2	184	0	217	303
STB21	Kayan Sst (Bungo Range)	115	82	16	95	34	13	14	0	44	55	8	24	0	0	0	500	468	4.8	228	27	213	342
STB20b	Kayan Sst (Bungo Range)	137	67	30	26	12	5	1	7	19	69	0	69	1	7	0	500	423	13.8	133	56	234	272
TB135	Kayan Sst (Bungo Range)	92	68	8	56	9	8	7	54	24	58	2	97	5	12	0	500	384	19.4	201	15	168	233
TB122	Kayan Sst (Bungo Range)	97	81	20	57	11	7	3	28	22	33	3	57	0	11	0	500	429	11.4	151	80	198	266
TB124b	Kayan Sst (Bungo Range)	156	98	36	65	3	0	6	2	12	22	1	75	0	4	0	500	420	15.0	104	26	290	358
STB65	Kayan Sst (Matang/Serapi)	117	89	8	71	13	5	3	3	15	34	1	63	2	6	0	500	428	12.6	146	68	214	298
STB63	Kayan Sst (Matang/Serapi)	150	101	5	75	16	9	6	15	34	38	1	22	1	17	0	500	459	4.4	178	25	256	347
TB21b	Kayan Sst (Matang/Serapi)	203	137	17	22	2	0	0	4	7	20	1	76	2	7	0	498	412	15.3	55	0	357	381
TB21	Kayan Sst (Matang/Serapi)	266	62	43	6	0	7	2	0	6	41	1	40	5	21	0	500	433	8.0	53	9	371	377
STB18c	Kayan Sst (Matang/Serapi)	80	49	7	77	50	8	9	13	61	32	2	104	2	6	0	500	386	20.8	233	17	136	263
STB18a	Kayan Sst (Matang/Serapi)	136	90	8	40	3	3	1	17	29	41	0	9	0	3	0	500	368	25.8	130	4	234	277
TB167	?Kayan Sst (Santubong)	180	119	17	39	0	5	0	7	21	19	0	93	0	0	0	500	407	18.6	86	5	316	355

STB50	Kayan Sst (Santubong)	129	73	19	76	36	16	30	21	41	71	0	7	0	0	0	500	493	1.4	226	46	221	333
STB48b	Kayan Sst (Santubong)	109	119	12	3	15	0	4	21	20	40	0	36	0	1	0	500	463	7.2	219	4	240	378
STB48a	Kayan Sst (Santubong)	124	148	35	102	31	3	2	0	27	20	0	8	0	0	0	500	492	1.6	180	5	307	440
TB63a	Kayan Sst (Kayan Syncline)	94	103	21	65	8	4	0	59	29	49	0	66	1	1	0	500	432	13.2	210	4	218	291
TB107	Kayan Sst (Kayan Syncline)	120	92	14	66	10	15	32	31	26	37	2	48	1	6	0	500	443	9.6	170	47	226	302
STB10	Kayan Sst (Kayan Syncline)	97	59	18	92	21	0	2	18	24	79	1	72	0	17	0	500	410	14.4	234	2	174	287
TB96	Kayan Sst (Kayan Syncline)	90	58	23	42	13	3	23	3	64	65	0	108	1	7	0	500	384	21.6	187	26	171	226
TB95b	Kayan Sst (Kayan Syncline)	125	84	5	73	14	4	55	10	12	28	2	69	1	8	0	500	420	13.8	137	69	214	301
TB92c	Kayan Sst (Kayan Syncline)	202	48	30	27	2	6	22	0	12	4	0	144	0	3	0	500	353	28.8	45	28	280	309
STB06	Kayan Sst (Kayan Syncline)	124	77	66	55	26	3	16	0	47	59	0	27	0	0	0	500	473	5.4	187	19	267	348
STB01	Kayan Sst (Kayan Syncline)	128	89	45	66	0	5	23	8	54	30	0	32	0	0	0	500	468	6.4	178	28	262	348
TB104	Kayan Sst (Kayan Syncline; base cgl)	71	59	7	72	31	0	0	33	46	65	1	100	0	15	0	500	384	20.0	247	0	137	240
TB99	Kayan Sst (Kayan Syncline; base cgl)	98	57	22	64	9	0	3	28	74	69	0	63	1	12	0	500	424	12.6	244	3	177	250

Table 2a

Sample	Formation	Zr (total)	Rutile	Brookite	Anatase	Garnet	Titanite	Tourmaline	Biotite	Cassiterite	Andalusite	Sillimanite	Kyanite	Apatite	Hornblende	Monazite	Chrome spinel	Hercynite	Pyx (augite)	Epidote	Clinozoisite	Actinolite	Chlorite	Chloritoid	Sphalerite	Siderite	Ankerite	Hypersthene	Enstatite	Jadeite	Mica	Serpentine	Allanite	Calcite	Wolframit	Huebnerite	Total translucent
TB																																				
22		9	4		1			4																												2
7	Tutoop Sst	2	7	1	2			2	4			1				1	9						1														1
TB		2																																			0
22		7	4		1			4																													4
3	Tutoop Sst	9	7	6	5	2		6	3							6				1	2																0
TB		1						1																													7
21		3	3	1	2			1												1																	3
5	Tutoop Sst	8	7	6	9		3	1	3						3	4				4			1	1													6
ST		1																																			0
B9		1	2		2			2																													2
5	Tutoop Sst	3	7	5	1	1		7	3						2		1			1																	0
ST		1																																			1
B8		9	3					5																													3
8	Tutoop Sst	8	1	7	4			5		1					2	4	3			3	1																0
TB		1																																			9
17	Bako-Mintu	1	3	1	1			7																													2
1	Sst	4	1	3	2			5		2		1				2				2												2					5
TB		1						1																													4
14	Bako-Mintu	3	2	1	1			0																													3
4	Sst	4	6	9	4			6							1	5	2			1												1					0
TB		1																																			9
21	Temudok	0	5		1			6																													2
8	Sst Mbr	0	1		2			8							4	3	2				3					4						3					5
TB						1																															0
21	Marup Sst	9	1		1	0		4																		1											3
7	Mbr	3	5		0	1	6	9									4			1	2		1			9			1						1	0
																																					2

TB210	Marup Sst Mbr	**86**	**32**	16	5			**94**				1	3	3	1			10	1					1				1						**254**
STB75b	Ngili Sst	**96**	**48**	13	18			**7**			2							3			1		6	9	1			1	1	1				**207**
STB75	Ngili Sst	**254**	**13**		9		4	**8**							2			7	1				16											**314**
TB119	Penrissen Sst	**53**	**2**		12	33	14	**22**				16					3	128	24			3	8		3		3							**324**
TB121	Penrissen Sst	**47**	**7**			53	11	**23**				28						339	58		4				2		4							**576**
TB89b	Kayan Sst (Pueh)	**93**	**47**	30	27	11	2	**28**					1					9	9															**257**
TB124b	Kayan Sst (Bungo Range)	**121**	**10**	1				**46**	4		1		3	1	1			10	10	1														**209**
STB24	Kayan Sst (Bungo Range)	**88**	**26**	4	10			**72**	2			1	1	2				2	1						4	3		3	8					**227**
STB21	Kayan Sst (Bungo Range)	**124**	**22**		12	4	2	**31**							24								2			2								**223**
STB20a	Kayan Sst (Bungo Range)	**86**	**45**	13	3	2		**25**										8	6		2	2	3		2				3					**200**
TB21	Kayan Sst (Matang/Serapi)	**26**	**8**					**2**	6	270						10								8				8			5	1	1	**343**
STB18b	Kayan Sst (Matang/Serapi)	**68**	**8**	6				**17**					1	2	1		2	1																**106**

STB18a	Kayan Sst (Matang/Serapi)	105	22	3	33			37												4	3					1											208
TB167	?Kayan Sst (Santubong)	46	90	36	3			0	1	5				7	1	1	2			21	1							1									215
STB50	Kayan Sst (Santubong)	110	38	4	1			101						3	3	2			2	6	5			1				1				2					279
STB48c	Kayan Sst (Santubong)	69	69	22	9		3	14		1						4	10			1								3									205
TB106	Kayan Sst (Kayan Syncline)	89	27	4	1		1	76						1		2				1			2		1												205
STB10	Kayan Sst (Kayan Syncline)	164	34	1	30			67	5			1	2							4								1									309
STB01	Kayan Sst (Kayan Syncline)	104	40	2	15			51							1		2						2		1												218

Table 2b

Sample	Formation	Zr (total)	Rutile	Brookite	Anatase	Garnet	Titanite	Tourmaline	Biotite	Cassiterite	Andalusite	Sillimanite	Kyanite	Apatite	Hornblende	Monazite	Chrome spinel	Hercynite	Pyx (augite)	Epidote	Clinozoisite	Actinolite	Chlorite	Chloritoid	Sphalerite	Siderite	Ankerite	Hypersthene	Enstatite	Jadeite	Mica	Serpentine	Allanite	Calcite	Wolframit	Huebnerite	Total translucent
TB		**43**	**2**	0	5				1			0				0							0														**1**
22		**.8**	**2.**	.	.			**2**	.			.				.	4.						.														**0**
7	Tutoop Sst	**1**	**4**	5	7	0	0	**0**	9	0	0	5	0	0	0	5	3	0	0	0	0	0	5	0	0	0	0	0	0	0	0	0	0	0	0	**0**
TB		**68**	**1**	1	3	0.		**1**	0							1				0.	0															**1**
22		**.5**	**1.**	.	.	4		**1.**	.							.	0.			2	.															**0**
3	Tutoop Sst	**5**	**5**	5	7	9	0	**3**	7	0	0	0	0	0	0	5	0	0	0	5	5	0	0	0	0	0	0	0	0	0	0	0	0	0	0	**0**
TB		**38**	**1**	4	8		0	**3**	0						0	1				3.			0	0													**1**
21		**.3**	**0.**	.	.		.	**0.**	.						.	.	0.			8			.	.													**0**
5	Tutoop Sst	**3**	**3**	4	1	0	8	**8**	8	0	0	0	0	0	8	1	0	0	0	9	0	0	3	3	0	0	0	0	0	0	0	0	0	0	0	**0**
ST		**56**	**1**	2				**1**	1																											**1**
B9		**.2**	**3.**	.	1	0.		**3.**	.								0.			0.																	**0**
5	Tutoop Sst	**2**	**4**	5	0	5	0	**4**	5	0	0	0	0	0	1	0	5	0	0	5	0	0	0	0	0	0	0	0	0	0	0	0	0	0	0	**0**
ST		**64**		2	1			**1**		0					0	1				0.	0															**1**
B8		**.0**	**1**	.	.			**7.**		.					.	.	1.			9	.															**0**
8	Tutoop Sst	**8**	**0**	3	3	0	0	**8**	0	3	0	0	0	0	6	3	0	0	0	7	3	0	0	0	0	0	0	0	0	0	0	0	0	0	0	**0**
TB		**44**	**1**	5	4			**2**		0		0				0				0.												0				**1**
17	Bako-Mintu	**.8**	**2.**	.	.			**9.**		.		.				.	0.			7												.				**0**
1	Sst	**8**	**2**	1	7	0	0	**5**	0	8	0	4	0	0	0	8	0	0	0	9	0	0	0	0	0	0	0	0	0	0	0	8	0	0	0	**0**
TB		**43**	**8.**	6	4			**3**							0	1				0.												0				**1**
14	Bako-Mintu	**.3**	**4**	.	.			**4.**							.	.	0.			3												.				**0**
4	Sst	**7**	**1**	1	5	0	0	**3**	0	0	0	0	0	0	3	6	6	0	0	2	0	0	0	0	0	0	0	0	0	0	0	3	0	0	0	**0**
TB			**2**		4			**2**							1	1					1					1						1				**1**
21	Temudok		**0.**		.			**7.**							.	.	0.				.					.						.				**0**
8	Sst Mbr	**40**	**4**	0	8	0	0	**2**	0	0	0	0	0	0	6	2	8	0	0	0	2	0	0	0	0	6	0	0	0	0	0	2	0	0	0	**0**
TB		**30**	**4.**		3	3		**1**												0.	0		0			6			0						0		**1**
21	Marup Sst	**.7**	**9**		.	3.		**6.**									1.			3	.		.			.			.						.		**0**
7	Mbr	**9**	**7**	0	3	4	2	**2**	0	0	0	0	0	0	0	0	3	0	0	3	7	0	3	0	0	3	0	0	3	0	0	0	0	0	3	0	**0**

TB		**33**	**1**	6										0	1	1				3.	0						0				0									**1**
21	Marup Sst	**.8**	**2.**	.				**3**						.	.	.	0.			9	.						.				.									**0**
0	Mbr	**6**	**6**	3	2	0	0	**7**	0	0	0	0	0	4	2	2	4	0	0	4	4	0	0	0	0	0	4	0	0	0	4	0	0	0	0	0				**0**
ST		**46**	**2**	6	8			**3.**												1.			0			2	4	0			0	0	0							**1**
B7		**.3**	**3.**	.	.			**3**									0.			4			.			.	.	.			.	.	.							**0**
5b	Ngili Sst	**8**	**2**	3	7	0	0	**8**	0	0	0	1	0	0	0	0	0	0	0	5	0	0	5	0	0	9	3	5	0	0	5	5	5	0	0	0				**0**
ST		**80**	**4.**		2		1	**2.**												2.	0					5													**1**
B7		**.8**	**1**		.		.	**5**									0.			2	.					.													**0**
5	Ngili Sst	**9**	**4**	0	9	0	3	**5**	0	0	0	0	0	0	0	0	6	0	0	3	3	0	0	0	0	1	0	0	0	0	0	0	0	0	0	0				**0**
TB		**16**	**0.**		3	1	4	**6.**						4					0	3	7			0		2		0		0									**1**
11	Penrissen	**.3**	**6**		.	0.	.	**7**						.			0.		.	9.	.			.		.		.		.									**0**
9	Sst	**6**	**2**	0	7	2	3	**9**	0	0	0	0	0	9	0	0	0	0	9	5	4	0	0	9	0	5	0	9	0	9	0	0	0	0	0	0				**0**
TB			**1.**				1	**3.**						4						5			0				0		0									**1**
12	Penrissen	**8.**	**2**			9.	.	**9**						.			0.			8.	1		.				.		.									**0**
1	Sst	**16**	**2**	0	0	2	9	**9**	0	0	0	0	0	9	0	0	0	0	0	9	0	0	7	0	0	0	0	3	0	7	0	0	0	0	0	0				**0**
TB		**36**	**1**			4.	0	**1**							0						3																		**1**
89	Kayan Sst	**.1**	**8.**	1	1	2	.	**0.**							.		0.			3.	.																		**0**
b	(Pueh)	**9**	**3**	2	1	8	8	**9**	0	0	0	0	0	0	4	0	0	0	0	5	5	0	0	0	0	0	0	0	0	0	0	0	0	0	0	0				**0**
TB	Kayan Sst	**57**	**4.**	0					1			0			1	0				4.	4	0																	**1**
12	(Bungo	**.8**	**7**	.				**2**	.			.			.	.	0.			7	.	.																	**0**
4b	Range)	**9**	**8**	5	0	0	0	**2**	9	0	0	5	0	0	4	5	5	0	0	8	8	5	0	0	0	0	0	0	0	0	0	0	0	0	0	0				**0**
ST	Kayan Sst	**38**	**1**	1	4			**3**	0					0	0	0				0.	0							1	1		1	3							**1**
B2	(Bungo	**.7**	**1.**	.	.			**1.**	.					.	.	.	0.			8	.							.	.		.	.							**0**
4	Range)	**7**	**5**	8	4	0	0	**7**	9	0	0	0	0	4	4	9	0	0	0	8	4	0	0	0	0	0	0	8	3	0	3	5	0	0	0	0				**0**
ST	Kayan Sst	**55**	**9.**		5	1.	0	**1**									1									0			0									**1**
B2	(Bungo	**.6**	**8**		.	7	.	**3.**									0.									.			.									**0**
1	Range)	**1**	**7**	0	4	9	9	**9**	0	0	0	0	0	0	0	0	8	0	0	0	0	0	0	0	0	9	0	0	9	0	0	0	0	0	0	0				**0**
ST	Kayan Sst		**2**	6	1			**1**																		1					1								**1**
B2	(Bungo		**2.**	.	.			**2.**									0.									.						.								**0**
0a	Range)	**43**	**5**	5	5	1	0	**5**	0	0	0	0	0	0	0	0	0	0	0	4	3	0	1	1	0	5	0	1	0	0	0	5	0	0	0	0				**0**
	Kayan Sst		**2.**					**0.**	1		7							2								2				2			1	0	0				**1**
TB	(Matang/Se	**7.**	**3**					**5**	.		8.						0.	.								.				.			.	.	.				**0**
21	rapi)	**58**	**3**	0	0	0	0	**8**	7	0	7	0	0	0	0	0	0	9	0	0	0	0	0	0	0	0	3	0	0	0	3	0	0	5	3	3				**0**
ST	Kayan Sst	**64**	**7.**	5											0	1			1	0.																		**1**
B1	(Matang/Se	**.1**	**5**	.				**1**							.	.	0.		.	9																		**0**
8b	rapi)	**5**	**5**	7	0	0	0	**6**	0	0	0	0	0	0	9	9	9	0	9	4	0	0	0	0	0	0	0	0	0	0	0	0	0	0	0	0				**0**

ST	Kayan Sst	**50**	**1**	1			**1**													**1.**	1				0															**1**
B1	(Matang/Se	**.4**	**0.**	.	1		**7.**									0.				**9**	.				.															**0**
8a	rapi)	**8**	**6**	4	6	0	0	**8**	0	0	0	0	0	0	0	0	0	0	0	**2**	4	0	0	0	0	5	0	0	0	0	0	0	0	0	0	0	0	0	0	0	**0**
TB	?Kayan Sst		**4**		1				0	2				3	0	0				**9.**	0							0												**1**
16	(Santubong	**21**	**1.**	1	.				.	.				.	.	.	0.			**7**	.							.												**0**
7	)	**.4**	**9**	7	4	0	0	**0**	5	3	0	0	0	3	5	5	9	0	0	**7**	5	0	0	0	0	0	0	5	0	0	0	0	0	0	0	0	0	0	0	0	**0**
ST	Kayan Sst	**39**	**1**	1	0			**3**						1	1	0			0	**2.**	1			0				0				0								**1**
B5	(Santubong	**.4**	**3.**	.	.			**6.**						.	.	.	0.		.	**1**	.			.				.				.								**0**
0	)	**3**	**6**	4	4	0	0	**2**	0	0	0	0	0	1	1	7	0	0	7	**5**	8	0	0	4	0	0	0	4	0	0	0	7	0	0	0	0	0	0	0	0	**0**
ST	Kayan Sst	**33**	**3**		4		1	**6.**		0										**0.**								1												**1**
B4	(Santubong	**.6**	**3.**	1	.		.	**8**		.							4.			**4**								.												**0**
8c	)	**6**	**7**	1	4	0	5	**3**	0	5	0	0	0	0	0	2	9	0	0	**9**	0	0	0	0	0	0	0	5	0	0	0	0	0	0	0	0	0	0	0	0	**0**
TB	Kayan Sst	**43**	**1**		0		0	**3**						0						**0.**					0																**1**
10	(Kayan	**.4**	**3.**		.		.	**7.**						.			0.			**4**					.																**0**
6	Syncline)	**1**	**2**	2	5	0	5	**1**	0	0	0	0	0	5	0	1	0	0	0	**9**	0	0	1	0	5	0	0	0	0	0	0	0	0	0	0	0	0	0	0	0	**0**
ST	Kayan Sst	**53**		0	9			**2**	1			0	0							**1.**								0												**1**
B1	(Kayan	**.0**	**1**	.	.			**1.**	.			.	.				0.			**2**								.												**0**
0	Syncline)	**7**	**1**	3	7	0	0	**7**	6	0	0	3	6	0	0	0	0	0	0	**9**	0	0	0	0	0	0	0	3	0	0	0	0	0	0	0	0	0	0	0	0	**0**
ST	Kayan Sst	**47**	**1**	0	6			**2**							0								0		0																**1**
B0	(Kayan	**.7**	**8.**	.	.			**3.**							.		0.						.		.																**0**
1	Syncline)	**1**	**3**	9	9	0	0	**4**	0	0	0	0	0	0	5	0	9	0	0	0	0	0	9	0	5	0	0	0	0	0	0	0	0	0	0	0	0	0	0	0	**0**

Table 3

Sample	Formation	Zr (colourless) euhedral	subhedral	anhedral	subrounded	rounded	Zr (colour) euhedral	subhedral	anhedral	subrounded	rounded	Zr (total)	Zr (sub-) angular (%)	Zr (sub-) rounded (%)	Tourmaline brown	green	blue	(rounded)	(other)	Tourmaline (total)	Tourmaline (other %)	Tourmaline (rounded %)
TB227	Tutoop Sst	12	15	18	18	8		6	3	5	7	92	**58.7**	**41.3**	38	2	2	16	26	42	**61.9**	**38.1**
TB223	Tutoop Sst	20	46	32	73	36	2	9	9	28	24	279	**42.3**	**57.7**	41	4	1	21	25	46	**54.3**	**45.7**
TB215	Tutoop Sst	14	32	23	29	22		1	2	7	8	138	**52.2**	**47.8**	101	7	3	43	68	111	**61.3**	**38.7**
STB95	Tutoop Sst	15	23	24	23	9	4	2	5	6	2	113	**64.6**	**35.4**	26		1	13	14	27	**51.9**	**48.1**
STB88	Tutoop Sst	29	51	22	44	20	3	7	3	11	8	198	**58.1**	**41.9**	47	4	4	23	32	55	**58.2**	**41.8**
TB171	Bako-Mintu Sst	8	26	27	21	9	1	5	5	7	5	114	**63.2**	**36.8**	65	7	3	21	54	75	**72.0**	**28.0**
TB144	Bako-Mintu Sst	16	27	29	20	13	1	4	5	9	10	134	**61.2**	**38.8**	89	12	5	43	63	106	**59.4**	**40.6**
TB218	Temudok Sst Mbr	11	22	20	17	9	1	4	5	6	5	100	**63.0**	**37.0**	45	18	5	26	42	68	**61.8**	**38.2**
TB217	Marup Sst Mbr	16	20	16	14	14	2		3		8	93	**61.3**	**38.7**	43		6	21	28	49	**57.1**	**42.9**
TB210	Marup Sst Mbr	5	15	11	22	13	2	5		8	5	86	**44.2**	**55.8**	81	9	4	33	61	94	**64.9**	**35.1**
STB75b	Ngili Sst	9	14	15	26	9	2	5		14	2	96	**46.9**	**53.1**	6	1		5	2	7	**28.6**	**71.4**
STB75	Ngili Sst	33	39	49	44	27	6	8	15	18	15	254	**59.1**	**40.9**	8			5	3	8	**37.5**	**62.5**
TB119	Penrissen Sst	8	12	6	2	10			6	4	5	53	**60.4**	**39.6**	21	1		9	13	22	**59.1**	**40.9**
TB121	Penrissen Sst	3	11	12	7	1		3	6	3	1	47	**74.5**	**25.5**	21	2		7	16	23	**69.6**	**30.4**
TB89b	Kayan Sst (Pueh)	15	31	16	19	1	2	3		4	2	93	**72.0**	**28.0**	20	5	3	13	15	28	**53.6**	**46.4**

TB124b	Kayan Sst (Bungo Range)	19	36	16	37	2		3		8		121	**61.2**	**38.8**	38	7	1	14	32	46	**69.6**	**30.4**
STB24	Kayan Sst (Bungo Range)	14	16	15	12	4	2	6	3	9	7	88	**63.6**	**36.4**	59	11	2	23	49	72	**68.1**	**31.9**
STB21	Kayan Sst (Bungo Range)	13	16	38	20	9	2	4	7	10	5	124	**64.5**	**35.5**	27	3	1	13	18	31	**58.1**	**41.9**
STB20a	Kayan Sst (Bungo Range)	16	24	31	8			3	2	2		86	**88.4**	**11.6**	19	6		10	15	25	**60.0**	**40.0**
TB21	Kayan Sst (Matang/Serapi)	6	2	1	2	2			1	6	6	26	**38.5**	**61.5**	2			2	2		**100.0**	**0.0**
STB18b	Kayan Sst (Matang/Serapi)	11	12	12	10	5	2	4	3	6	3	68	**64.7**	**35.3**	15	2		5	12	17	**70.6**	**29.4**
STB18a	Kayan Sst (Matang/Serapi)	14	21	28	16	6	2	6	4	6	2	105	**71.4**	**28.6**	31	6		12	25	37	**67.6**	**32.4**
TB167	?Kayan Sst (Santubong)	5	7	10	9	7	2			4	2	46	**52.2**	**47.8**						0		
STB50	Kayan Sst (Santubong)	10	20	30	20	5	2	4	3	12	4	110	**62.7**	**37.3**	87	12	2	35	66	101	**65.3**	**34.7**
STB48c	Kayan Sst (Santubong)	6	8	19	14	6	2	3	2	2	7	69	**58.0**	**42.0**	14			10	4	14	**28.6**	**71.4**
TB106	Kayan Sst (Kayan Syncline)	6	14	17	18	14		4	2	6	8	89	**48.3**	**51.7**	61	14	1	32	44	76	**57.9**	**42.1**
STB10	Kayan Sst (Kayan Syncline)	18	32	30	26	28	2	6	4	7	11	164	**56.1**	**43.9**	62	5		28	39	67	**58.2**	**41.8**
STB01	Kayan Sst (Kayan Syncline)	12	24	19	20	9	3	3	3	6	5	104	**61.5**	**38.5**	48	3		21	30	51	**58.8**	**41.2**

Table 4

Sample	Formation	Zircon	Rutile	Anatase	Brookite	Tourmaline	Apatite	Garnet	Chrome spinel	Monazite	Total HM (translucent)	ZTR	ZTi	GZi	ATi	RZi	RuZi (only Rutile)	CZi	MZi
TB227	**Tutoop Sst**	92	47	12	1	42	0	0	9	1	210	86.19	68.66	0.00	0.00	39.47	33.81	8.91	1.08
TB223	**Tutoop Sst**	279	47	15	6	46	0	2	0	6	407	91.40	85.85	0.71	0.00	19.60	14.42	0.00	2.11
TB215	**Tutoop Sst**	138	37	29	16	111	0	0	0	4	360	79.44	55.42	0.00	0.00	37.27	21.14	0.00	2.82
STB95	**Tutoop Sst**	113	27	21	5	27	0	1	1	0	201	83.08	80.71	0.88	0.00	31.93	19.29	0.88	0.00
STB88	**Tutoop Sst**	198	31	4	7	55	0	0	3	4	309	91.91	78.26	0.00	0.00	17.50	13.54	1.49	1.98
TB171	**Bako-Mintu Sst**	114	31	12	13	75	0	0	0	2	254	86.61	60.32	0.00	0.00	32.94	21.38	0.00	1.72
TB144	**Bako-Mintu Sst**	134	26	14	19	106	0	0	2	5	309	86.08	55.83	0.00	0.00	30.57	16.25	1.47	3.60
TB218	**Silantek**	100	51	12	0	68	0	0	2	3	250	87.60	59.52	0.00	0.00	38.65	33.77	1.96	2.91
TB217	**Silantek**	93	15	10	0	49	0	101	4	0	302	51.99	65.49	52.06	0.00	21.19	13.89	4.12	0.00
TB210	**Silantek**	86	32	5	16	94	1	0	1	3	254	83.46	47.78	0.00	1.05	38.13	27.12	1.15	3.37
STB75b	**Ngili Sst**	96	48	18	13	7	0	0	0	0	207	72.95	93.20	0.00	0.00	45.14	33.33	0.00	0.00
STB75	**Ngili Sst**	254	13	9	0	8	0	0	2	0	314	87.58	96.95	0.00	0.00	7.97	4.87	0.78	0.00
TB119	**Penrissen Sst**	53	2	12	0	22	16	33	0	0	324	23.77	70.67	38.37	42.11	20.90	3.64	0.00	0.00
TB121	**Penrissen Sst**	47	7	0	0	23	28	53	0	0	576	13.37	67.14	53.00	54.90	12.96	12.96	0.00	0.00
TB89b	**Kayan Sst (Pueh)**	93	47	27	30	28	0	11	0	0	257	65.37	76.86	10.58	0.00	52.79	33.57	0.00	0.00
TB124b	**Kayan Sst (Bungo Range)**	121	10	0	1	46	0	0	1	1	209	84.69	72.46	0.00	0.00	8.33	7.63	0.82	0.82
STB24	**Kayan Sst (Bungo Range)**	88	26	10	4	72	1	0	0	2	227	81.94	55.00	0.00	1.37	31.25	22.81	0.00	2.22
STB21	**Kayan Sst (Bungo Range)**	124	22	12	0	31	0	4	24	0	223	79.37	80.00	3.13	0.00	21.52	15.07	16.22	0.00
STB20a	**Kayan Sst (Bungo Range)**	86	45	3	13	19	0	2	0	0	200	75.00	81.90	2.27	0.00	41.50	34.35	0.00	0.00
TB21	**Kayan Sst (Matang/Serapi)**	26	8	0	0	2	0	0	0	0	343	10.50	92.86	0.00	0.00	23.53	23.53	0.00	0.00
STB18b	**Kayan Sst (Matang/Serapi)**	68	8	0	6	17	0	0	1	2	106	87.74	80.00	0.00	0.00	17.07	10.53	1.45	2.86
STB18a	**Kayan Sst (Matang/Serapi)**	105	22	33	3	37	0	0	0	0	208	78.85	73.94	0.00	0.00	35.58	17.32	0.00	0.00

TB167	**?Kayan Sst (Santubong)**	46	90	3	36	0	7	0	2	1	215	63.26	100.00	0.00	100.00	73.71	66.18	4.17	2.13
STB50	**Kayan Sst (Santubong)**	110	38	1	4	101	3	0	0	3	279	89.25	52.13	0.00	2.88	28.10	25.68	0.00	2.65
STB48c	**Kayan Sst (Santubong)**	69	69	9	22	14	0	0	10	4	205	74.15	83.13	0.00	0.00	59.17	50.00	12.66	5.48
TB106	**Kayan Sst (Kayan Syncline)**	89	27	1	4	76	1	0	0	2	205	93.66	53.94	0.00	1.30	26.45	23.28	0.00	2.20
STB10	**Kayan Sst (Kayan Syncline)**	164	34	30	1	67	0	0	0	0	309	85.76	71.00	0.00	0.00	28.38	17.17	0.00	0.00
STB01	**Kayan Sst (Kayan Syncline)**	104	40	15	2	51	0	0	2	0	218	89.45	67.10	0.00	0.00	35.40	27.78	1.89	0.00

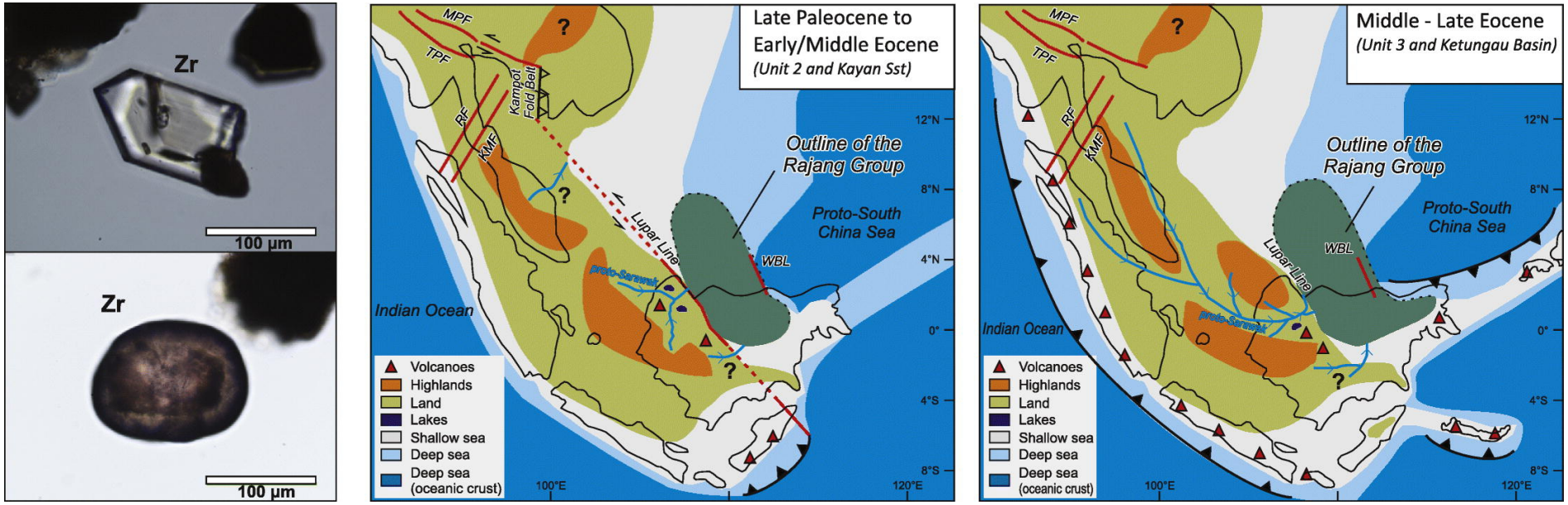

Graphics Abstract

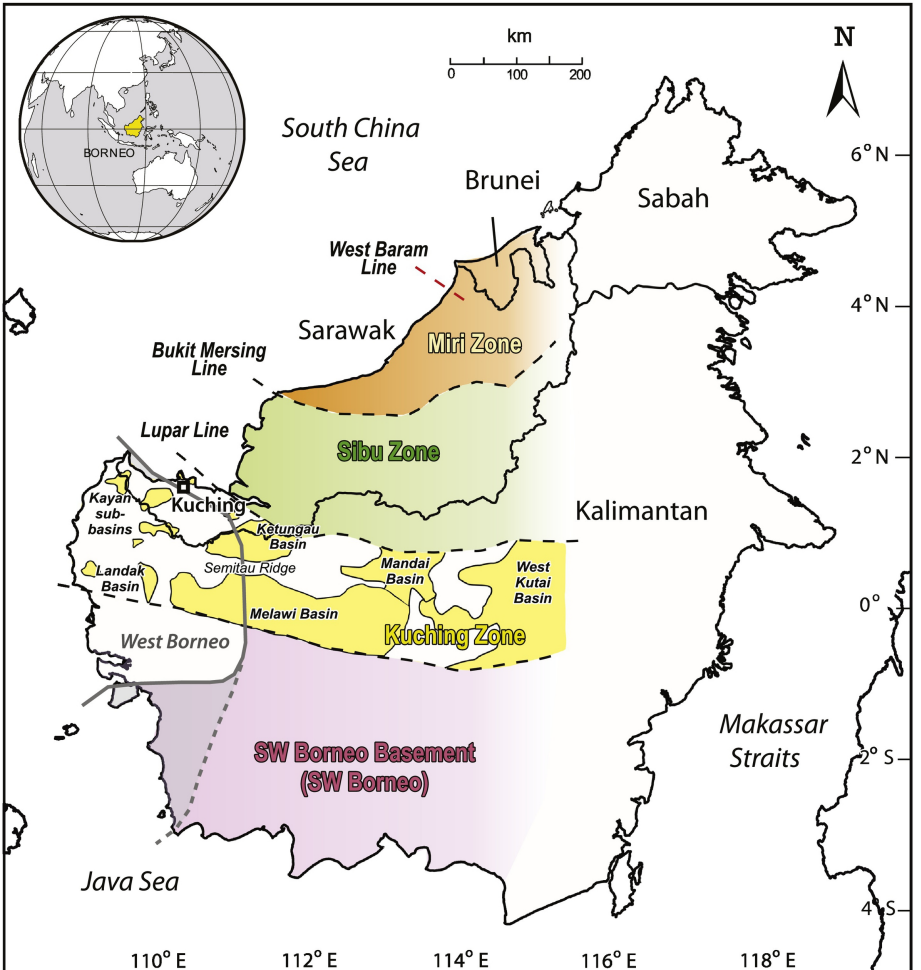
BORNEO
km
0
100
200
N
South China Sea
Brunei
Sabah
West Baram Line
Sarawak
Miri Zone
Bukit Mersing Line
Lupar Line
Sibu Zone
Kuching
Kayan sub-basins
Ketungau Basin
Kalimantan
Semitau Ridge
Mandai Basin
West Kutai Basin
Landak Basin
Melawi Basin
Kuching Zone
West Borneo
Makassar Straits
SW Borneo Basement (SW Borneo)
Java Sea
6° N
4° N
2° N
0°
2° S
4° S
110° E
112° E
114° E
116° E
118° E

Figure 1

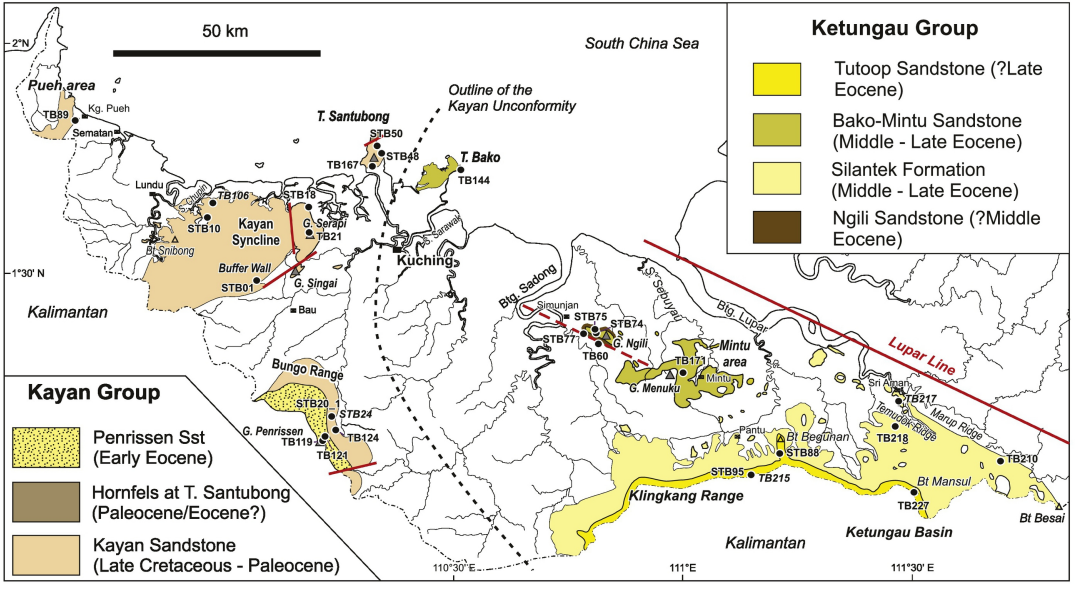
50 km
2°N
1°30' N
110°30' E
111°E
111°30' E
South China Sea
Kalimantan
Kalimantan
Outline of the
Kayan Unconformity
Pueh area
Kg. Pueh
TB89
Sematan
Lundu
Gunung
TB106
STB16
STB10
Kayan
Syncline
G. Serabi
TB21
Bt Snibong
Buffer Wall
STB01
G. Singai
Bau
T. Santubong
STB50
STB48
TB167
T. Bako
TB144
Sarawak
Kuching
Bung Sadong
Simunjan
STB75
STB74
STB77
TB60
G. Ngili
Mintu
area
TB171
Mintu
G. Menuku
Bung Lupar
Lupar Line
Sri Aman
TB217
Temurun Ridge
Marup Ridge
Pantu
Bt Begunan
STB88
TB218
TB210
STB95
TB215
Bt Mansul
TB227
Bt Besai
Klingkang Range
Ketungau Basin
Bungo Range
STB20
STB24
G. Penrissen
TB119
TB124
TB121
Ketungau Group
Tutoop Sandstone (?Late Eocene)
Bako-Mintu Sandstone (Middle - Late Eocene)
Silantek Formation (Middle - Late Eocene)
Ngili Sandstone (?Middle Eocene)
Kayan Group
Penrissen Sst (Early Eocene)
Hornfels at T. Santubong (Paleocene/Eocene?)
Kayan Sandstone (Late Cretaceous - Paleocene)

Figure 2

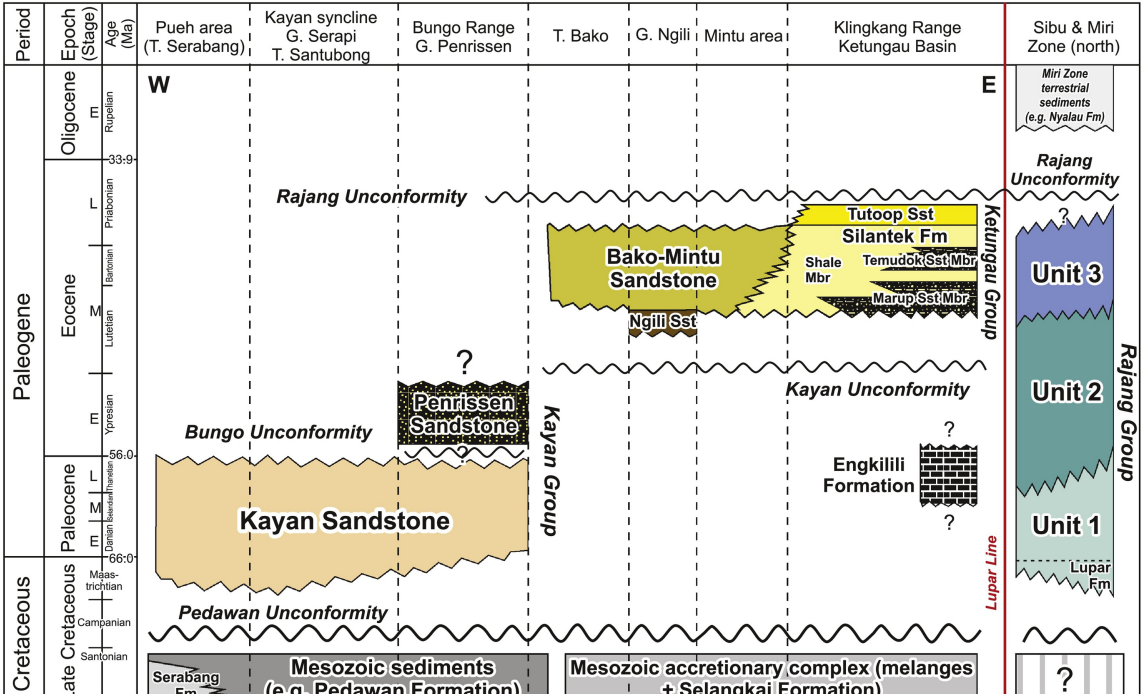
Period
Epoch (Stage)
Age (Ma)
Pueh area (T. Serabang)
Kayan syncline G. Serapi T. Santubong
Bungo Range G. Penrissen
T. Bako
G. Ngili
Mintu area
Klingkang Range Ketungau Basin
Sibu & Miri Zone (north)
Paleogene
Cretaceous
Oligocene
Eocene
Paleocene
Late Cretaceous
Rupelian
Priabonian
Bartonian
Lutetian
Ypresian
Thanetian
Selandian
Danian
Maas-trichtian
Campanian
Santonian
33.9
56.0
66.0
W
E
Miri Zone terrestrial sediments (e.g. Nyalau Fm)
Rajang Unconformity
Tutoop Sst
Silantek Fm
Shale Mbr
Temudok Sst Mbr
Marup Sst Mbr
Bako-Mintu Sandstone
Ngili Sst
Ketungau Group
Unit 3
Unit 2
Unit 1
Rajang Group
Lupar Fm
Penrissen Sandstone
Kayan Unconformity
Bungo Unconformity
Kayan Group
Kayan Sandstone
Engkilili Formation
Lupar Line
Pedawan Unconformity
Serabang Fm
Mesozoic sediments (e.g. Pedawan Formation)
Mesozoic accretionary complex (melanges + Selangkai Formation)

Figure 3

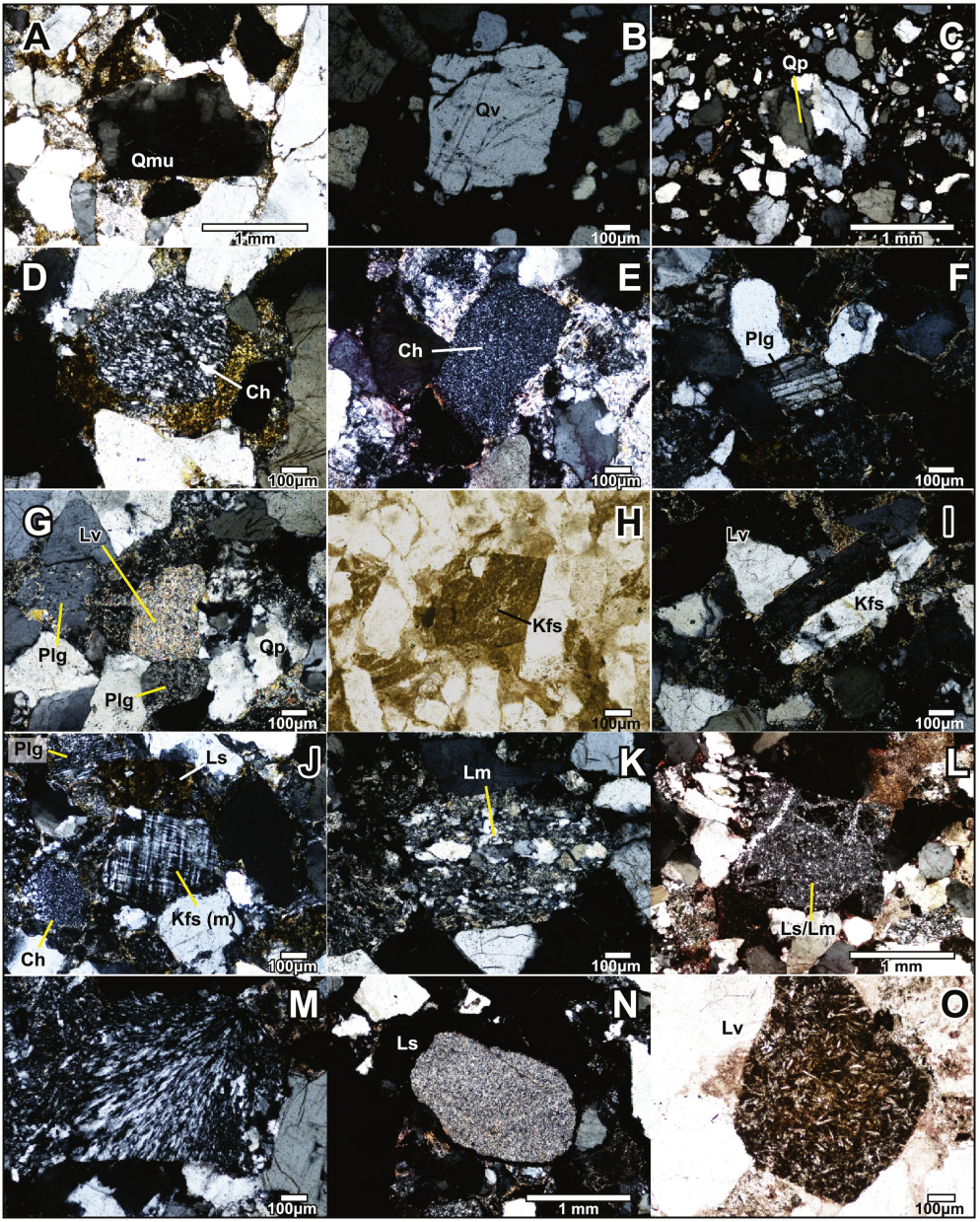
A
Qmu
1 mm
B
Qv
100µm
C
Qp
1 mm
D
Ch
100µm
E
Ch
100µm
F
Plg
100µm
G
Lv
Plg
Qp
Plg
100µm
H
Kfs
100µm
I
Lv
Kfs
100µm
Plg
Ls
J
Kfs (m)
Ch
100µm
K
Lm
100µm
L
Ls/Lm
1 mm
M
100µm
N
Ls
1 mm
O
Lv
100µm

Figure 4

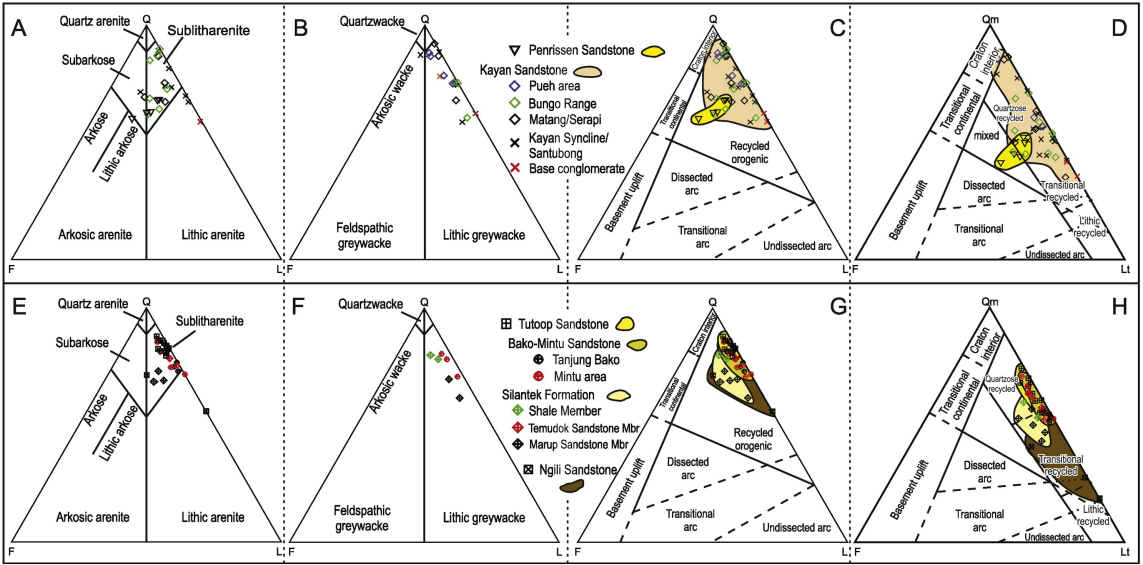
A
Quartz arenite
Q
Sublitharenite
Subarkose
Arkose
Lithic arkose
Arkosic arenite
Lithic arenite
F
L
B
Quartzwacke
Arkosic wacke
Feldspathic greywacke
Lithic greywacke
Penrissen Sandstone
Kayan Sandstone
Pueh area
Bungo Range
Matang/Serapi
Kayan Syncline/ Santubong
Base conglomerate
C
Craton interior
Transitional continental
Recycled orogenic
Basement uplift
Dissected arc
Transitional arc
Undissected arc
D
Qm
Lt
Quartzose recycled
mixed
Transitional recycled
Lithic recycled
E
F
G
H
Tutoop Sandstone
Bako-Mintu Sandstone
Tanjung Bako
Mintu area
Silantek Formation
Shale Member
Temudok Sandstone Mbr
Marup Sandstone Mbr
Ngili Sandstone

Figure 5

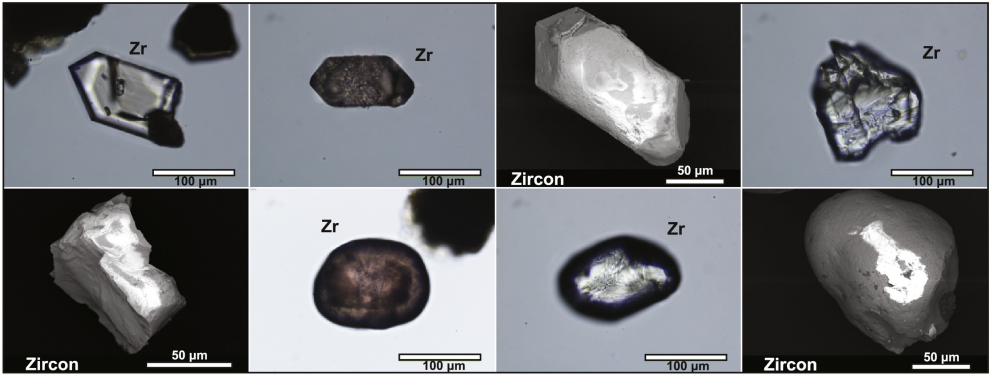
Zr
100 µm
Zr
100 µm
Zircon
50 µm
Zr
100 µm
Zircon
50 µm
Zr
100 µm
Zr
100 µm
Zircon
50 µm

Figure 6

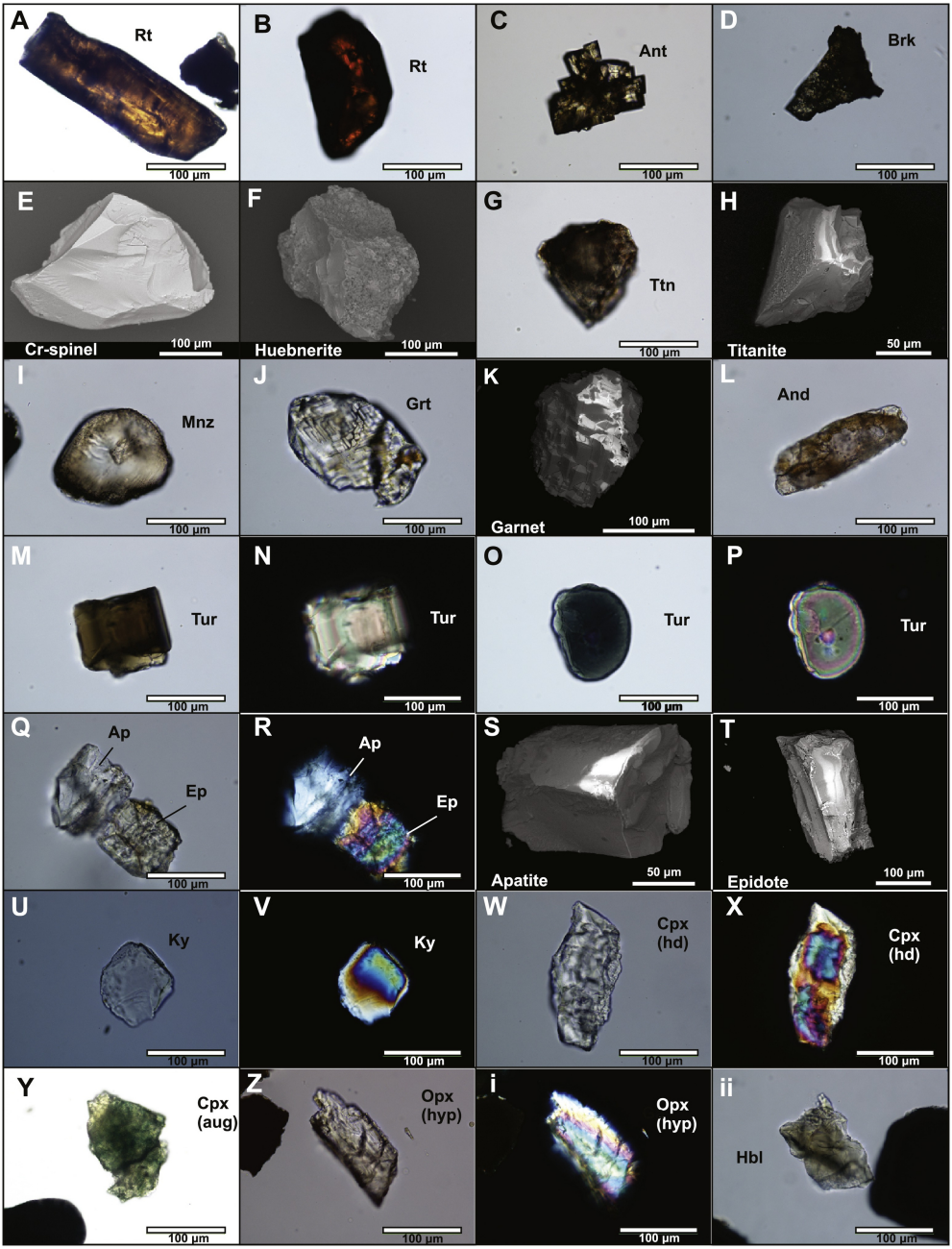
A
Rt
100 µm
B
Rt
100 µm
C
Ant
100 µm
D
Brk
100 µm
E
Cr-spinel
100 µm
F
Huebnerite
100 µm
G
Ttn
100 µm
H
Titanite
50 µm
I
Mnz
100 µm
J
Grt
100 µm
K
Garnet
100 µm
L
And
100 µm
M
Tur
100 µm
N
Tur
100 µm
O
Tur
100 µm
P
Tur
100 µm
Q
Ap
Ep
100 µm
R
Ap
Ep
100 µm
S
Apatite
50 µm
T
Epidote
100 µm
U
Ky
100 µm
V
Ky
100 µm
W
Cpx
(hd)
100 µm
X
Cpx
(hd)
100 µm
Y
Cpx
(aug)
100 µm
Z
Opx
(hyp)
100 µm
i
Opx
(hyp)
100 µm
ii
Hbl
100 µm

Figure 7

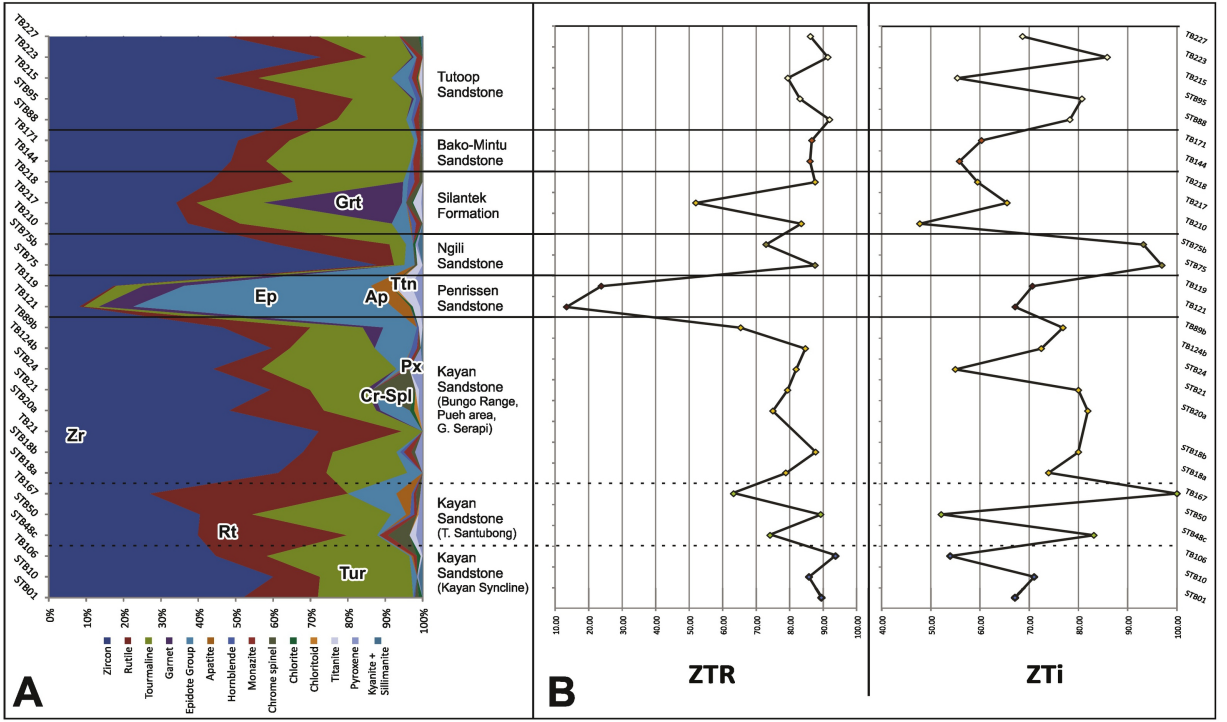
TB227
TB223
TB215
STB95
STB88
TB171
TB144
TB218
TB217
TB210
STB75b
STB75
TB119
TB121
TB88b
TB124b
STB24
TB21
STB20a
TB31
STB18b
STB18a
TB167
STB50
STB48c
TB106
STB10
STB01
Tutoop Sandstone
Bako-Mintu Sandstone
Silantek Formation
Ngili Sandstone
Penrissen Sandstone
Kayan Sandstone (Bungo Range, Pueh area, G. Serapi)
Kayan Sandstone (T. Santubong)
Kayan Sandstone (Kayan Syncline)
Grt
Ep
Ttn
Ap
Px
Cr-Spl
Zr
Rt
Tur
0%
10%
20%
30%
40%
50%
60%
70%
80%
90%
100%
Zircon
Rutile
Tourmaline
Garnet
Epidote Group
Apatite
Hornblende
Monazite
Chrome spinel
Chlorite
Chloritoid
Titanite
Pyroxene
Kyanite + Sillimanite
A
10.00
20.00
30.00
40.00
50.00
60.00
70.00
80.00
90.00
100.00
ZTR
B
40.00
50.00
60.00
70.00
80.00
90.00
100.00
ZTi

Figure 8

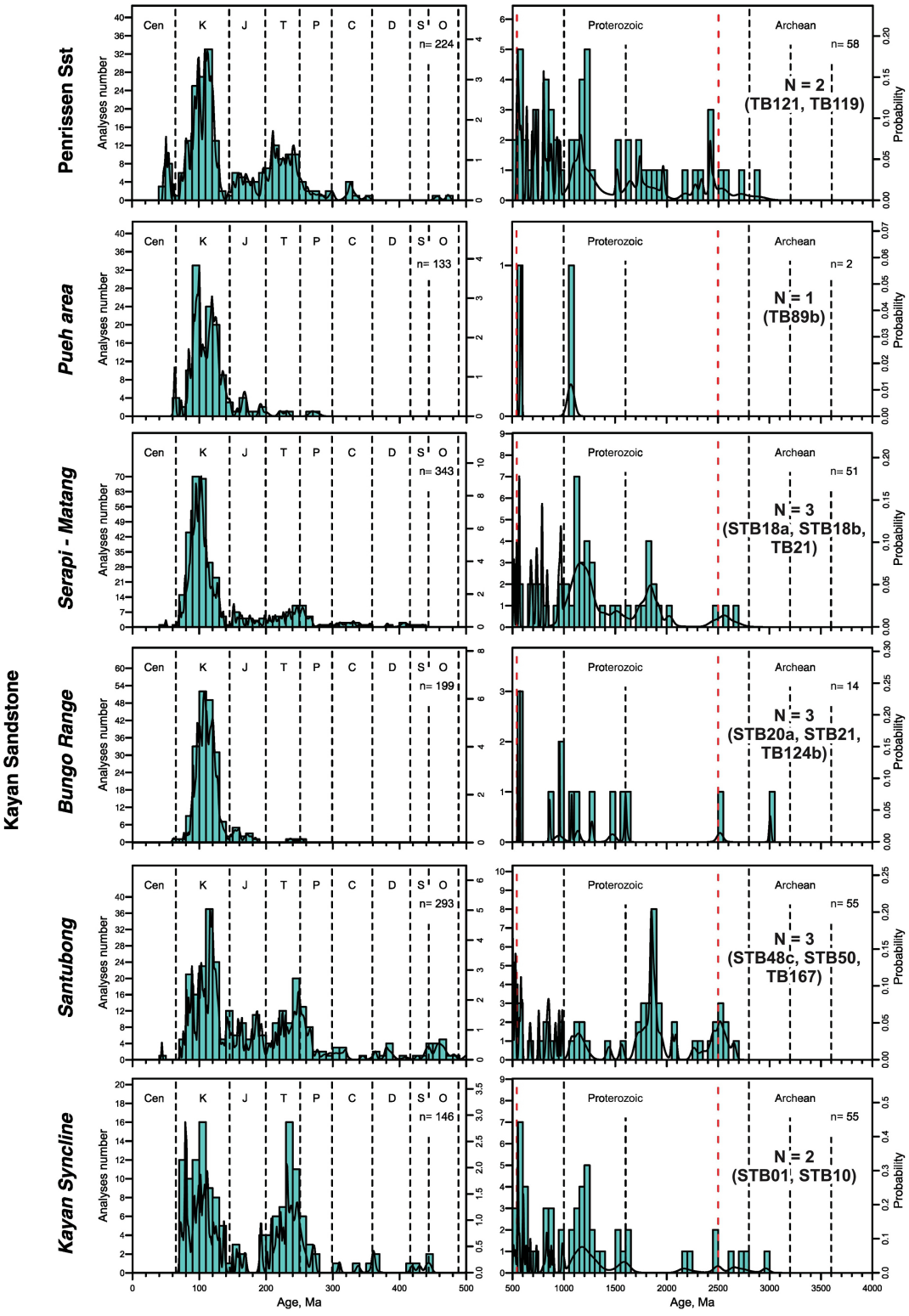
Kayan Sandstone
Penrissen Sst
Pueh area
Serapi - Matang
Bungo Range
Santubong
Kayan Syncline
Cen
K
J
T
P
C
D
S
O
Proterozoic
Archean
n= 224
n= 58
N = 2
(TB121, TB119)
n= 133
n= 2
N = 1
(TB89b)
n= 343
n= 51
N = 3
(STB18a, STB18b,
TB21)
n= 199
n= 14
N = 3
(STB20a, STB21,
TB124b)
n= 293
n= 55
N = 3
(STB48c, STB50,
TB167)
n= 146
n= 55
N = 2
(STB01, STB10)
Analyses number
Probability
Age, Ma

Figure 9

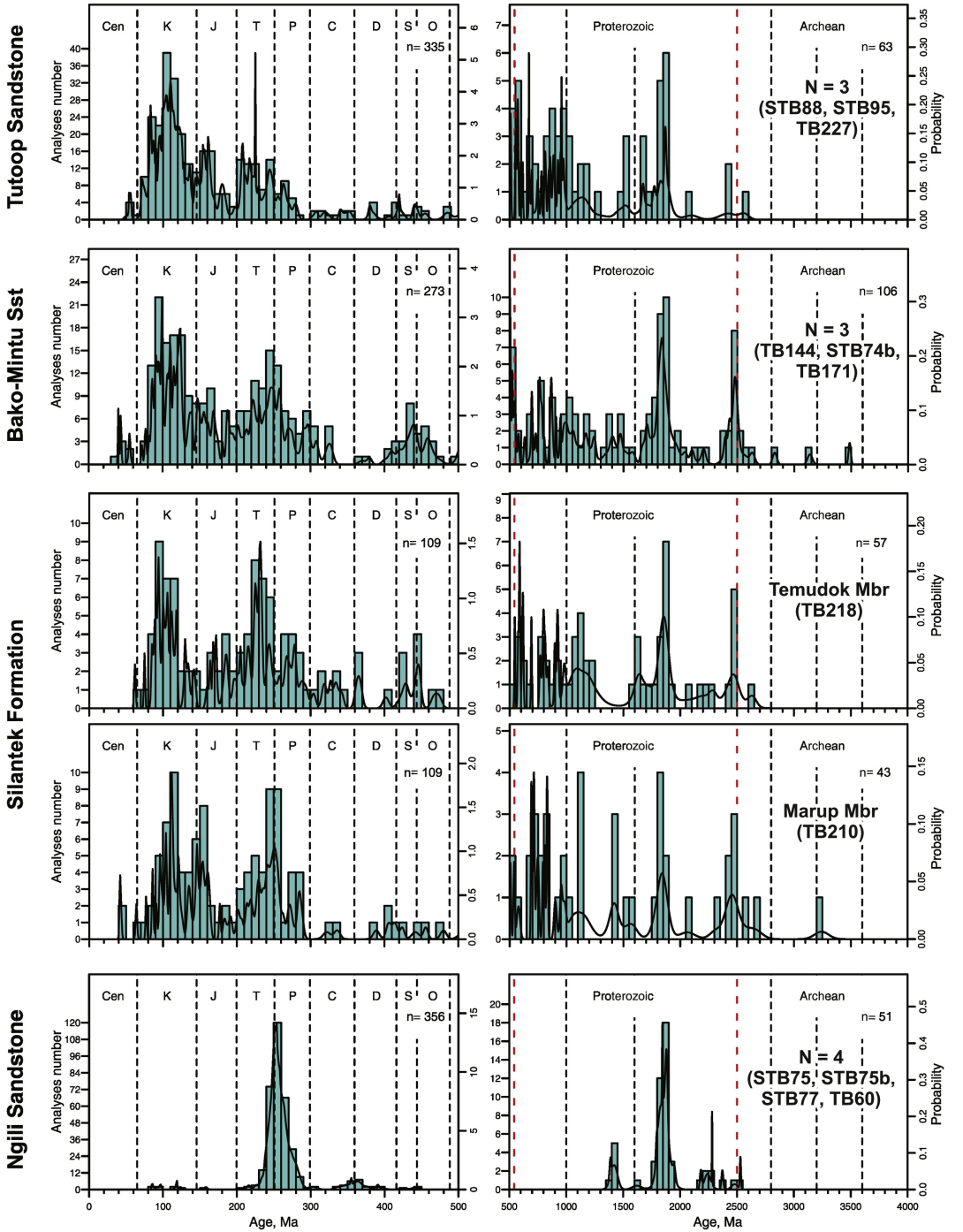
Tutoop Sandstone
Bako-Mintu Sst
Silantek Formation
Ngili Sandstone
Cen
K
J
T
P
C
D
S
O
Proterozoic
Archean
Analyses number
Probability
n= 335
n= 63
N = 3
(STB88, STB95,
TB227)
n= 273
n= 106
N = 3
(TB144, STB74b,
TB171)
n= 109
n= 57
Temudok Mbr
(TB218)
n= 109
n= 43
Marup Mbr
(TB210)
n= 356
n= 51
N = 4
(STB75, STB75b,
STB77, TB60)
Age, Ma

Figure 10

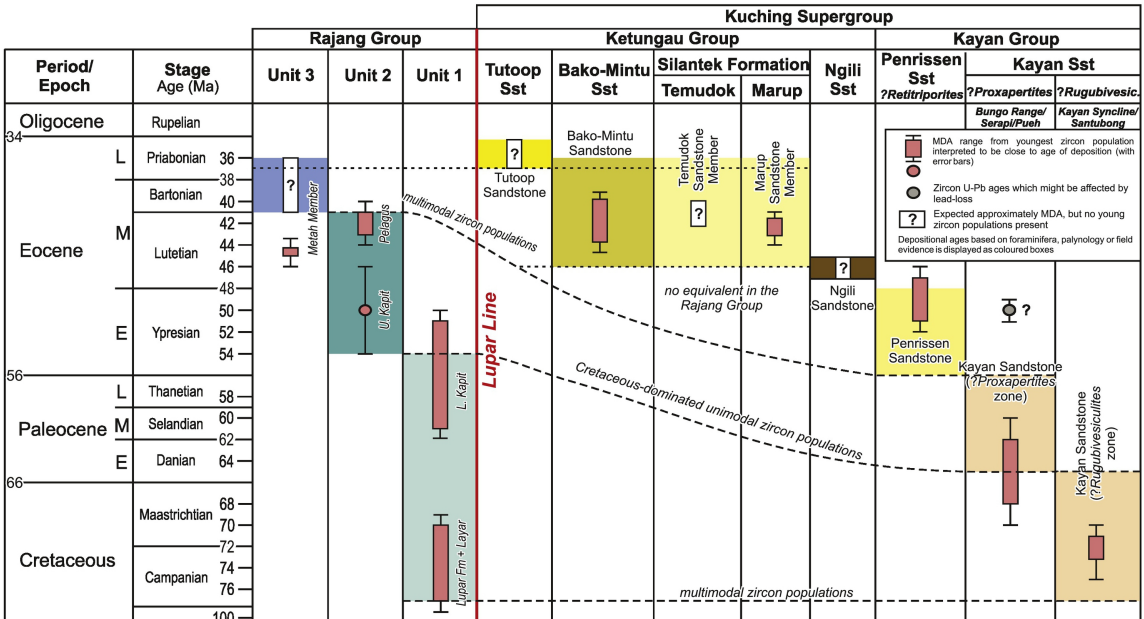
Kuching Supergroup
Rajang Group
Ketungau Group
Kayan Group
Period/ Epoch
Stage Age (Ma)
Unit 3
Unit 2
Unit 1
Tutoop Sst
Bako-Mintu Sst
Silantek Formation
Temudok
Marup
Ngili Sst
Penrissen Sst
?Retitriporites
Kayan Sst
?Proxapertites
?Rugubivesic.
Bungo Range/ Serapi/Pueh
Kayan Syncline/ Santubong
Oligocene
Rupelian
34
Eocene
L
M
E
Priabonian
Bartonian
Lutetian
Ypresian
36
38
40
42
44
46
48
50
52
54
56
Paleocene
L
M
E
Thanetian
Selandian
Danian
58
60
62
64
66
Cretaceous
Maastrichtian
Campanian
68
70
72
74
76
100
Metah Member
Pelagus
U. Kapit
L. Kapit
Lupar Fm + Layar
Tutoop Sandstone
Bako-Mintu Sandstone
Temudok Sandstone Member
Marup Sandstone Member
Ngili Sandstone
Penrissen Sandstone
Kayan Sandstone (?Proxapertites zone)
Kayan Sandstone (?Rugubivesiculites zone)
Lupar Line
multimodal zircon populations
no equivalent in the Rajang Group
Cretaceous-dominated unimodal zircon populations
multimodal zircon populations
MDA range from youngest zircon population interpreted to be close to age of deposition (with error bars)
Zircon U-Pb ages which might be affected by lead-loss
Expected approximately MDA, but no young zircon populations present
Depositional ages based on foraminifera, palynology or field evidence is displayed as coloured boxes

Figure 11

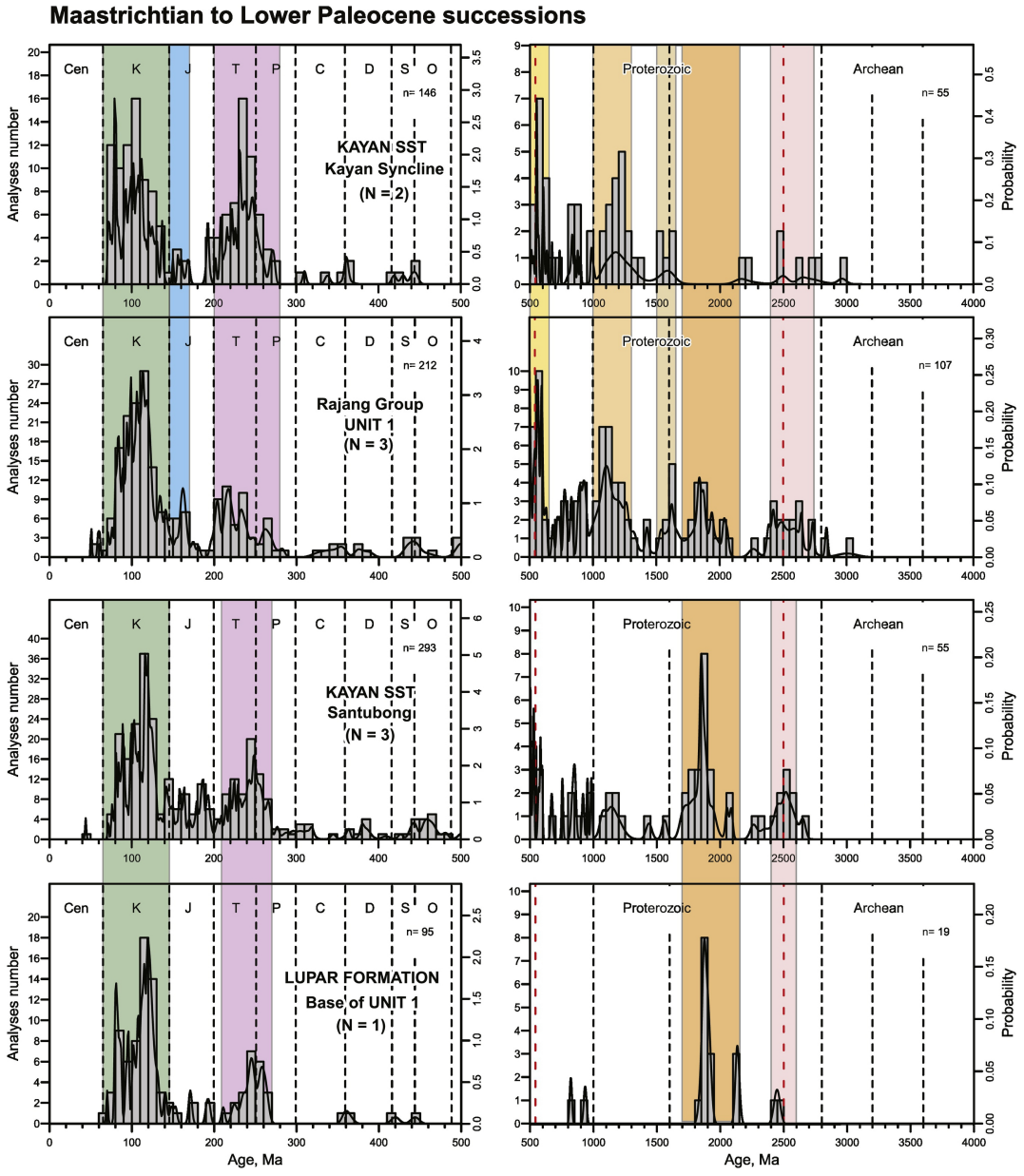
Maastrichtian to Lower Paleocene successions
Cen
K
J
T
P
C
D
S
O
n= 146
KAYAN SST
Kayan Syncline
(N = 2)
Proterozoic
Archean
n= 55
Analyses number
Probability
n= 212
Rajang Group
UNIT 1
(N = 3)
n= 107
n= 293
KAYAN SST
Santubong
(N = 3)
n= 55
n= 95
LUPAR FORMATION
Base of UNIT 1
(N = 1)
n= 19
Age, Ma

Figure 12

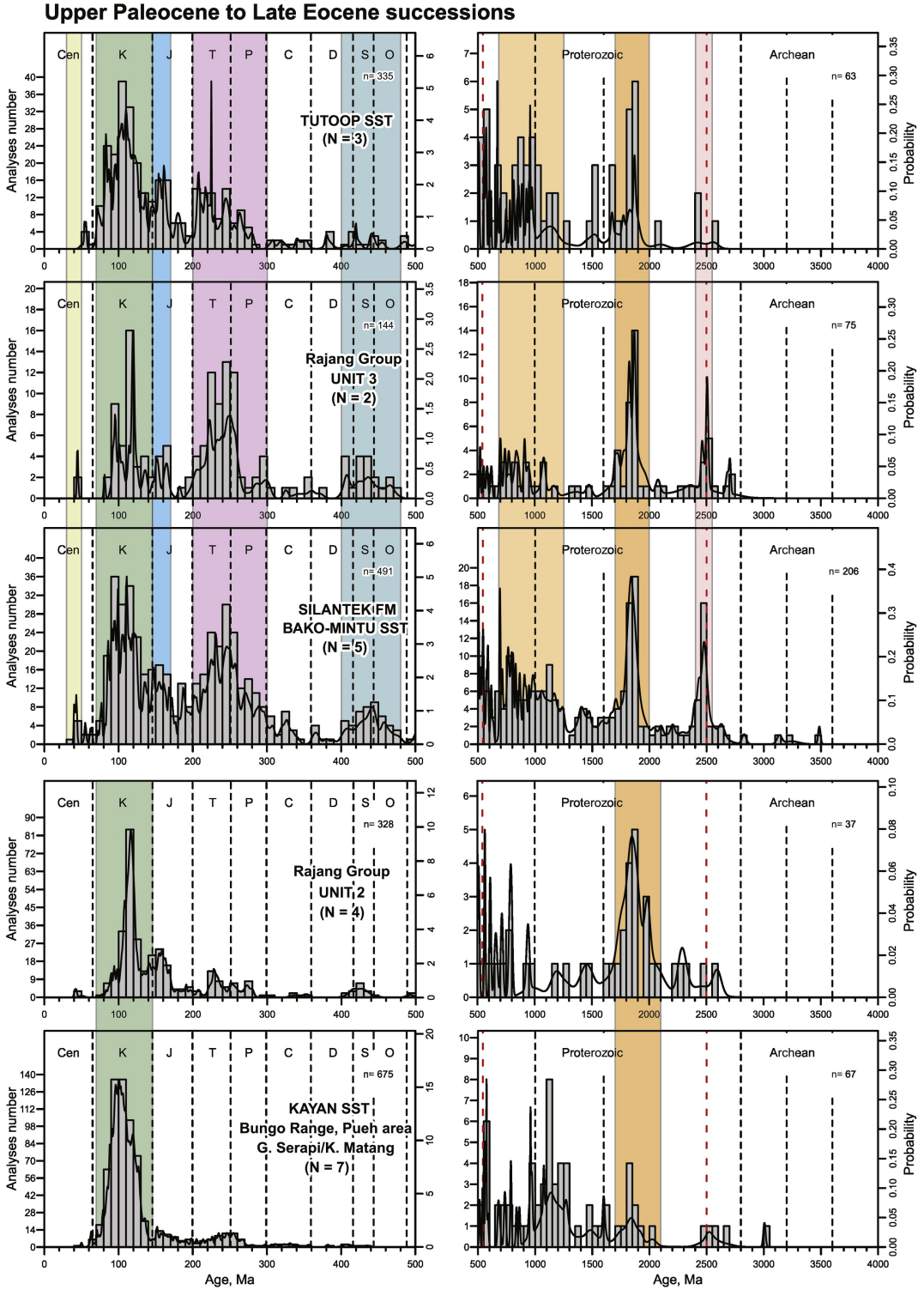
Upper Paleocene to Late Eocene successions
Cen
K
J
T
P
C
D
S
O
n= 335
TUTOOP SST
(N = 3)
n= 144
Rajang Group
UNIT 3
(N = 2)
n= 491
SILANTEK FM
BAKO-MINTU SST
(N = 5)
n= 328
Rajang Group
UNIT 2
(N = 4)
n= 675
KAYAN SST
Bungo Range, Pueh area
G. Serapi/K. Matang
(N = 7)
Proterozoic
Archean
n= 63
n= 75
n= 206
n= 37
n= 67
Analyses number
Probability
Age, Ma

Figure 13

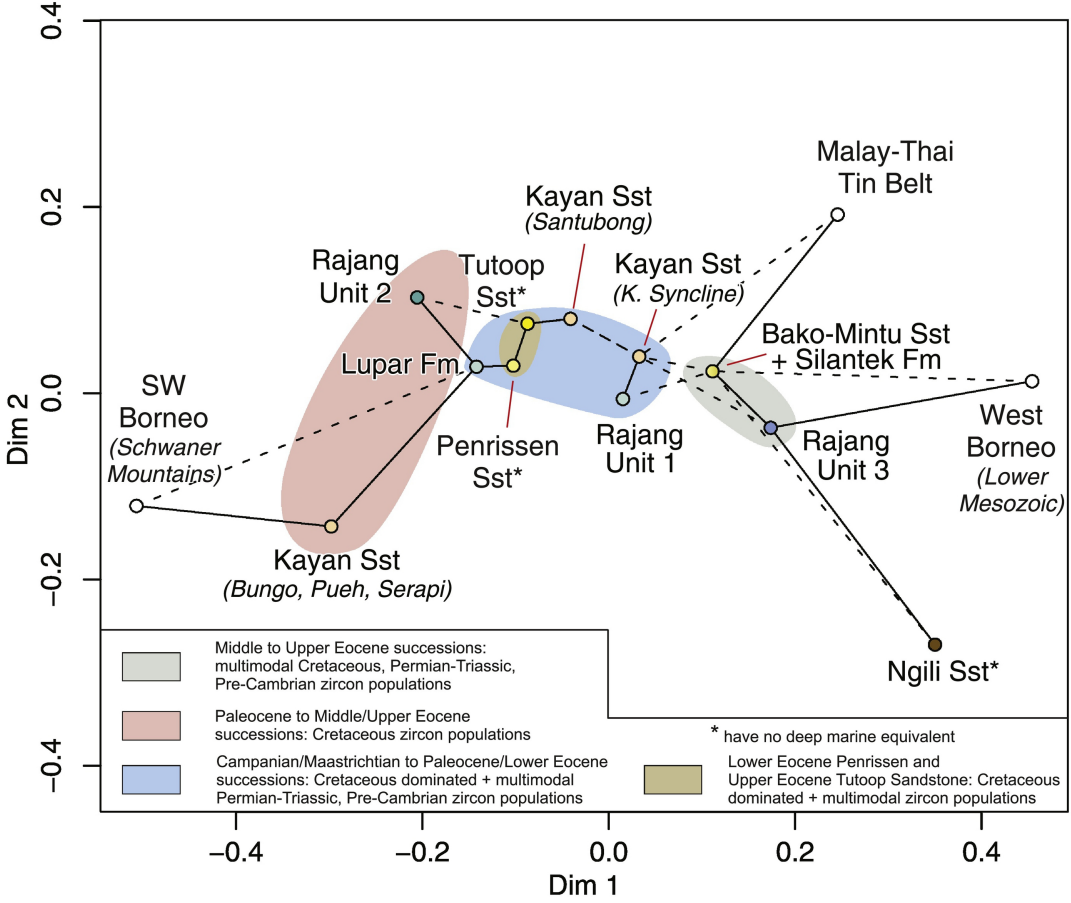
Malay-Thai
Tin Belt
Kayan Sst
(Santubong)
Rajang
Unit 2
Tutoop
Sst*
Kayan Sst
(K. Syncline)
Bako-Mintu Sst
+ Silantek Fm
Lupar Fm.
SW
Borneo
(Schwaner
Mountains)
Penrissen
Sst*
Rajang
Unit 1
Rajang
Unit 3
West
Borneo
(Lower
Mesozoic)
Kayan Sst
(Bungo, Pueh, Serapi)
Ngili Sst*
Middle to Upper Eocene successions:
multimodal Cretaceous, Permian-Triassic,
Pre-Cambrian zircon populations
Paleocene to Middle/Upper Eocene
successions: Cretaceous zircon populations
Campanian/Maastrichtian to Paleocene/Lower Eocene
successions: Cretaceous dominated + multimodal
Permian-Triassic, Pre-Cambrian zircon populations
* have no deep marine equivalent
Lower Eocene Penrissen and
Upper Eocene Tutoop Sandstone: Cretaceous
dominated + multimodal zircon populations
Dim 2
0.4
0.2
0.0
−0.2
−0.4
−0.4
−0.2
0.0
0.2
0.4
Dim 1

Figure 14

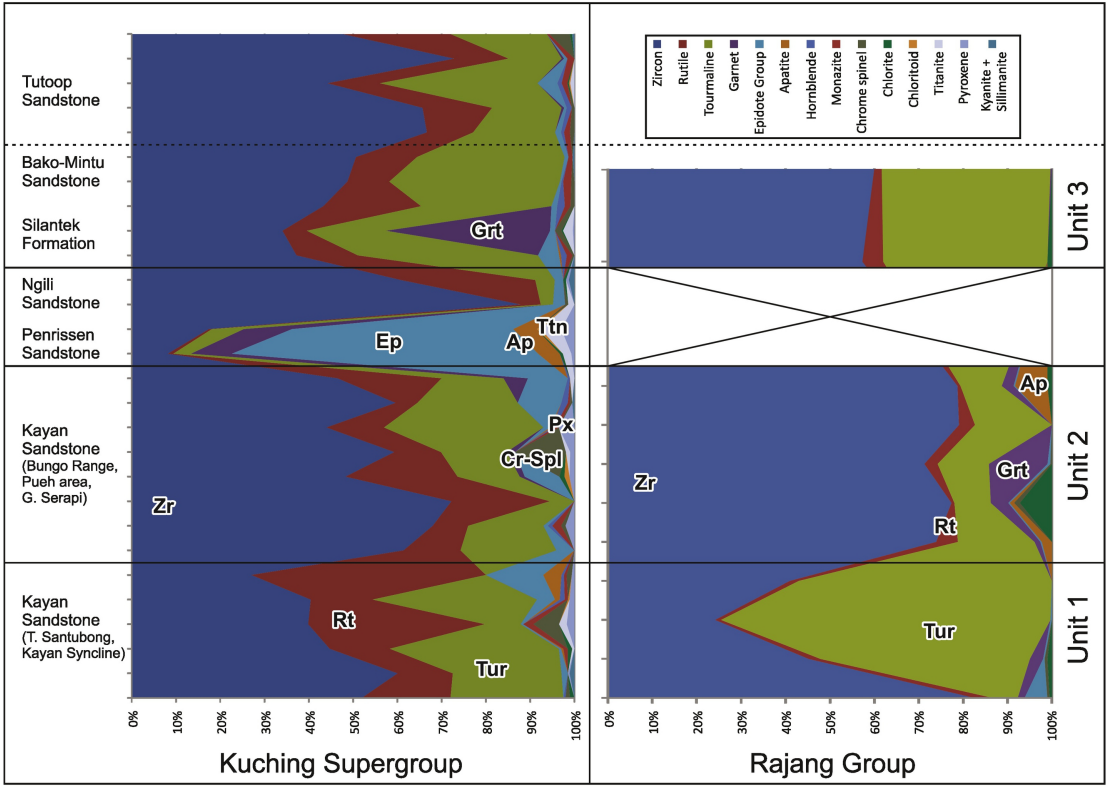
Zircon
Rutile
Tourmaline
Garnet
Epidote Group
Apatite
Hornblende
Monazite
Chrome spinel
Chlorite
Chloritoid
Titanite
Pyroxene
Kyanite + Sillimanite
Tutoop Sandstone
Bako-Mintu Sandstone
Silantek Formation
Ngili Sandstone
Penrissen Sandstone
Kayan Sandstone (Bungo Range, Pueh area, G. Serapi)
Kayan Sandstone (T. Santubong, Kayan Syncline)
Grt
Ep
Ap
Ttn
Px
Cr-Spl
Zr
Rt
Tur
Unit 3
Unit 2
Unit 1
0%
10%
20%
30%
40%
50%
60%
70%
80%
90%
100%
Kuching Supergroup
Rajang Group

Figure 15

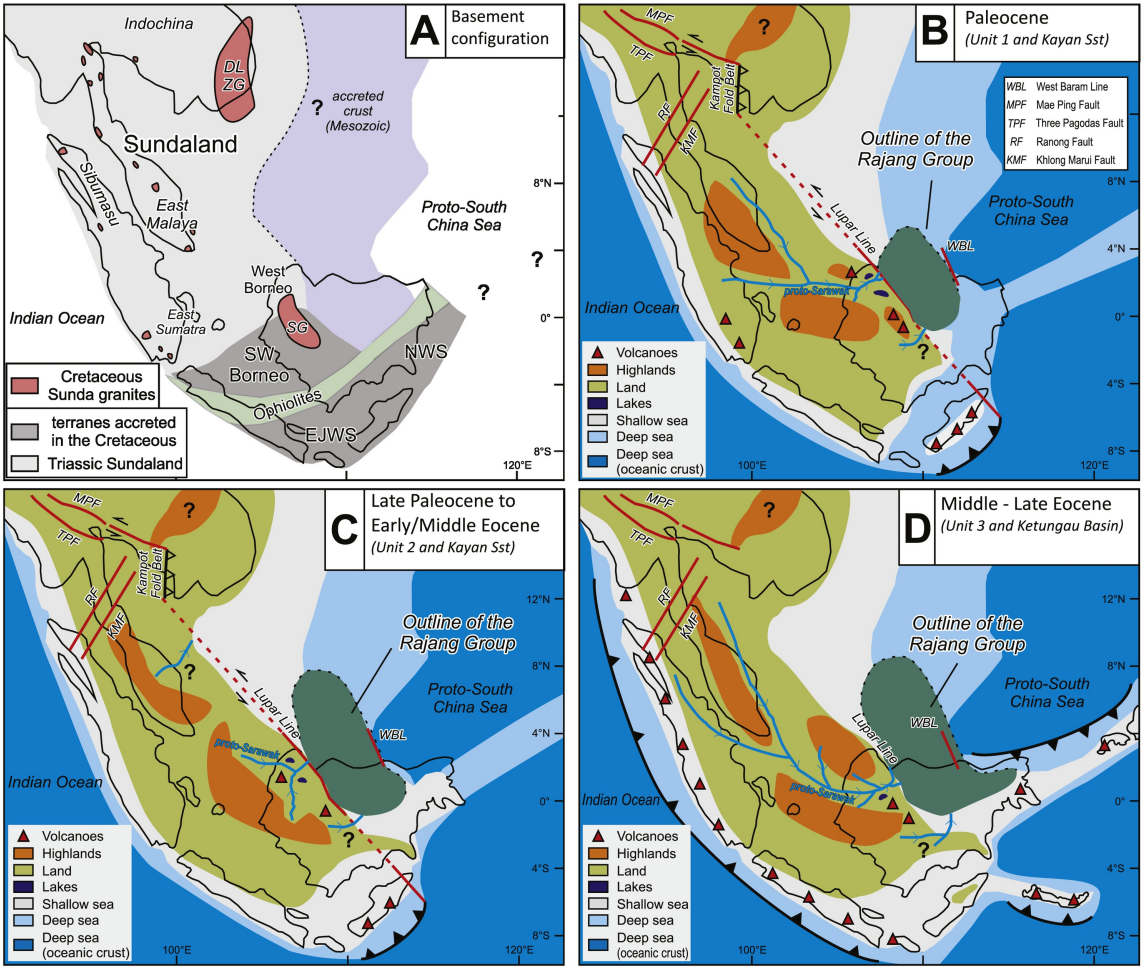
A
Basement configuration
Indochina
DL
ZG
accreted crust (Mesozoic)
Sundaland
Sibumasu
East Malaya
Proto-South China Sea
West Borneo
SG
East Sumatra
Indian Ocean
SW Borneo
NWS
Ophiolites
EJWS
Cretaceous Sunda granites
terranes accreted in the Cretaceous
Triassic Sundaland
8°N
0°
8°S
120°E
B
Paleocene
(Unit 1 and Kayan Sst)
MPF
TPF
RF
KMF
Kampot Fold Belt
WBL West Baram Line
MPF Mae Ping Fault
TPF Three Pagodas Fault
RF Ranong Fault
KMF Khlong Marui Fault
Outline of the Rajang Group
Lupar Line
proto-Sarawak
WBL
Proto-South China Sea
Indian Ocean
Volcanoes
Highlands
Land
Lakes
Shallow sea
Deep sea
Deep sea (oceanic crust)
8°N
4°N
0°
4°S
8°S
100°E
120°E
C
Late Paleocene to Early/Middle Eocene
(Unit 2 and Kayan Sst)
12°N
8°N
4°N
0°
4°S
8°S
100°E
120°E
D
Middle - Late Eocene
(Unit 3 and Ketungau Basin)

Figure 16